

Development of cyclic peptide inhibitors of coagulation factor Xla for safer anticoagulation

Thèse N° 7223

Présentée le 9 août 2019

à la Faculté des sciences de base

Laboratoire de protéines et peptides thérapeutiques

Programme doctoral en chimie et génie chimique

pour l'obtention du grade de Docteur ès Sciences

par

Vanessa CARLE

Acceptée sur proposition du jury

Prof. S. Gerber, présidente du jury

Prof. C. Heinis, directeur de thèse

Dr D. Obrecht, rapporteur

Dr L. Walport, rapporteuse

Prof. M. Dal Peraro, rapporteur

2019

“Nothing in life is to be feared, it is only to be understood. Now is the time to understand more, so that we may fear less.”

Marie Curie

Acknowledgements

First, I would like to deeply thank my thesis supervisor Prof. Christian Heinis. Thank you for giving me the opportunity to perform exciting research in LPPT, your guidance has been crucial to achieve the goals of my projects. I would also like to thank you for supporting me in exploring the world of translational research – an opportunity that very few PhD students have. I have grown a lot as a scientist during these four years and I want to thank you for this.

I would like to thank Dr Daniel Obrecht, Dr Louise Walport and Prof. Matteo Dal Peraro for being members of my exam jury and for evaluating my work. I am also very grateful to Prof. Sandrine Gerber for chairing the jury of my PhD exam.

I am extremely grateful to Béatrice Bliesener-Tong and Anne Lene Odegaard for all the support and availability during these four years.

A big thank you to the LPPT crew! You all contributed to making my PhD an amazing experience of both personal growth and fun. Thanks to the “old” lab members that welcomed me in the lab in 2015 - Ale, Camille, Xudong, Davide, Jonas, Simon, Kaycie, Sangram, Kahn, Hiro. You helped me have a great start in the lab and were always available when I needed your help! I would also like to thank the members that joined after – Patrick, Christina, Sevan, Yu Teng, Joao, Carl, Gontran, Manuel, Jun, Rakesh, Cristina, Mischa, Solenne, Ganesh M., Mahn, Milan and Ganesh S. Thank you for all the fun and the scientific discussions.

I am very grateful to all the people that have contributed to my thesis project. Thanks to Yu Teng, Rakesh, Xudong and Christina from LPTT, who have collaborated in the development of the FXI inhibitor. Your input and feedbacks have been essential for the success of the project. Thank you to Prof. Bernd Stegmayr and Dr Junko Goto for giving us the opportunity

to test the lead compound in the *ex vivo* hemodialysis model. It has been great working together and I learned a lot during the week I spent in Umeå. I would also like to express my gratitude to Prof. Urs Von Gunten and Dr Jaedon Shin for allowing me to test the on-rate of the peptides with the stopped-flow spectrophotometer. A special thank you to Sangram for the advices on chemistry, to Camille and Xudong for the help with phage display and NGS, and to Sevan, Cristina and Xudong for proof-reading this thesis. Finally, I would like to thank the students that have worked with me: Cécile, Quentin, Chelsea, Alice, Enza and Chloé. I have really enjoyed working with you and you have added a lot of value to the project!

A special thank you goes to my friends. Thanks to Ale, who has always been available since the very first day. I cannot even imagine a PhD without you in the lab. Thank you also for making the atmosphere always enjoyable! Patrick, thank you for always being available for discussing science (but not only!), for the feedbacks and for the great experience we had with Velox! I will never forget the amazing pitches we have been working on and especially our presentation at the Sachs Forum. Tami, your energy, enthusiasm and kindness have really added a lot to my life in Lausanne. Thank you for always being there for me and for your generosity. Thank you, Yu Teng, for making the lab a fun place to work in and for the time you spent to discuss science with me. Thanks to Nora, Eduard and Yann for all the fun and adventures outside the lab! Finally a big thank you to Sonia, Samu and Rico for being such great friends and for visiting me wherever I move. You are an important pillar in my life and I know I can count on you.

I would like to thank my family, that has always supported me no matter what they were going through. Thank you for allowing me to follow my dreams and for always believing in me. I could never have achieved all this without you.

Finally, thank you Stefano for making my life so incredible. Thank you for always understanding me, for always having the right words to make me feel confident and for always supporting my choices. You are my biggest fan! I hope soon we can enjoy our lives together.

Abstract

Hemostasis is a complex physiological process responsible for the prevention of blood loss caused by vascular injury. The dysregulation of this delicate mechanism can lead to thromboembolic diseases, the leading cause of death worldwide. Anticoagulants are drugs applied for the treatment and prevention of this class of diseases. Their major side effect – severe bleeding, which is a life-threatening condition – strongly limits their potential and leads to events of inappropriate treatment. Thus, there is a strong unmet need for a safer class of anticoagulants.

Coagulation factor XI (FXI), a serine protease from the intrinsic pathway of coagulation, has been identified as a promising target for safer anticoagulation. Studies in various animal models and epidemiological data have shown that FXI is involved in the pathogenesis of thrombosis, while not being essential for hemostasis. Various FXI-targeting molecules are currently in development, including small molecules, monoclonal antibodies and antisense oligonucleotides. Peptide-based FXIa inhibitors have not yet been developed, despite the attractive properties of peptides as a drug format, including high affinity and selectivity, tunable pharmacokinetic properties, a fast onset of action and absence of toxic metabolic products.

The aim of my thesis was the development of cyclic peptide-based FXIa inhibitors for safer anticoagulation. In a first project, I have developed a large cyclic peptide phage display library with unprecedentedly high structural diversity. In a proof-of-concept selection performed with the library, peptides displaying long consensus sequences were enriched and potent binders were isolated, confirming the importance of having access to large and structurally diverse libraries.

Next, I had applied the new phage display library for selecting cyclic peptide inhibitors of FXIa. Isolated peptides were characterized, and a particularly potent inhibitor was further optimized. The resulting peptide ($K_i = 3 \pm 0.2$ nM) showed a strong anticoagulation effect *ex vivo*, which was comparable to the effect of heparin at therapeutic concentrations, and a wide therapeutic window (100-fold larger than heparin). I then PEGylated the peptide, which improved its plasma stability and prolonged the circulation time *in vivo*. The PEGylated peptide inhibited plasma coagulation after administration to rabbits and in an *ex vivo* model of hemodialysis using human blood.

Finally, I had stumbled over a cyclic peptide FXIa inhibitor that had a moderate inhibitory constant but a particularly strong anticoagulation activity. In a structure-activity relationship analysis of the peptide, I identified a lysine in the peptide as the most important residue for the strong anticoagulation activity, which pointed to an electrostatic interaction and to potentially fast binding kinetics. The peptide indeed bound much faster than other FXIa inhibitors, showing that rapid engagement with the FXIa is important for efficient anticoagulation. Based on these findings, I concluded that it is worth to take into consideration the binding on-rate of inhibitors of coagulation proteases in the future development of anticoagulants.

Keywords

phage display, cyclic peptides, bicyclic peptides, protease inhibitors, pharmacokinetics, half-life extension, therapeutics, thrombosis, anticoagulants, anticoagulation, antithrombotic, coagulation factor XI, hemodialysis, *ex vivo* hemodialysis, rabbit pharmacokinetics, rabbit model, on-rate, binding kinetics

Sommario

L'emostasi è una complessa risposta fisiologica che previene la perdita di sangue causata da lesioni vascolari. Anomalie in questo processo possono portare allo sviluppo di malattie tromboemboliche, la principale causa mondiale di morte. Gli anticoagulanti sono farmaci utilizzati per il trattamento e la prevenzione di questi disturbi. Il loro effetto collaterale più importante – l'emorragia, una condizione potenzialmente letale – limita fortemente il loro potenziale e porta ad eventi di trattamento inappropriato. Quindi, c'è un forte bisogno di una classe di anticoagulanti più sicura.

Il fattore di coagulazione XI (FXI), una serin proteasi della via intrinseca della coagulazione, è stato identificato come un target promettente per una terapia anticoagulante più sicura. Studi in diversi modelli animali e dati epidemiologici hanno dimostrato che FXI è coinvolto nella patogenesi della trombosi, pur non essendo essenziale per l'emostasi. Diverse molecole dirette a bloccare FXI sono attualmente in fase di sviluppo, e queste includono anticorpi monoclonali, "small molecules" e oligonucleotidi antisenso, ma al momento non è stato avviato alcun programma per lo sviluppo di terapie a base di peptidi. I peptidi sono un tipo di molecola che può soddisfare tutti i requisiti per lo sviluppo di questo tipo di farmaci, data la loro alta affinità e selettività, le proprietà farmacocinetiche modulabili, una rapida insorgenza d'azione e l'assenza di metaboliti tossici.

Lo scopo di questo lavoro era lo sviluppo di inibitori di FXI basati su peptidi ciclici per una terapia anticoagulante più sicura. In un primo progetto, ho sviluppato un'ampia libreria di peptidi ciclici per *phage display* con una diversità strutturale senza precedenti. Una selezione eseguita con la libreria ha confermato l'importanza di effettuare screening con librerie grandi e strutturalmente diverse, in quanto sono stati selezionati formati peptidici specifici, ampie

sequenze consenso e molecole potenti. Ci aspettiamo che tale libreria possa permettere la selezione di molecole con le proprietà desiderate contro diversi target molecolari.

In seguito, la libreria è stata ciclizzata con otto linker differenti e abbiamo effettuato uno screening contro FXIa, che ha permesso la selezione di diverse sequenze consenso. Alcuni dei peptidi sono stati caratterizzati e una hit è stata ottimizzata. L'inibitore ottenuto ($K_i = 3 \pm 0.2$ nM) ha mostrato un effetto anticoagulante molto potente *ex vivo*, comparabile a quello dell'eparina a concentrazioni terapeutiche, e un indice terapeutico molto ampio. In seguito, ho pegilato il peptide, che ha permesso di ottenere un'elevata stabilità in plasma e un effetto anticoagulante prolungato *in vivo* (conigli) ed *ex vivo* (modello di emodialisi). Questi risultati hanno mostrato che la molecola è adatta per l'applicazione come anticoagulante e può fornire vantaggi rispetto alle strategie attualmente in uso.

Infine, ho scoperto che una costante di associazione veloce può essere importante per ottenere un forte effetto anticoagulante e ho caratterizzato un peptide con una k_{on} particolarmente veloce. Ho identificato una lisina nel peptide come il residuo più importante per l'associazione veloce con il target, probabilmente grazie ad un'interazione elettrostatica. Sulla base dei risultati di questo studio, ho concluso che potrebbe essere importante considerare la k_{on} di inibitori di proteasi della coagulazione nei futuri programmi per lo sviluppo di nuovi farmaci.

Parole chiave

phage display, peptidi ciclici, peptidi biciclici, inibitori di proteasi, farmacocinetica, prolungamento dell'emivita, farmaci, trombosi, anticoagulanti, anticoagulazione, antitrombotici, fattore XI, emodialisi, emodialisi *ex vivo*, farmacocinetica in conigli, costante di associazione, cinetica di legame

Contents

Acknowledgements.....	I
Abstract.....	III
Sommario.....	V
Contents.....	VII
List of abbreviations	X
1 Introduction.....	1
1.1 Peptide therapeutics	1
1.1.1 Peptides in drug development.....	1
1.1.2 Cyclic peptide therapeutics.....	3
1.1.3 <i>In vitro</i> evolution and display technologies.....	5
1.1.4 Phage selection of cyclic peptides	9
1.1.5 Phage selection of bicyclic peptides	12
1.1.6 Strategies for half-life extension	17
1.2 Thrombotic diseases and coagulation factor XI	21
1.2.1 Hemostasis	21
1.2.2 Thromboembolic diseases.....	25
1.2.3 Current anticoagulants and limitations	27
1.2.4 Coagulation factor XI as therapeutic target.....	31
1.2.5 Coagulation factor XI-targeting molecules in development	34
2 Aim of this work.....	37
3 Generation and screening of a structurally diverse 100-billion cyclic peptide phage display library	39
3.1 Abstract.....	40
3.2 Introduction	41
3.3 Results and discussion	44
3.3.1 Design of a cyclic peptide library with high backbone diversity.....	44
3.3.2 Whole plasmid PCR of phagemid vector enables generation of large library.....	46

3.3.3	Phage need to be produced in large cultures to cover most of the library diversity	48
3.3.4	Phage panning experiments reveal importance of the backbone diversity	48
3.3.5	Isolated peptides display long consensus sequences	49
3.3.6	Bicyclic peptides bind FXIa with high affinity	51
3.4	Conclusions.....	52
3.5	Material and methods.....	54
3.6	Supplementary information.....	62
4	Development of selective FXIa inhibitors based on cyclic peptides and their application for safe anticoagulation.....	69
4.1	Abstract.....	70
4.2	Introduction.....	71
4.3	Results and discussion	73
4.3.1	Screening a 500-billion cyclic peptide library for FXIa inhibitors.....	73
4.3.2	Cyclic peptide inhibits FXIa with high affinity and selectivity	75
4.3.3	Peptide engineering affords inhibitor with long plasma half-life.....	77
4.3.4	Cyclic peptide has a 100-fold wider therapeutic range than heparin..	79
4.3.5	Inhibition of the intrinsic coagulation pathway in rabbits for hours..	81
4.3.6	Cyclic peptide suppresses coagulation in a hemodialysis model	81
4.4	Conclusions.....	84
4.5	Material and methods.....	87
4.6	Supplementary information.....	96
5	Fast binding kinetics of a coagulation factor inhibitor are key for strong anticoagulation.....	103
5.1	Abstract.....	104
5.2	Introduction.....	105
5.3	Results and Discussion	107
5.3.1	Anticoagulation activity and K_i do not correlate	107
5.3.2	Efficient anticoagulation is not based on multi-target inhibition	107
5.3.3	Alanine scan identifies key role for a lysine residue in peptide 4	109
5.3.4	Reducing the complexity of the inhibitor structure	111
5.3.5	Determination of the peptide binding on-rate.....	113

5.4	Conclusions.....	116
5.5	Material and methods	118
5.6	Supplementary information.....	123
6	Conclusion & Outlook	131
	References	137
	CV Vanessa Carle	151

List of abbreviations

ABS	Anion binding site
ACT	Activated clotting time
APC	Activated protein C
AMC	7-amino-4-methylcoumarin
aPTT	Activated partial thromboplastin time
AT	Antithrombin
BBMP	2,6-bis(bromomethyl)pyridine
BSA	Bovine serum albumin
CFU	Colony-forming unit
CKD	Chronic kidney disease
Da	Dalton
DOAC	Direct oral anticoagulant
DVT	Deep vein thrombosis
ECMO	Extracorporeal membrane oxygenation
EPO	Erythropoietin
ESI	Electrospray ionization
FDA	Food and drugs administration
Fmoc	Fluorenylmethyloxycarbonyl
FP	Fluorescence polarization
FIX	Coagulation factor IX
FV	Coagulation factor V
FVII	Coagulation factor VII
FVIII	Coagulation factor VIII
FX	Coagulation factor X
FXI	Coagulation factor XI
FXII	Coagulation factor XII

FXIII	Coagulation factor XIII
GI	Gastro-intestinal
GLP-1	Glucagon-like peptide-1
GP	Glycoprotein
HD	Hemodialysis
HIT	Heparin-induced thrombocytopenia
HK/HMWK	High molecular weight kininogen
HPLC	High performance liquid chromatography
IC ₅₀	Half maximal inhibitory concentration
Ig	Immunoglobulin
IL-17	Interleukin-17
IU	International unit
IV	Intravenous
K _D	Dissociation constant
K _i	Inhibition constant
k _{on}	Association constant
K _m	Michaelis-Menten constant
LCMS	Liquid Chromatography Mass Spectrometry
LICA	Ligand conjugated antisense
LMWH	Low molecular weight heparin
mAb	Monoclonal antibody
MOI	Multiplicity of infection
NHS	N-hydroxysuccinimide
NOAC	Non-Vitamin K antagonist oral anticoagulant
NZW	New Zealand White
OD	Optical density
PAR	Protease activated receptor
PBS	Phosphate Buffered Saline
PE	Pulmonary embolism
PEG	Polyethylene glycol

PF4	Platelet factor 4
pIII	Coat protein 3
pNA	p-nitroaniline
PPACK	D-Phenylalanyl-prolyl-arginyl Chloromethyl Ketone
PT	Prothrombin time
RBC	Red blood cell
RP	Reversed-phase
SAR	Structure-activity relationship
$t_{1/2}$	Half-life
TATA	1,3,5-triacryloyl-1,3,5-triazinane
TBAB	N,N',N''-(benzene-1,3,5-triyl)-tris(2-bromoacetamide)
TBMB	1,3,5-tris-(bromomethyl)benzene
TCEP	tris(carboxyethyl)phosphine
TFA	Trifluoroacetic acid
TFPI	Tissue factor pathway inhibitor
TIS	Triisopropylsilane
tPA	Tissue-type plasminogen activator
TxA2	Thromboxane A2
UFH	Unfractionated heparin
uPA	Urokinase-type plasminogen activator
VKA	Vitamin K antagonists
VT	Venous thrombosis
VTE	Venous thromboembolism
VWF	Von Willebrand's factor
WBCT	Whole blood clotting time

1 Introduction

1.1 Peptide therapeutics

1.1.1 Peptides in drug development

Peptides are molecules containing up to 50 amino acids, which is the typical boundary established to distinguish them from proteins. Having a size ranging from 0.5 to 5 kDa, they fit within small molecules and biologics and they combine some of the favorable properties of both classes¹⁻⁴. In particular, they share with biologics the ability to bind tightly and selectively to targets, achieved thanks to their large surface of interaction. This makes them also a suitable modality for targeting protein-protein interactions⁵. Also as for proteins, the metabolic degradation products of peptides are amino acids which are not toxic. Thanks to their small size, they present low risk of immunogenicity. In common with small molecules, peptides can be synthesized chemically, which allows more flexibility and can lower the manufacturing costs⁴.

Unfortunately, peptides also present some limitations. Their short biological half-life, which is due to fast renal clearance and degradation by proteases, limits their applications⁶. However, many strategies for half-life extension of peptides and proteins have been developed and will be presented in section 1.1.6 of this thesis. Poor oral availability is another aspect that reduces the attractiveness of this molecular format. It is commonly due to lack of membrane penetration and low stability in the gastro-intestinal tract. Many efforts have been made to address this issue, with strategies involving N-methylation of the backbone, introduction of

constraints in the molecule to decrease accessibility to proteases, peptide lipidation and use of specific formulations and permeation enhancers⁷⁻⁹. Notably, a peptide-based GLP-1 receptor agonist has recently been successfully delivered orally in patients¹⁰.

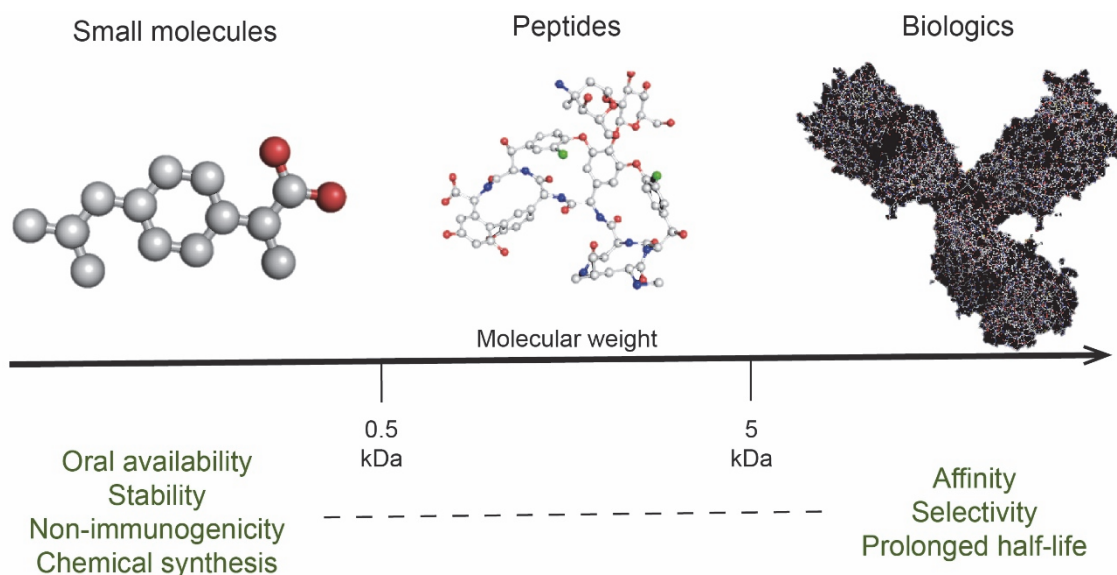


Figure 1. Size and properties of different drug modalities. Small molecules have generally a size below 500 Da, are usually orally available, cell permeable, stable and chemically synthesized. Biologics (> 5 kDa) have high potency and selectivity, and molecules like antibodies present a prolonged half-life. Peptides combine some of the favorable properties of the two classes. They can be chemically synthesized, provide high potency and selectivity and are usually non-immunogenic. However, they usually present a short systemic half-life, they are usually not orally available and can be degraded by proteases.

Over 100 drugs based on peptides are currently on the market and are applied for the treatment of various diseases, including cancer, cardiovascular diseases, and metabolic disorders. Examples of the top-selling peptide-based drugs include octreotide for the treatment of acromegaly and cancer, leuporelin and goserelin for breast and prostate cancer, and insulin glargine for diabetes³. Many other peptides are in clinical development^{11,12}.

Within the marketed peptide drugs, over 40 are based on cyclic peptides¹³. Cyclic peptides present several advantages in drug development over their linear version. They typically achieve tighter binding to the target thanks to their limited conformational flexibility and the resulting lower entropic penalty upon binding. In addition, they often show improved metabolic stability, as cyclization renders them more constrained. Finally, the particular

structure achieved upon cyclization might be more suitable to target specific surfaces, such as in the case of protein-protein interactions¹⁴.

1.1.2 Cyclic peptide therapeutics

As discussed above, the favorable properties of cyclic peptides make them a suitable modality for the application in drug development. Cyclization of peptides can generally be obtained via four strategies, involving head-to-tail, side chain-to-side chain, head-to-side chain and tail-to-side chain cyclization (Fig. 2), which can be achieved via the formation of disulfide bridges, thioethers and amide bonds, for example^{15,16}.

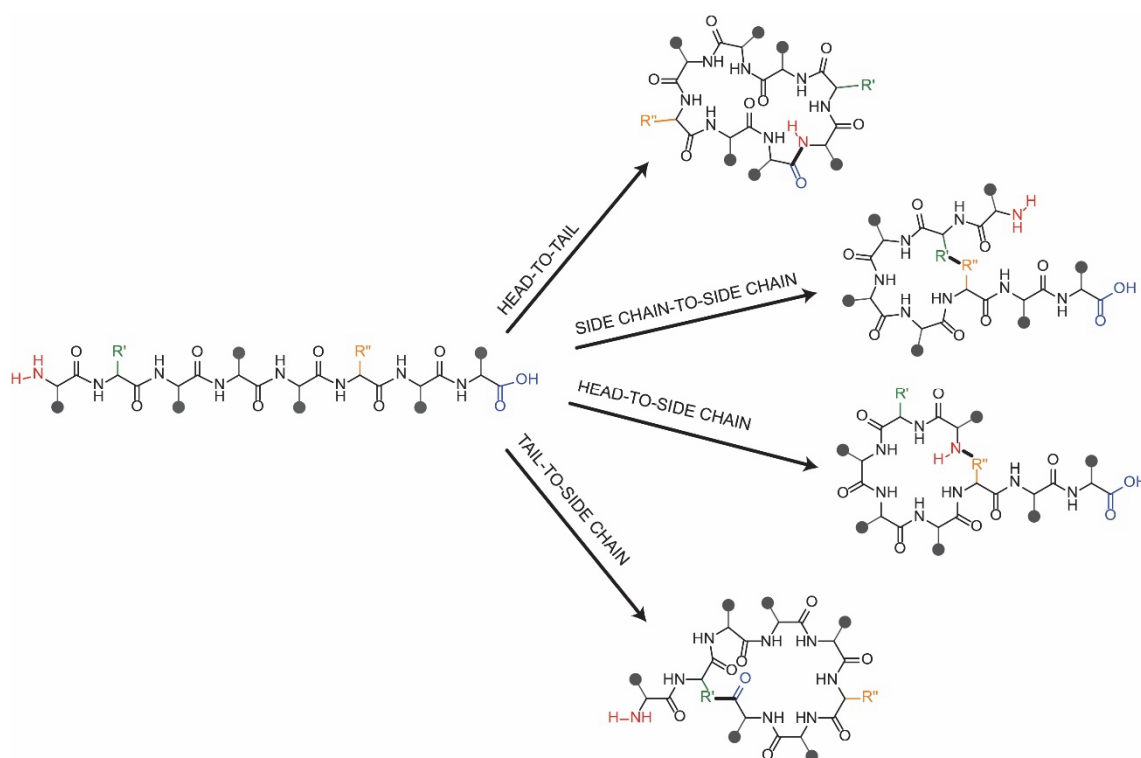


Figure 2. The four general strategies applied for peptide cyclization. Peptide head, tail and two of the side chains are shown in red, blue, green and orange, respectively. Approaches involve head-to-tail, side chain-to-side chain, head-to-side chain and tail-to-side chain macrocyclization.

As mentioned before, more than 40 cyclic peptide-based drugs have been approved to date. Examples of successful drugs include the blockbusters cyclosporine and octreotide.

Cyclosporine is an undecapeptide-based immunosuppressant used for the treatment of numerous conditions, including rheumatoid arthritis, psoriasis and prophylaxis of organ rejection in many transplants¹⁷. A special feature of this therapeutic is the oral bioavailability (29%), partly achieved thanks to its chemical properties, including N-methylations in the backbone, intramolecular hydrogen bonds, the cyclic structure and the lipophilicity, which have inspired scientists interested in the development of orally available peptides^{18,19}. Octreotide is a disulfide-cyclized octapeptide that exerts its therapeutic action by inhibiting the release of growth hormone. It is applied in the treatment of acromegaly and several hormone-secreting tumors²⁰.

While most of the marketed cyclic peptides derive from natural products, many of the molecules currently in clinical development have been discovered using *de novo* techniques, which include both *in vitro* evolution strategies and rational design¹³. The first cyclic peptide-based drug developed *de novo* to enter the market was peginesatide (in 2012)¹³. It is an erythropoietin receptor agonist, used to treat anemia caused by chronic kidney disease. It was identified using phage display from a library of disulfide-cyclized peptides and subsequently further engineered to improve its pharmacological properties²¹. In particular, it was dimerized, which allowed to achieve improved affinity to the receptor, and it was chemically conjugated to two 20 kDa PEG chains to prolong the *in vivo* half-life (Figure 3)²². Unfortunately, it was withdrawn from the market less than a year after approval due to the life-threatening anaphylactic reactions observed in one out of around 700 patients in a phase 4 trial. Studies have suggested that a post-approval change of formulation, namely the addition of phenols as preservatives in multi-dose vials, could have led to the adverse effects²³.

Cyclic peptide drugs developed *de novo* currently undergoing clinical evaluation include murepavadin, an antibacterial cyclic peptide with a novel mode of action for the treatment of *Pseudomonas aeruginosa* infections^{24,25}, APL-2, a PEGylated cyclic peptide targeting the complement protein C3 currently tested for paroxysmal nocturnal hemoglobinuria, geographic atrophy and other indications^{26,27}, and ALRN-6924, a stapled peptide that targets

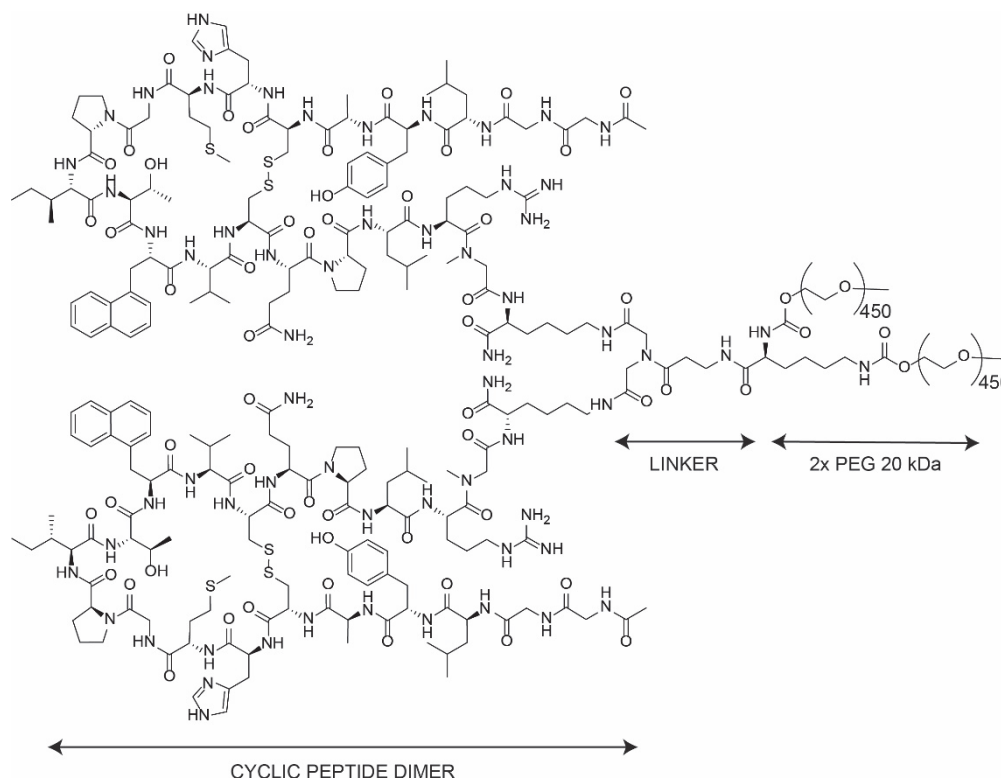


Figure 3. Structure of peginesatide. The molecule is composed by a dimer of the phage display-developed peptide conjugated via a linker to 2 chains of PEG 20 kDa.

physiological inhibitors of p53, evaluated in patients with different solid and hematological cancers^{28,29}.

1.1.3 *In vitro* evolution and display technologies

Drug development has relied for a long time on the development of active substances based on natural products³⁰. These molecules are a result of biological evolution driven by natural selection, which has fine-tuned their properties to achieve a specific function. However, it is not possible to find ligands in nature having the desired pharmacological properties for all therapeutic targets.

Thanks to the great advances in the fields of molecular biology and genetics achieved in the 20th century, scientists have started applying the mechanisms of natural selection in the

laboratory to engineer proteins. Since the rate of spontaneous mutations is too low for desired variants to be obtained in the laboratory within an acceptable time scale, libraries of genetic mutations are created to allow for rapid and efficient selection³¹. Similarly to natural evolution, *in vitro* evolution is an iterative process relying on the generation of billions of genetic variants that encode for phenotypes subjected to selection for specific properties. The selected variants are then passed on to the next generation and further improved. One of the most important aspects of *in vitro* evolution strategies is the link between the genotype and phenotype, which allows for the identification of the amino acid sequence of the selected peptide/protein variants (phenotype) by sequencing the corresponding DNA sequence (genotype). These methods represent a successful tool for *de novo* selection of proteins and peptides^{32,33}. Notably, the Nobel Prize in Chemistry 2018 was awarded to Frances H. Arnold “for the directed evolution of enzymes” and to George P. Smith and Sir Gregory P. Winter “for the phage display of peptides and antibodies”³⁴.

Many technologies for *in vitro* evolution of proteins and peptides are available to date, including phage display, yeast display, ribosome display and mRNA display³¹. Phage display, initially described in 1985 by G.P. Smith³⁵, was the first to be developed. In this method, large combinatorial libraries of proteins or peptides are inserted into a phage coat protein gene and cloned into plasmids, which are then transformed into phage competent *E. coli* cells. Transformed cells produce and assemble phage particles displaying the recombinant proteins and containing the DNA coding for them, thus allowing a physical link between genotype and phenotype (Fig. 4). Phage-encoded libraries are then subjected to biopanning to isolate specific binders with selected properties. In this selection process, libraries are incubated with the immobilized target, non-binders are washed away, and specific binders are isolated using different elution methods. Selected phage are then amplified and subjected to other runs of affinity selection, which allows for the enrichment of clones binding potently to the target. Finally, the DNA encoding for the amino acid sequence is sequenced in order to identify binders³⁶.

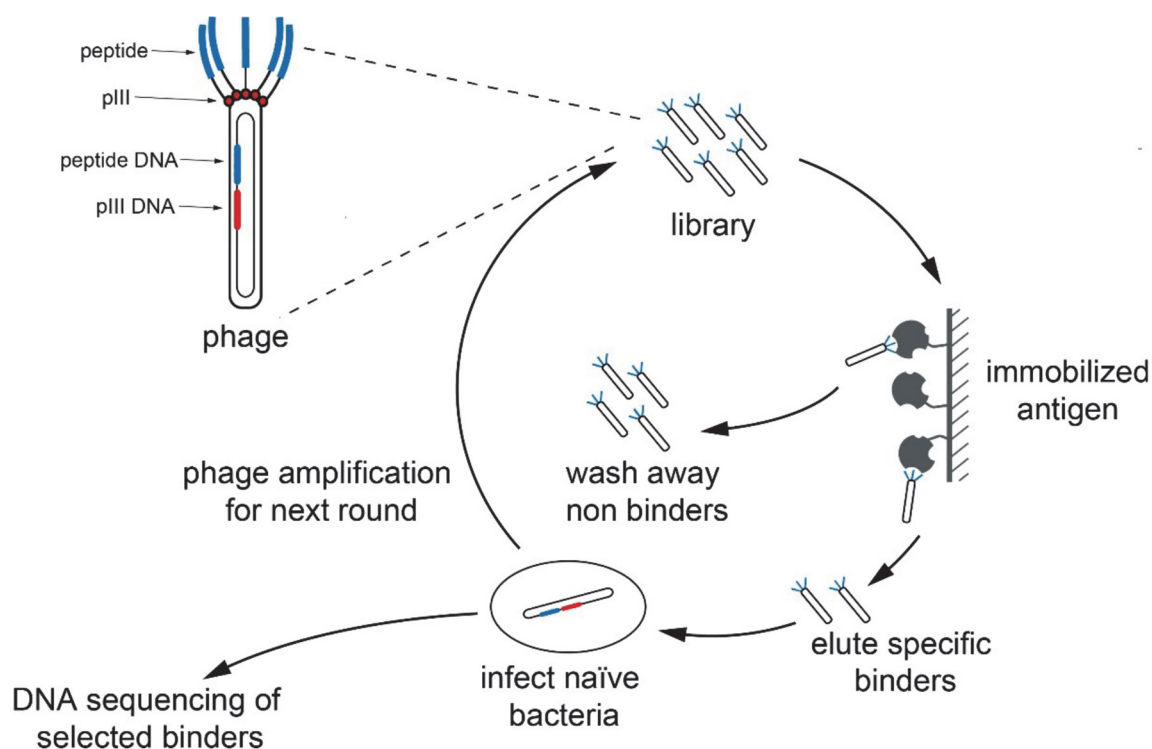


Figure 4. Schematic representation of phage display affinity selections of peptide libraries. The peptide (phenotype) and DNA sequence (genotype) encoding it are shown in blue. The coat protein pIII exploited for the display of the peptide is shown in red. Phage peptide libraries are subjected to affinity selections against an immobilized target. Non-binders are washed away, while specific binders are eluted and reamplified for the next round. Finally, DNA of selected phage is sequenced in order to identify binders.

Filamentous phage M13, fd and f1 are the most commonly used vectors and the minor coat protein pIII is often exploited for displaying peptide and protein libraries. pIII is a 406 amino acid protein found in five copies on one tip of the phage particle (Fig. 4).

The size of phage libraries is generally limited to $10^9 - 10^{10}$ unique clones, which corresponds to the maximum number of bacterial transformants that can be obtained in one experiment during library generation³¹. A strategy for improving transformation efficiency during the creation of phage libraries involves the use of phagemid systems. Phagemids are vectors containing the gene for a phage coat protein (often pIII) with cloning sites, an origin of replication, the phage intergenic region, a promoter, a signal peptide sequence and an antibiotic-resistance gene^{37,38}. The improved transformation efficiency is achieved thanks to

their smaller size in comparison with phage vectors, which instead contain genes coding for all the phage coat proteins. In addition, the small size allows to insert larger fragments of foreign DNA into phage. Phagemids are also more genetically stable than phage vectors and allow to control the expression of fusion proteins³⁷. When a library is constructed using a phagemid, the other coat protein genes necessary for particle formation must be provided using a helper phage. Helper phage are useful when monovalent display is desired, since they provide a wild-type pIII that competes with the phagemid-derived pIII fusion protein during phage packing. However, as a result around 90% of the resulting phage does not display the recombinant protein³⁹. An alternative is provided by hyperphage, a helper phage lacking the pIII gene in its genome, that allows multivalent display and higher panning efficiency⁴⁰.

Display methods that allow to achieve larger library sizes by avoiding the bacterial transformation step are mRNA and ribosome display. With these techniques, combinatorial libraries with diversities higher than 10^{12} can be achieved⁴¹. In mRNA display (Fig. 5), a cDNA library is transcribed into mRNA *in vitro* and coupled to a spacer containing puromycin at its end. *In vitro* translation of the mRNA molecules into the corresponding peptides is then performed by ribosomes. Once the ribosome approaches the end of the mRNA, it encounters puromycin, which gets covalently attached to the peptide chain, thus linking the mRNA to the encoded polypeptide. The peptide can then be further modified before being subjected to affinity selections (e.g. cyclized) and the mRNA is reverse-transcribed to allow subsequent PCR amplification. Affinity selection against the immobilized target is then performed similarly as previously described for phage display and finally the cDNA of the selected binders is amplified. The amplification can also be made error-prone to create further diversity. Several of such selection rounds can be performed in order to enrich specific binders to the target of interest. In contrast with phage display, mRNA display is always monovalent, which can be advantageous as it can avoid the selection of weak binders due to avidity effect. In addition, unnatural amino acids can be incorporated more easily in the peptide^{32,41}.

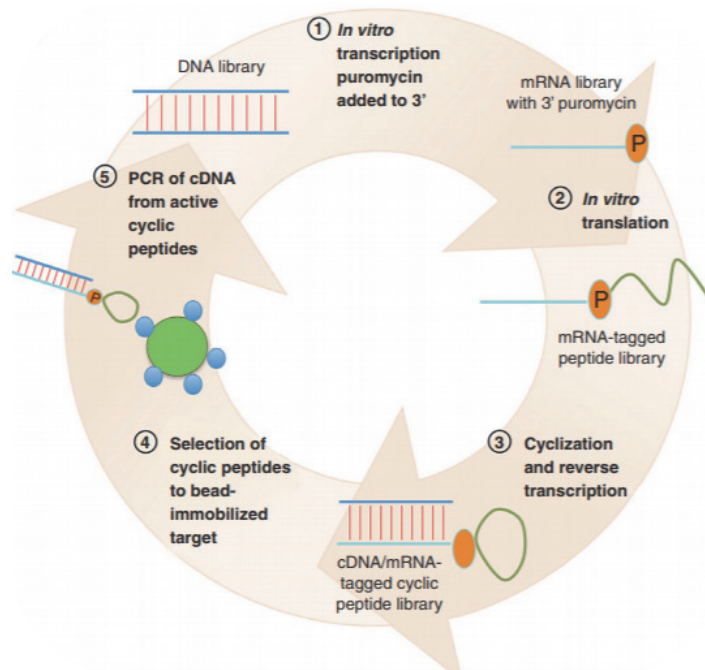


Figure 5. Schematic representation of mRNA display affinity selections of peptide libraries. The DNA library is transcribed and puromycin is coupled to the mRNA molecules. Peptides are synthesized by *in vitro* translation, covalently attached to the corresponding mRNA via puromycin and subsequently cyclized. mRNA is reverse transcribed and affinity selection against the immobilized target is performed. Finally, DNA of selected binders is amplified. Adapted with permission from ⁴¹, reprinting license number 4586131196494 Copyright © 2014, Elsevier Ltd.

1.1.4 Phage selection of cyclic peptides

Phage display has allowed to select cyclic peptide binders to many protein targets. The first peptide libraries subjected to phage selections were composed of linear peptides. However, peptides containing two cysteine residues were enriched from such libraries during phage display, suggesting the isolation of disulfide-cyclized peptides⁴². Based on this observation, new phage libraries were constructed, characterized by peptides showing two cysteine residues spaced by a random amino acid sequence. Peptides of these libraries were cyclized on phage by oxidizing their cysteines and subsequently subjected to affinity selection (Fig. 6a)^{43–47}.

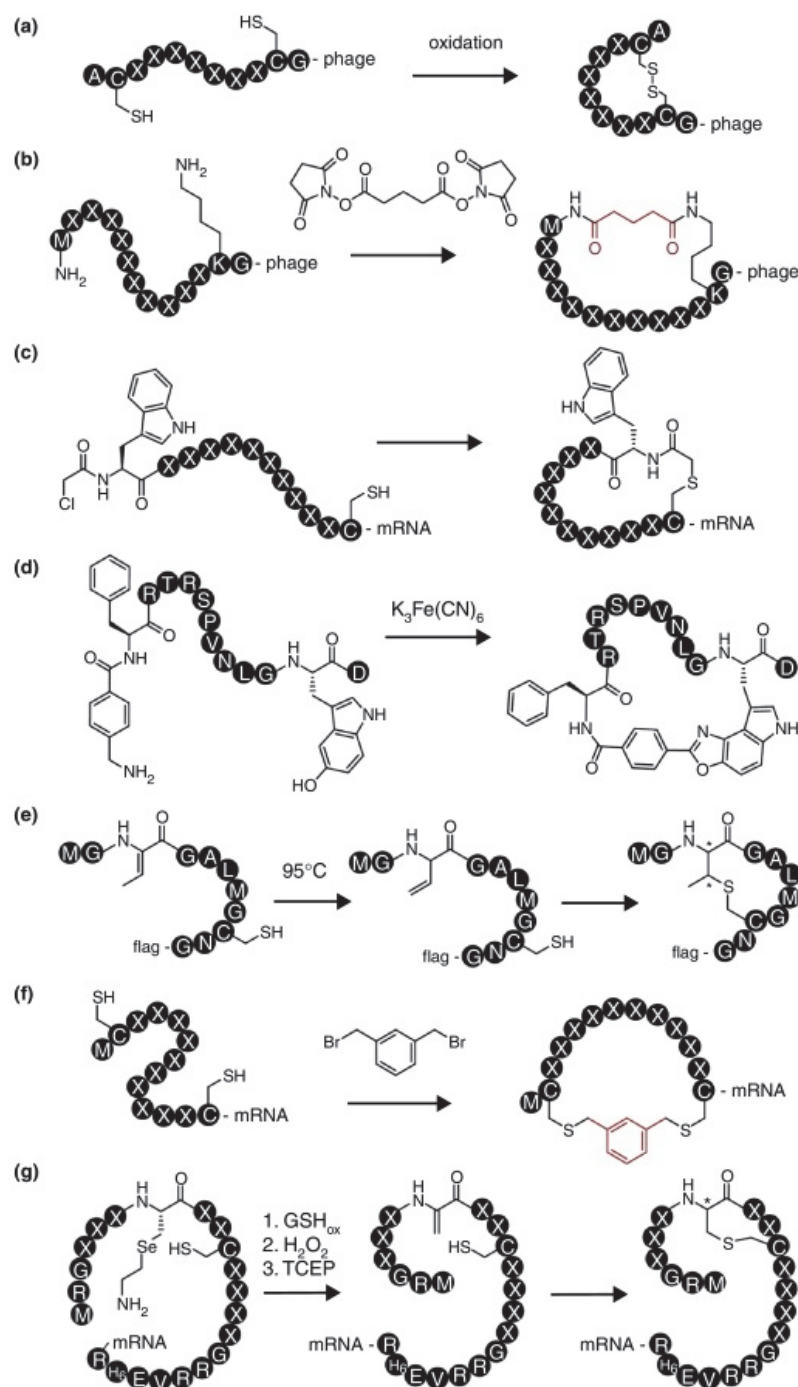


Figure 6. Encoded cyclic peptide libraries. a) Cyclization by oxidation of two cysteines. b) Cyclization by chemical linkage of the N-terminus and a lysine amino group with DSG. c) Cyclization by spontaneous reaction of a chloroacetamide group with a cysteine. d) Oxidative cyclization of peptides. e) Linkage of the thiol of a cysteine to dehydrobutyryne. f) Linkage of two cysteines with a thiol-reactive molecule. g) Cyclization of a cysteine residue to dehydroalanine. Adapted with permission from⁴⁸, reprinting license number 4586961279887, copyright © 2015 Elsevier.

Initial selections using these libraries confirmed the advantage of cyclic peptides over their linear counterparts, as they achieved binding affinities to specific targets up to three orders of magnitude higher than previously developed linear peptides^{43,45}. In addition, screening of libraries with variable loop size developed by Fairbrother *et al.*⁴⁷ showed that each target leads to the selection of specific peptide formats, thus underlying the importance of topological diversity in combinatorial libraries⁴². Based on this observation, phage libraries of peptides containing a cysteine residue in a fixed position flanked by random amino acid sequences were developed in order to increase the number of possible formats^{45,46,49}. These libraries rely on the presence of a second cysteine in the random amino acid sequence (in a fraction of the peptides). After phage display selections, most of the isolated peptides presented a second cysteine and thus were successfully selected as cyclic peptides.

The only approved cyclic peptide selected by phage display is peginesatide, which has been discussed in section 1.1.2 (Figure 3). Peginesatide was initially identified by screening a phage display peptide library with format CX₈C against the extracellular part of the erythropoietin (EPO) receptor²¹. In order to improve the binding properties of the selected peptide, secondary libraries were created, and a lead with nanomolar affinity was identified. The peptide was then dimerized, based on the binding mechanism elucidated with the help of a crystal structure⁵⁰, which improved potency. Finally, the dimer was PEGylated to increase its plasma half-life. As mentioned before, shortly after approval for the treatment of anemia in CKD patients, the drug was withdrawn from the market due to the observation of lethal side effects²².

More recently, new cyclization strategies based on non-reducible linkers have been applied to solve the problems related to cyclization via disulfide bridges. Some examples are shown in Figure 6b-g. The use of different cyclization strategies can further increase the diversity of peptide libraries, as it may lead to different peptide topologies and to the introduction of new chemical groups⁴⁸.

1.1.5 Phage selection of bicyclic peptides

Encouraged by the recent achievements with phage-selected cyclic peptides, Heinis *et al.* developed a new technology for phage display selection of bicyclic peptides⁵¹. This new molecular format allows to obtain more constrained peptide structures, thereby potentially achieving higher potency and stability. Bicyclic peptides are characterized by two macrocyclic rings, obtained by reacting three reduced cysteine residues with a trivalent thiol-reactive chemical linker. Both rings of bicyclic peptides can engage in binding, which allows to achieve a high number of binding interactions and thus high affinity and specificity⁴⁸, providing a potential advantage compared to monocyclic peptides.

Heinis *et al.* showed that the cyclization reaction used to obtain bicyclic peptides, which was previously developed by Timmerman *et al.*⁵², could be successfully applied on peptides displayed by phage without perturbing the infectivity of the virions (Fig. 7). They created a large combinatorial library containing more than 10^9 peptides, characterized by the format ACX₆CX₆CG, thereby yielding two rings of six random amino acids each upon cyclization. After phage production, the cysteine residues on peptides were reduced using tris(carboxyethyl)phosphine (TCEP) and subsequently cyclized (Fig. 7). The trivalent reagent used for cyclization in this study was 1,3,5-tris-(bromomethyl)benzene (TBMB).

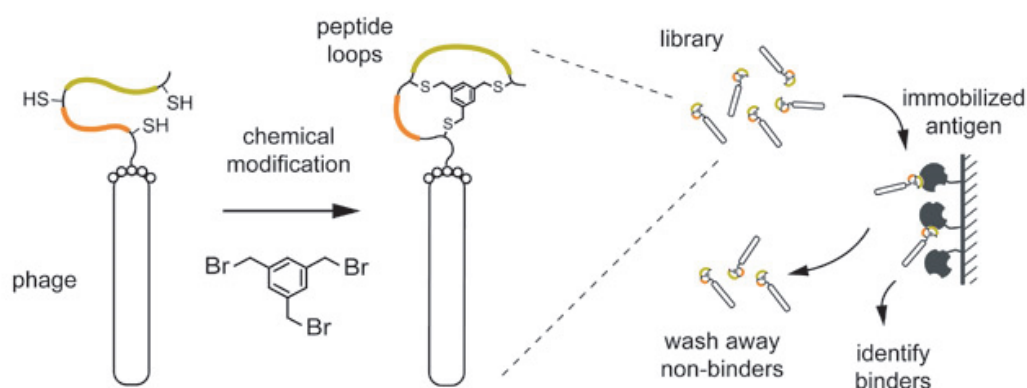


Figure 7. Schematic representation of phage display affinity selections of bicyclic peptide libraries. Peptide libraries are cyclized on phage and subjected to affinity selections against an immobilized target. Non-binders are washed away, while specific binders are eluted and reamplified for the next round. Finally, DNA of selected binders is sequenced to identify binders.

Three rounds of phage selection were performed against immobilized plasma kallikrein (PK). This yielded binders that inhibited the enzymatic activity of PK with nanomolar affinities. In addition, corresponding linear peptides were tested and showed > 200-fold lower binding affinities⁵¹.

While the selections performed using the library mentioned above (format ACX₆CX₆CG, also called 6x6 library) yielded potent and specific binders^{51,53}, a lot of potential still remained to improve library diversity and thus potentially obtain even better binders. The two main strategies for increasing structural diversity of such libraries involve the variation of ring sizes and the cyclization with different chemical linkers. As discussed previously, screening monocyclic peptide libraries with various loop sizes was found to be important, as targets often show preferences for specific peptide formats (section 1.1.4). To this end, new phage libraries of bicyclic peptides containing combinations of differently sized rings were developed⁵⁴. The library format was CX_mCX_nC, where m and n correspond to 3, 4, 5 or 6 amino acids (Fig. 8).

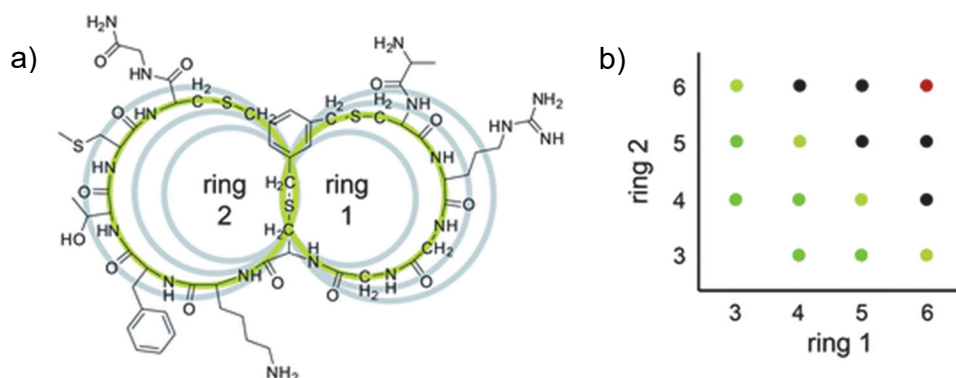


Figure 8. Phage libraries of bicyclic peptides having various combinations of loop sizes. a) Combination of different ring sizes shown on a model peptide. b) Scheme of the different ring sizes in the generated libraries. The dots in green, light green and black represent the combinations of ring sizes found in the three new libraries. The dot in red represents the previous 6x6 library. Reprinted with permission from⁵⁴, reprinting license number 4590250579850, copyright © 2013 Royal Society of Chemistry.

These libraries were screened against the target urokinase-type plasminogen activator (uPA) and led to the identification of more diverse consensus sequences compared to the ones found in previous selections with the 6x6 library.

As mentioned previously, another strategy that can be applied to increase the diversity of bicyclic peptide libraries involves the use of different chemical linkers for peptide cyclization. This can lead to different topologies upon cyclization and different interactions between the chemical linker and the peptide. To this end, Chen *et al.* applied two new molecules to bicyclic peptide libraries displayed on phage, namely 1,3,5-triacryloyl-1,3,5-triazinane (TATA) and N,N',N''-(benzene-1,3,5-triyl)-tris(2-bromoacetamide) (TBAB). These molecules present multiple polar groups and thus have the potential to form more noncovalent interactions than TBMB⁵⁵ (Fig. 9).

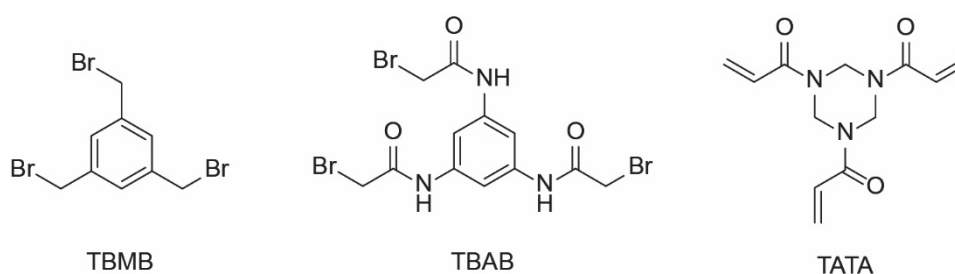


Figure 9. The three organic linkers applied for the cyclization of bicyclic peptides displayed by phage. TBMB was the first molecule used by Heinis *et al.*, while TBAB and TATA were applied by Chen *et al.* to increase diversity and to favor noncovalent interactions between the small molecule and the peptide.

NMR and crystallography data demonstrated that the new linkers impose different backbone conformations and form noncovalent interactions with peptides, which can lead to higher binding affinities thanks to the stabilization of the 3D structure of the molecules in solution (and thus lower entropic penalty when binding the target)^{55,56}. In addition, phage selections of libraries modified with these linkers against uPA yielded various consensus sequences, which were strongly dependent on the linker used⁵⁵. Therefore, the application of these molecules can triple the library diversity.

An example of a peptide selected by combining the two strategies mentioned above is the coagulation factor XIIa (FXIIa) inhibitor FXII618. This molecule was developed by screening three libraries (with formats 3x3, 4x4 and 6x6), which were cyclized with two linkers (TBAB and TATA) and by further engineering the best peptide⁵⁷. The obtained peptide FXII618, which was cyclized with TATA, showed a K_i for FXIIa of 22 nM and efficiently suppressed

coagulation driven by the intrinsic pathway *ex vivo*. In addition, it showed high selectivity when tested against homologous proteases, while inhibiting mouse FXIIa, important feature for the preclinical testing of the molecule. In later studies, FXII618 was further improved by substituting its residues with D- or unnatural amino acid analogs^{58,59}, which allowed to further increase binding affinity, stability and other properties.

Inspired by the successful application of these approaches for increased library diversity, Kale *et al.* developed a new format based on peptide cyclization with two chemical bridges⁶⁰. Cyclization can be performed on phage via four reactive cysteines, bridged using two bivalent linkers per molecule (Fig. 10a). Thanks to the large number of possible combinations of cysteine positions, this strategy allows for the creation of libraries containing thousands of different scaffolds, an unprecedented increase in topological diversity (Fig. 10b). Upon cyclization, three topological isomers are formed, which further increases diversity by three-fold. Another advantage relies on the commercial availability of several molecules with two thiol-reactive groups that are compatible with peptide cyclization on phage. This allows for a further increased diversity, which gets multiplied by the number of linkers (around 20 linkers tested to date, unpublished).

In the study by Kale *et al.*, during affinity selections against PK and interleukin-17 (IL-17), specific peptide formats were enriched, which further underscored the importance of screening structurally diverse libraries. Selected peptides showed high potency (with some PK inhibitors reaching subnanomolar K_i values) and high proteolytic stability, remaining stable for several days when incubated in human plasma at 37°C. It was observed that the impressive stability was achieved thanks to the interconnection between two bridges, which probably reduced the accessibility to proteases.

Thanks to its favorable properties, this new format allows for the construction of highly diverse libraries that could be applied for the selection of binders to challenging targets, such as protein-protein interactions, where high diversity is essential to select optimal binders^{61,62}.

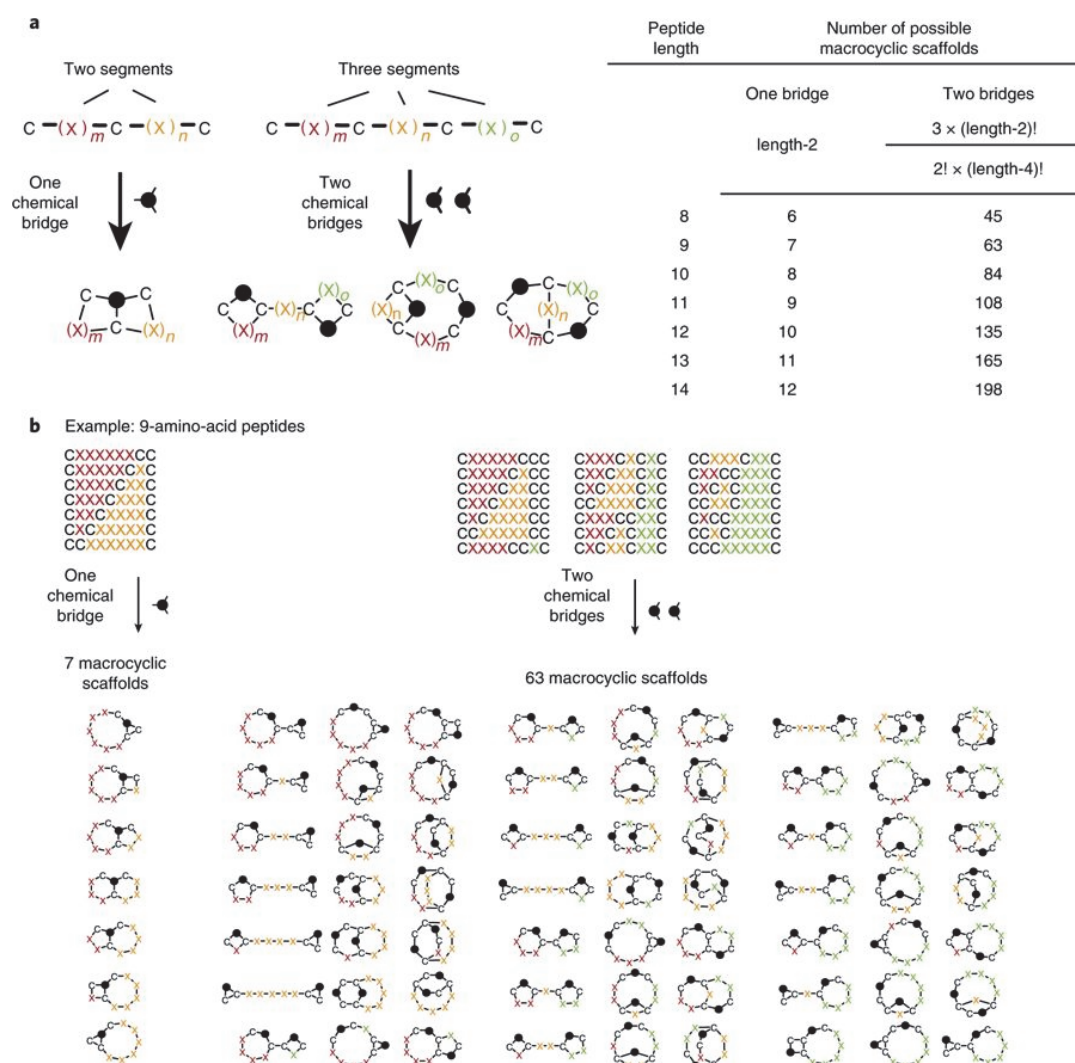


Figure 10. Novel peptide format based on peptide cyclization forming two bridges. a) The new strategy allows for the generation of many more scaffolds compared to previous format, which relied on cyclization with one linker per molecule. This is achieved thanks to the possibility to vary the position of 4 cysteines in the peptide and to the formation of 3 regioisomers upon cyclization. b) Examples of formats that can be obtained with the new strategy compared with cyclization with one chemical bridge. Reprinted with permission from⁶⁰, reprinting license number 4587130648317, copyright © 2018 Springer Nature.

In addition, smaller, monocyclic peptides that can fit into smaller binding pockets could also be selected from such libraries.

1.1.6 Strategies for half-life extension

A major limitation for the application of peptides as therapeutics is their short *in vivo* half-life, which is typically on the order of minutes after IV injection⁶³. The short half-life is generally due to two main factors: rapid renal filtration, and the proteolytic instability of certain peptides. This leads to insufficient residence times in the body for peptide-based drugs to exert their effect, and therefore they have to be frequently administered parenterally and in high dose. This represents a considerable problem both in terms of patient compliance and clinical costs^{63,64}. Renal clearance of drugs is a result of glomerular filtration and is mostly dependent on molecule size and net charge. The glomerular epithelium is characterized by pores with a diameter of 8 nm and is negatively charged. Thus, molecules with molecular weight lower than 60 kDa and a net positive charge are eliminated rapidly by the kidneys⁶⁴.

Several half-life extension strategies have been developed to date. They commonly rely on increasing the hydrodynamic volume of peptides and proteins to avoid renal filtration. These strategies can be classified in covalent (genetic or chemical) fusion to large molecules (endogenous and exogenous), and non-covalent binding to plasma proteins.

For binding to plasma proteins (covalent and non-covalent), albumin and IgGs are often exploited, as they are found at high concentrations in plasma and show the longest half-lives (19 and 21 days in humans, respectively)⁶⁴. Non-covalent binding can be achieved *in vivo* directly by the peptide or by conjugation of the peptide with a ligand of the plasma protein (e.g. fatty acids for albumin). Many examples of drugs exploiting albumin and IgGs for half-life prolongation exist^{64,65}. However, these strategies present some disadvantages. First, it is challenging to fine-tune the drug's half-life to achieve the desired residence time in the body⁶⁴. In addition, conjugation or non-covalent binding to such large proteins often leads to loss in potency of the peptide, typically due to a decrease in binding on-rate or to steric hindrance⁶⁵.

Within the strategies based on covalent chemical fusion to polymers, conjugation to polyethylene glycol (PEG) is the most commonly exploited. It is a well-established half-life extension technique that has been widely employed since the approval of the first PEGylated biologic in 1990⁶⁶. PEG has been classified as safe and well-tolerated and has been applied to 17 approved drugs (Table 1) and to many other drugs currently in clinical trials^{67,68}.

Table 1. Approved PEGylated therapeutics^{67,69}. The names in brackets are the generic drug name.

Name	PEG size	Indication	Year approved
Adagen (pegadamas)	Multiple x 5 kDa	Severe combined immunodeficiency disease	1990
Oncaspar (pegaspargase)	Multiple x 5 kDa	Acute lymphoblastic leukemia	1994
PegIntron (peginterferon alpha-2b)	12 kDa	Hepatitis C	2001
Pegasys (peginterferon alpha-2a)	40 kDa, branched	Chronic hepatitis C, B	2002
Neulasta (pegfilgrastim)	20 kDa	Neutropenia	2002
Somavert (pegvisomant)	4-6 x 5 kDa	Acromegaly	2003
Macugen (pegaptanib)	40 kDa, branched	Age-related macular degeneration	2004
Mircera (PEG-EPO)	30 kDa	Anemia associated with chronic kidney disease	2007
Cimzia (certolizumab pegol)	40 kDa, branched	Rheumatoid arthritis, Chron's disease and others	2008
Krystexxa (pegloticase)	9-11 x 10 kDa	Chronic gout	2010
Sylatron (peginterferon alpha-2b)	12 kDa	Melanoma	2011
Omontys (peginesatide)	40 kDa, branched	Anemia associated with chronic kidney disease	2012 (withdrawn)
Plegridy (peginterferon beta-1a)	20 kDa	Relapsing from multiple sclerosis	2014
Adynovate (Antihemophilic Factor (Recombinant), PEGylated)	20 kDa	Hemophilia A	2015
Rebinyn (coagulation factor IX (recombinant), glycopegylated)	40 kDa	Hemophilia B	2017
Jivi (antihemophilic factor (recombinant), PEGylated-aucl)	60 kDa	Hemophilia A	2018
Palynziq (pegvaliase)	20 kDa	Phenylketonuria	2018

The molecular weight of PEG chains is dependent on the number of attached units, with common length ranging from 5 to 50 kDa. The possibility to use PEGs with different molecular weights allows to fine-tune the half-life of peptides, as it has been shown that the *in vivo* half-life of PEG is dependent on its size. In particular, elimination of PEG chains above 8 kDa is dependent on molecular weight, with a dramatic increase in half-life observed with PEGs larger than 30 kDa⁷⁰. The reason behind this is that PEG 30 kDa has a diameter of 8 nm, similarly to the pores in the glomerular epithelium⁷¹. However, due to the typical flexibility and deformability, large PEGs are still filtered by kidneys at very slow rates. The observed 30 kDa threshold for glomerular filtration is lower than previously mentioned (60 kDa) thanks to the fact that PEG can coordinate many water molecules, thus having a larger hydrodynamic volume than the actual size⁶⁴. In addition to the ability to slow down glomerular filtration, PEG also presents other useful properties. It can shield the peptide from proteolytic degradation, thus improving stability, and it can decrease the immunogenicity potential of proteins. In addition, it can increase the solubility of drugs.

PEG with a molecular weight of 40 kDa (and thus above the 30 kDa threshold) is often applied to peptides and small proteins in order to achieve longer half-lives. As an example, peginesatide (peptide conjugated to a branched 40 kDa PEG, with total molecule size of 45 kDa, Fig. 3) shows a half-life of 25 hours upon IV injection in healthy volunteers⁷². Branched 40 kDa PEG, characterized by two 20 kDa chains linked together (Fig. 3), is the most common type used in approved molecules (Table 1) and in molecules undergoing clinical trials. Branched PEG was found to increase half-lives and reduce immunogenicity more efficiently than its linear counterpart. However, it was also associated with a greater reduction in binder activity⁶⁸.

Even though PEGylation is successfully applied to several molecules and considered safe, some issues have emerged. In some cases, PEGylation can lead to loss in activity and potency of the drug. Due to its nondegradable nature, it can cause renal tubular vacuolation. Although no toxicologic significance has been attributed to vacuolation, long-term effects cannot be

easily predicted, and thus more studies are required. In addition, anti-PEG antibodies have been observed for PEG-protein conjugates during animal studies, but their impact on the conjugates has not been fully characterized yet. Finally, allergic reactions to PEG-containing molecules have been documented, although the mechanism for the development of such allergies is not yet clear^{64,73}.

In order to address these problems, alternative strategies exploiting natural polymers have been developed. These include glycosylation, conjugation to polysaccharides like hyaluronic acid, polysialic acid, dextran and hydroxy-ethyl-starch, and recombinant fusion to specific unstructured amino acid sequences, achieved for example via XTENylation, ELPylation and PASylation. However, more studies are required in order to fully characterize these alternative strategies and to benchmark them against PEG⁷⁴.

1.2 Thrombotic diseases and coagulation factor XI

1.2.1 Hemostasis

Hemostasis is a complex physiological process responsible for the prevention of blood loss caused by vascular injury. The rapid closure of the site of injury is ensured thanks to the formation of a hemostatic thrombus (a fibrin-rich platelet plug). In parallel, normal blood flow in the circulation is maintained. This subtle balance is preserved thanks to the coordinated activity of platelets, coagulation cascade, fibrinolytic system and physiological anticoagulation mechanisms⁷⁵. Dysregulation of this balance can lead on one hand to impaired hemostasis and thus risk of hemorrhage, and on the other hand to increased fibrin deposition and thus risk of thrombosis⁷⁶.

Hemostasis is divided in two main steps: primary and secondary hemostasis. Primary hemostasis involves platelet activation and aggregation at the site of injury, leading to the formation of a platelet plug. Secondary hemostasis culminates in the formation of insoluble fibrin, which is added into and around the platelet plug and has the function to stabilize the clot. In addition, the fibrinolytic pathway is another important mechanism that, together with several anticoagulation processes, helps maintain the hemostatic balance. These processes occur concurrently and are interconnected⁷⁷.

Platelets are small disc-shaped cell fragments without nuclei deriving from megakaryocytes in the bone marrow⁷⁸. In normal physiological conditions, platelets are found in blood without adhering to endothelial cells or to each other. However, they have the ability to rapidly react to vascular injury, upon which they get activated and form a primary plug localized at the injured site. This is achieved through a complex network of interactions between components of the subendothelial matrix, soluble ligands, and receptors on platelets. Examples of adhesive ligands include fibrinogen, von Willebrand's factor (VWF), and

fibronectin⁷⁹. The most important platelet receptors mediating adhesion are GPVI and GPIb-IX-V. Briefly, initial adhesion occurs when GPIb-IX-V binds to the immobilized form of VWF, forming an interaction dependent on blood flow velocity and shear rate⁸⁰. GPVI then binds collagen, which is found in the subendothelial matrix, stabilizing the thrombus. These interactions are important to start adhesion of platelets to the site of injury and to activate them⁷⁷. Platelet activation in turn leads to a conformational change in the structure of integrins found in the membrane (α IIB β 3, α 2 β 1, α v β 3), that allows them to bind their ligands with higher affinity and consequently promote aggregation⁸¹. α IIB β 3 (also named GPIIb/IIIa), which appears to be the most important integrin for aggregation, binds to collagen, VWF, fibronogen, fibronectin, and other ligands and promotes platelet-platelet aggregation and clot stabilization (Fig. 11)^{77,80}. An important mechanism for further aggregation is the feedback-activation of other platelets, which is achieved by activated platelets through the release of ligands like ADP and serotonin (present in their α -granules) and thromboxane A2 (TxA₂)⁸⁰. These agonists act by binding receptors found on inactive platelets, which leads to their activation. Finally, the serine protease thrombin, a component of secondary hemostasis, can also activate platelets by cleaving the receptors PAR1 and PAR4⁸². The platelet clot is then stabilized through fibrin deposition, which is achieved by secondary hemostasis⁷⁷.

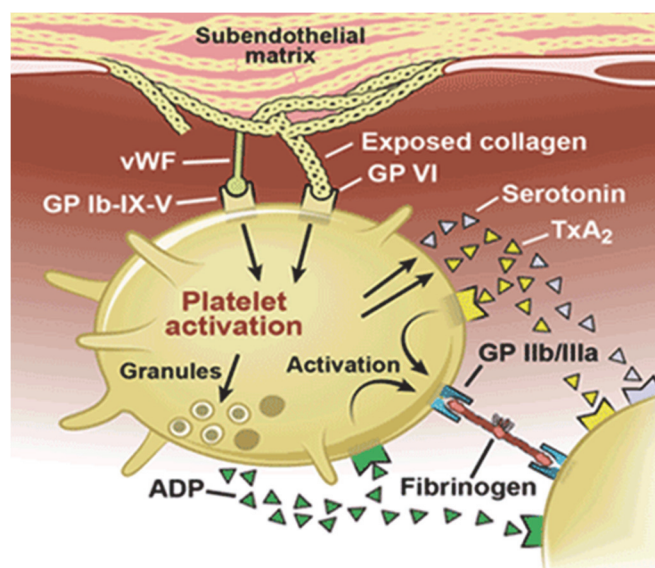


Figure 11. Overview of the complex network of interactions that govern platelet adhesion, activation and aggregation. Reprinted with permission from ⁸³. CCF © 2016.

Secondary hemostasis is achieved by the coagulation cascade of serine proteases via a series of proteolytic activations. When injury occurs, blood gets in contact with tissues rich in the membrane protein tissue factor (TF), which, in complex with factor VIIa (FVIIa), activates factor X (FX), forming FXa. In addition, the TF-FVIIa complex also cleaves factor IX (FIX) to form FIXa. FXa, in presence of factor Va (FVa), activates prothrombin to form thrombin. The pathway in which coagulation is activated via FVIIa and TF has been named “extrinsic pathway” (Figure 12). A parallel pathway, called “intrinsic pathway” of coagulation, also leads to the activation of thrombin. In particular, when blood is exposed to negatively charged surfaces, small amounts of factor XII (FXII) are activated to FXIIa due to a conformational change in the protein. FXIIa cleaves PK, which further activates FXII. FXIIa cleaves factor XI (FXI) to form FXIa, which in turn activates factor IX (FIX). FIXa activates FX and at this point the two pathways converge in a common pathway^{84,85}. Finally, activated thrombin leads to the formation of insoluble fibrin by cleavage of fibrinogen (Fig. 12)^{86,87}, which happens concurrently with platelet plug formation.

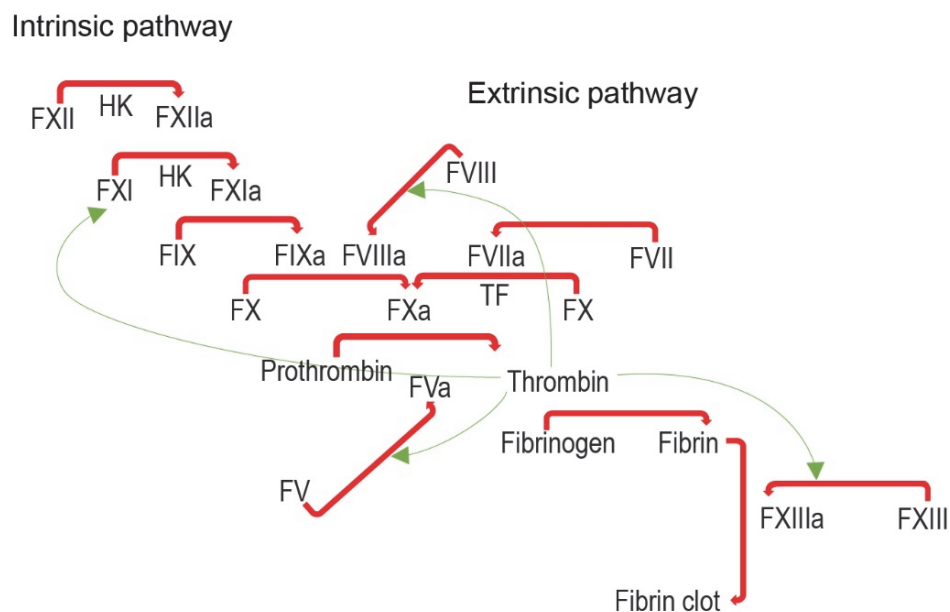


Figure 12. Scheme of the coagulation cascade of serine proteases. Protease zymogens are represented with roman numbers, while their activated form is indicated with “a”. Red arrows indicate activation reactions as represented in the standard model, while green arrows indicate some of the feedback reactions that were not part of classic coagulation models. HK: high molecular weight kininogen.

In addition, thrombin activates other factors, such as FXI, in a positive feedback loop mechanism (Fig. 12). This is considered to be essential for clot propagation⁷⁷.

The importance of interconnections between primary and secondary hemostasis and of the concept of cell-based coagulation has recently become clear^{84,88}. Briefly, TF-FVIIa-driven thrombin production, the initiation phase, takes place on the surface of subendothelial cells. Subsequently, thrombus amplification and propagation (achieved by thrombin via the different feedback activations) takes place on platelet surface, creating active complexes such as the prothrombinase (FVa/FXa) and Xase (FVIIa/FIXa) complexes. This accelerates the production of FXa and thrombin, leading to clot formation. In addition, as mentioned previously, generated thrombin has the ability to further activate platelets at the site of injury. Thus, the mechanisms of hemostasis appear more complex and interconnected than previously described with classical coagulation models, with localization on platelets probably being important for restricting clot formation to the site of injury⁸⁸.

The coagulation cascade and clot localization are controlled by several physiological inhibitory systems. The most important are antithrombin, protein C, protein S, tissue factor pathway inhibitor (TFPI) and the fibrinolytic system. Antithrombin is an inhibitor of serine proteases, including FXa and thrombin, and member of the serpin superfamily⁸⁹. While alone it is a weak inhibitor, its inhibitory activity is increased by around 300-fold upon binding to heparin and heparans, which are found on the surface of vascular endothelium⁹⁰. Protein C is a serine protease activated by the complex formed by thrombin and thrombomodulin, a protein found on the surface of endothelial cells. Its activated form, APC, can regulate the activity of FVa and FVIIIa⁸⁶. Protein S (a serine protease) acts as a cofactor of protein C, supporting its activity⁸⁹. Thanks to activation involving heparin-like molecules and thrombomodulin, activities of both protein C and antithrombin are thus localized at the endothelium surface. TFPI is a serine protease inhibitor (Kunitz-type) that blocks the activity of FXa. Upon FXa binding, it can in turn inhibit the FVIIa-TF complex⁹¹.

Fibrinolysis is another important control mechanism involved in clot dissolution during wound healing and in clot localization specifically at the site of injury. The system includes three serine proteases: plasmin, urokinase-type plasminogen activator (uPA) and tissue-type plasminogen activator (tPA). Plasmin is activated by uPA and tPA and is responsible for fibrin cleavage and degradation, thus leading to clot removal⁹². The activity of proteases from the fibrinolytic system is in turn controlled by inhibitors from the serpin superfamily⁹³.

1.2.2 Thromboembolic diseases

Dysregulation of hemostasis can cause the formation of thrombi that obstruct blood vessels, leading to thromboembolic diseases, the leading cause of mortality and morbidity⁹⁴. Thrombosis can occur both in arterial and in venous circulations. These two conditions differ in the pathophysiological mechanisms and thus they are treated differently. Normally, thrombosis in the arterial circulation is treated with antiplatelet agents, while the treatment of venous thrombosis involves the use anticoagulants, which are drugs targeting the serine proteases of the coagulation cascade⁹⁵. Currently available antithrombotic agents are efficacious, but they present a main limitation – they increase the risk of severe bleeding.

Arterial thrombosis is generally caused by the rupture of an atherosclerotic plaque (Fig. 13). Such plaques form mainly in medium and large-sized elastic arteries and are due to the accumulation of lipids and foam cells (macrophages laden with lipids) in the artery^{96,97}. Upon rupture, the endothelium is damaged, exposing ligands of platelet receptors, like collagen and VWF. This leads to platelet adhesion and aggregation and the rapid formation of blood clots that are typically platelet-rich⁹⁸. An important role is also played by the coagulation cascade. High levels of TF are present in the ruptured plaque, which leads to the activation of the cascade and ultimately to fibrin deposition. In addition, thrombin further activates platelets by activating the PAR1 receptor.

As mentioned above, the treatment of arterial thrombosis generally involves agents targeting

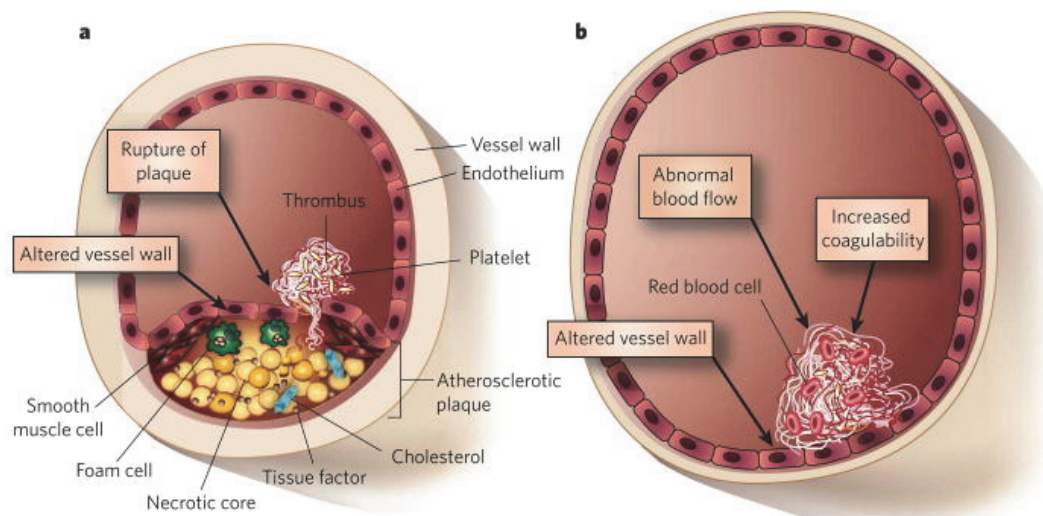


Figure 13. The mechanism involved in arterial and venous thrombosis. a) Arterial thrombosis. Upon rupture of an atherosclerotic plaque, the endothelium is damaged, and ligands of platelet receptors are exposed and lead to platelet aggregation to the site rupture, together with fibrin deposition. b) Venous thrombosis. The endothelium can lose its anticoagulation properties and can become procoagulant, which leads to thrombus formation. Many risk factors can lead to thrombosis, including altered flow of blood, abnormal changes in the endothelium and alterations in the blood components. Reprinted with permission from⁹⁵, reprinting license number 4590090704495, copyright © 2008 Springer Nature.

platelet activation and aggregation, including cyclooxygenase inhibitors, ADP-receptor antagonists, PAR-1 inhibitors and $\alpha\text{IIb}\beta 3$ inhibitors⁹⁵.

Venous thromboembolism (VTE), which includes venous thrombosis (VT) and pulmonary embolism (PE), is a major cause of death. Deep VT (DVT) is caused by the formation of a blood clot generally in the large veins of the legs. PE is a life-threatening complication that occurs when a thrombus or a fraction thereof detaches from the primary location and migrates to the lungs, where it leads to the occlusion of a pulmonary artery. Venous thrombi, in contrast with the ones formed in the arteries, contain large amounts of fibrin and red blood cells (RBCs) and thus are often called “red clots”^{95,99,100}.

The triggers of DVT can be classified into three main groups. The first group includes modifications of blood components that lead to a procoagulant state. This is usually related to increased activity of procoagulant factors or impaired activity of physiological anticoagulants. The second group involves changes in the wall of the vessel. Evidence suggests

that local inflammation might be the cause for thrombosis related to vessel alterations. Finally, the third group includes abnormal blood flow. In particular, blood stasis has been strongly linked to high risk of thrombosis as it can lead to accumulation of procoagulant factors and to hypoxia, which can activate the endothelium and favor the release of TF^{95,101}. All these triggers involve the activation of the coagulation cascade. Inherited risk of VTE is often due to alterations in blood components, while non-inherited risk factors include major surgical operations, cancer and obesity^{101,102}.

VTE is usually treated with anticoagulants, which target the coagulation cascade of serine proteases. In the next section the properties and limitations of the main classes of anticoagulants currently available will be discussed.

1.2.3 Current anticoagulants and limitations

Currently available anticoagulants are classified based on their mode of action into heparins, vitamin K antagonists (VKAs) and direct inhibitors of thrombin and FXa.

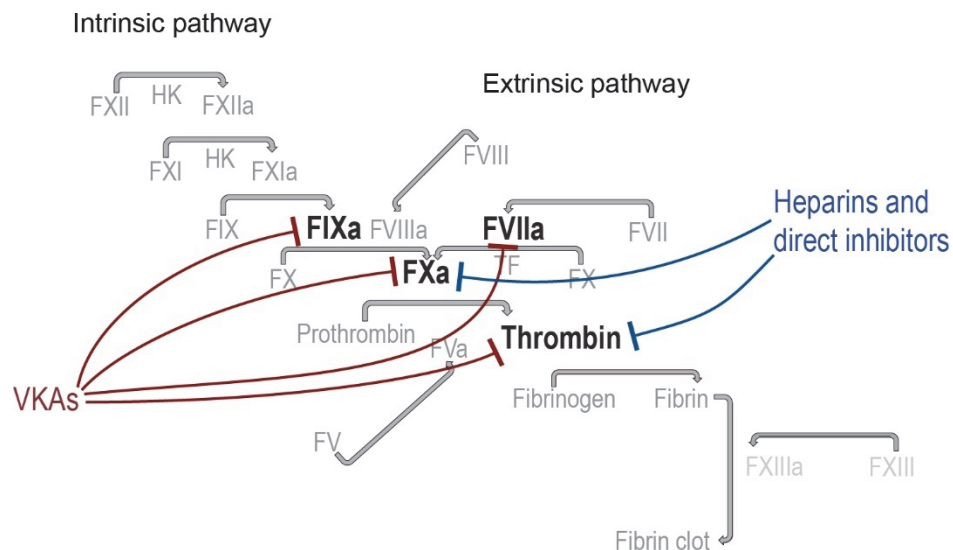


Figure 14. Direct and indirect targets of the main classes of anticoagulants. VKAs (in red) target mainly FIXa, FVIIa, FXa and thrombin. Heparin and direct inhibitors (in blue) target FXa and thrombin.

The drug class of heparins includes unfractionated heparin (UFH) and low molecular weight heparins (LMWHs). UFH is the oldest anticoagulant, in use since the 1920s¹⁰³. It is a glycosaminoglycan derived from natural sources. As mentioned previously, it acts by binding to antithrombin (AT), a natural inhibitor of several serine proteases, including FXa and thrombin. The motif necessary for high affinity binding to AT is a specific pentasaccharide sequence, that is present in around 30% of UFH molecules¹⁰⁴. Upon binding, AT undergoes a conformational change, that dramatically increases its affinity for FXa and thrombin, thus exerting an anticoagulation activity⁹⁰. The application of UFH in indications like prevention of VTE, acute coronary syndrome, vascular surgery, and prevention of clotting in extracorporeal circuits is well established. However, UFH presents several disadvantages (Table 2). It is associated with an increased risk of severe bleeding, with an incidence of 2.0 - 4.5 %, depending on the indication¹⁰⁵. In addition, the use of heparins can lead to heparin-induced thrombocytopenia (HIT), an immune response-driven side effect occurring in 1-5% of patients taking UFH. HIT is caused by the generation of antibodies targeting complexes of heparin and platelet factor 4 (PF4), a molecule found in platelets. Such antibody-heparin-PF4 complexes can activate platelets, leading to a hypercoagulable state and can paradoxically cause thrombosis¹⁰⁶. UFH presents a short and dose-dependent *in vivo* half-life, corresponding to around 1.5 hours upon IV injection¹⁰⁷. Finally, heparins cannot be administered orally. LMWHs have been developed more recently and are smaller heparin fragments, usually derived by enzymatic or chemical degradation of UFH¹⁰⁸. In contrast with UFH, they do not favor the inhibition of thrombin by AT, as this requires the interaction with a long polysaccharide (minimum length 18 saccharides). Thus LMWHs mainly target FXa, as its potentiated inhibition occurs only via the interaction with the conformationally changed-AT¹⁰⁹. In comparison with UFH, LMWHs lead to a smaller risk of severe bleeding in selected indications, ranging from 1.5 – 4.7 %¹⁰⁵. In addition, the risk to develop HIT is lower, probably because the affinity of heparins for PF4 depends on the molecular weight¹⁰⁶. Finally, LMWHs show improved PK properties, including a longer half-life and higher bioavailability upon SC injection¹⁰⁴. Despite the improvements, LMWHs are still affected by the main limitations of

UFH.

Table 2. The three main classes of anticoagulants and their main properties. Data from^{95,105,110–112}.

	Heparins	VKA	Direct inhibitors
Mechanism of action	Bind AT, inhibition FXa (and thrombin)	Inhibition of vitamin K epoxide reductase	Direct inhibition of FXa or thrombin
Application	Acute and chronic anticoagulation	Chronic anticoagulation	Acute and chronic anticoagulation
Advantages			Orally available
			Fast onset of action
	Fast onset of action	Orally available	No need for routine monitoring
	Safe during pregnancy	Well established	Predictable PK
	Well established	Reversal agents available	Little food/drug interactions
	Reversal agents available		Lower intracranial bleeding risk
Disadvantages	Risk of major bleeding	Risk of major bleeding	Risk of major bleeding (especially in GI tract)
	Risk of HIT	Activity/PK affected by diet and genetic	Less established reversal agents
	Parenteral administration	Narrow therapeutic window	No long-term safety data
	Variable PK profile	Slow onset of action	
	Narrow therapeutic window	Need for routine monitoring	Higher cost

VKAs are oral small molecule anticoagulants targeting vitamin K epoxide reductase. This enzyme is essential for the vitamin K-dependent post-translational modification of several proteases of the coagulation cascade. Its inhibition by VKAs leads to the reduction of functional coagulation factors, causing the anticoagulation effect¹¹⁰. They are applied for

long-term prophylaxis and treatment of VTE, after myocardial infarction, in patients with atrial fibrillation, and in many other indications. They have been for a long time the only oral anticoagulants available on the market¹¹¹. VKAs present serious disadvantages. They increase the risk of severe bleeding, with an incidence of 2 – 5 % for patients treated with warfarin (the most used VKA)¹¹³. In addition, they have an unpredictable dose-response profile, with inter- and intra-patient variability and a narrow therapeutic index, also due to the influence of diet and other drugs. This often leads to inappropriate anticoagulation and bleeding side effects and thus patients require constant monitoring¹¹⁰. Finally, they show a slow onset of action, as they cannot block the activity of coagulation factors already present in circulation, and thus are not suitable for acute indications¹¹⁴.

Direct inhibitors of thrombin and FXa, often named NOACs (non-vitamin K oral anticoagulants) or DOACs (direct oral anticoagulants), are a novel class of anticoagulants developed to overcome the limitations of VKAs, which were the only class of oral drugs present at the time of their development. Their mechanism of action relies on the specific inhibition of the activity of either FXa or thrombin¹¹¹. Examples of these drugs include dabigatran (thrombin inhibitor), apixaban, and rivaroxaban (FXa inhibitors). They are used for the treatment and prevention of VTE and thrombosis prevention in patients with atrial fibrillation and acute coronary syndrome. Their main advantages over VKAs include a better risk/benefit ratio, lower incidence of intracranial bleeding, wider therapeutic range and no need for routine monitoring (Table 2)¹¹¹. However, they still present bleeding side effects, with incidence of 0.6 – 3.3 % depending on indication and drug^{112,115–119}. In addition, there is less data about long-term effects than VKAs and reversal agents have been only recently approved¹²⁰.

Although many advances in the field of anticoagulation therapy have been made, all the available drug classes still present major disadvantages, especially in terms of safety profile. Therefore, there is still a clear unmet need for safer anticoagulation strategies with an improved risk/benefit profile. The new agents should fulfill important requirements,

including: non-inferiority in safety compared to NOACs, predictable PK profile and low risk of interactions with other agents, large therapeutic window, fast onset and offset of action, no monitoring required, lack of (or little) side effects and bleeding, access to a reversal agent, and non-renal clearance¹²¹.

1.2.4 Coagulation factor XI as therapeutic target

As previously discussed, anticoagulants currently in use strongly interfere with hemostasis and thus lead to an increased risk of severe bleeding, which represents a major side effect. Because of this safety issue, many patients are not treated, or receive inappropriate treatment with insufficient doses of drugs, as severe bleeding poses an important health risk that in some cases is considered unacceptable^{122,123}. For this reason, there is a strong unmet need for safer anticoagulants for the prevention and treatment of thrombotic diseases.

In recent years, studies in animal models of thrombosis have shown that components of the intrinsic pathway of coagulation, and in particular FXI and FXII, are involved in thrombosis without being essential for hemostasis¹²⁴. Patients deficient in FXII do not suffer from a bleeding disorder and FXI deficiency leads to a mild bleeding phenotype, with excessive bleeding occurring rarely and only upon injury to tissues with high fibrinolytic activity^{125,126}. However, results from epidemiological studies suggest that targeting FXI could provide a more efficacious strategy, as its plasma levels were found to be strongly linked to thrombosis incidence. In contrast, there is no solid clinical evidence for a role of FXII in thrombosis in humans¹²⁷. This could be explained with the hypothesis that feedback activation of FXI by thrombin plays a role in thrombosis, a mechanism that could not be stopped through FXII inhibition¹²⁸.

FXI is a trypsin-like serine protease found at a concentration of around 30 nM in plasma, where it forms a complex with HK¹²⁹. It is composed of a light and a heavy chain, with molecular weights of 35 and 48 kDa, respectively. The heavy chain, which contains four 90-

91 amino acid domains named apple domains, is found at the N-terminal part of the protein, while the catalytic domain is located in the C-terminal portion of the protease after the apple four domain (Figure 15)¹³⁰. The catalytic triad of the active site is composed of the residues serine 557, histidine 413 and aspartic acid 462 (highlighted in black in figure 15)¹²⁹. The activation of the FXI zymogen takes place upon cleavage of the amide bond between the residues arginine 369 and isoleucine 370, which can be performed by FXIIa, by thrombin, or by FXI via autoactivation, in a reaction stimulated by polyanions^{129,131,132}. In the activated form, the two chains are kept together by a disulfide bridge between two cysteine residues found in the catalytic domain and in the apple four domain (Fig. 15)¹³³.



Figure 15. Structure of coagulation FXIa. The sequence, disulfide bridges and domains of the serine protease are shown. The apple domains are labelled as A1-4. Cysteines are shown in yellow and amino acids forming the catalytic triad in black. Important residues are labelled with colors, including orange – residues involved in interactions with thrombin, magenta - residues involved in interactions with high molecular weight kininogen, green - residues involved in interactions factor IX, with red - residues involved in interactions with polyanions (ABS: anion binding site), grey - residues involved in interactions with the receptor GPIb and blue - residues found at the dimer interface. Finally, sites of glycosylation are indicated with a diamond symbol. Reprinted with permission from¹²⁹, reprinting license number 4591411281031, copyright © 2018 Elsevier.

Under normal physiological conditions, FXIa circulates as a dimer, with the two monomers bound through a disulfide bridge between the cysteines 321 found in the apple four domains¹³⁴ and additionally held together by non-covalent interactions¹³⁵. The homodimer formation is unique within the coagulation proteases and it is conserved in several species^{129,136}.

FXI can form interactions with several molecules, including thrombin, HK, FIX, polyanions (whose binding enhances FXI activation) and the GPIb receptor found on platelets (leading to procoagulant and proinflammatory activity upon binding)¹²⁹. These interactions involve residues found mostly in the heavy chain (Fig. 15). FXIa activation of FIXa requires calcium and involves binding mediated by the apple three domain of FXIa, cleavage of a first bond (Arg145-Ala146), and finally cleavage of a second bond (Arg180-Val181)^{130,137}.

Patients with FXI plasma concentrations above the 90th percentile of the normal distribution had a risk two times higher than the population with lower values to develop VTE¹³⁸. In other studies, a connection between the risk of ischemic stroke and myocardial infarction with FXI levels has been observed, although FXI contribution to myocardial infarction is still debated^{139,140}. In addition, plasma levels of FXI in women taking hormonal contraceptives were found to correlate with risk of stroke¹²⁴. In parallel, a protective effect against cardiovascular events (stroke, transient ischemic attack, and myocardial infarction) and venous thromboembolism has been observed in patients with severe FXI deficiency¹⁴¹. A clinical proof of concept for FXI activity reduction as a new anticoagulation strategy has been achieved in 2016 in a small phase II clinical trial, when an antisense oligonucleotide targeting the synthesis of FXI proved to be efficacious in the prevention of thrombosis after total knee arthroplasty (even showing higher efficacy than enoxaparin) without bleeding side effects¹⁴².

Based on its biological role and on available clinical data, it is possible to identify many indications where molecules targeting FXI could be suitable alternatives to current drugs. These include primary VTE prophylaxis, thrombosis prevention in acute coronary syndrome,

atrial fibrillation, and end-stage renal disease patients. In addition, they could be applied for anticoagulation in extracorporeal circuits and in patients undergoing hemodialysis (HD)¹²⁷. Patients on HD would particularly benefit from a safer anticoagulation strategy, as cardiovascular events lead to 50% of mortality in this patient group¹²⁷. The pharmacological requirements of specific indications differ from each other (e.g. acute/chronic treatment, pharmacokinetic requirements). This suggests that various drugs based on different molecular formats might be useful to achieve an optimal therapeutic effect in different settings.

1.2.5 Coagulation factor XI-targeting molecules in development

Many strategies have been applied to date to target FXI. Developed molecules can be classified based on their molecular format and mode of action into mAbs, protein-based natural inhibitors, antisense oligonucleotides, small molecule active site inhibitors and small molecule allosteric inhibitors^{121,126,143,144}. An overview of drugs currently in clinical development is shown in Table 3.

Several mAbs have been developed and they present different modes of action. O1A6 (aXIMAb, binding the apple 3 domain) and MAA868 (binding the catalytic domain) block FXI activation as well as FXIa activation of FIX^{145–147}. AB023 (Xisomab 3G3) binds the apple 2 domain and blocks exclusively the activation of FXI by FXIIa^{148,149}. In addition, BAY-1213790 binds a region next to the active site and inhibits exclusively the active form of FXI^{150,151}. Many mAbs are currently in clinical development (Table 3). Protein-based natural inhibitors include Desmolaris, an inhibitor binding the active site derived from saliva of vampire bat¹⁵² and the Kunitz domain of protein nexin-2, an active site inhibitor derived from a physiological inhibitor of FXIa¹⁵³.

Table 3. Overview of FXI-targeting molecules currently in clinical development. The indication(s) for which the molecules have been tested in phase II studies are listed, where applicable. ASO: antisense oligonucleotide; mAb: monoclonal antibody; HD: hemodialysis.

Molecule	Molecular format	Company	Development stage	Indication(s)
IONIS-FXI _{Rx} (IONIS-416858)	ASO	IONIS Pharmaceuticals/ Bayer	Phase II	HD (NCT02553889) (NCT03358030) Total knee replacement (NCT01713361)
IONIS-FXI-L _{Rx}	ASO	IONIS Pharmaceuticals/ Bayer	Phase I	-
BAY1213790	mAb	Bayer	Phase II	Total knee replacement (NCT03276143)
AB023	mAb	Aronora Inc.	Phase II	HD (NCT03612856)
MAA868	mAb	Novartis/ Anthos Therapeutics	Phase I	-
				HD (NCT03000673)
BMS-986177	Small molecule	BMS/Janssen	Phase II	Total knee replacement (NCT03891524) Acute Ischemic Stroke/Transient Ischemic Attack (NCT03766581)
EP-7041	Small molecule	eXIthera	Phase I	-

Antisense oligonucleotides targeting FXI include IONIS-416858 (also IONIS-FXI_{Rx}), which has been mentioned before as the first FXI-targeting molecule investigated in a clinical proof of concept study^{142,144,154}. In this study, IONIS-416858 was found to reduce FXI levels in a dose-dependent manner and to safely prevent VTE after total knee replacement¹⁴². IONIS-416858 is currently being tested in another phase II clinical study (Table 3). In addition, IONIS-FXI-L_{Rx}, a “ligand conjugated antisense (LICA)” version of IONIS-FXI_{Rx}, that should

allow more specific targeting of the ASO to liver cells, is also in clinical development.

Several small molecules targeting FXI have been developed. The active site inhibitors include BMS-986177, an oral inhibitor of FXIa currently in clinical development¹⁴⁴, BMS-262084, an irreversible inhibitor¹⁵⁵, BMS-962212, a parenterally-delivered inhibitor¹⁵⁶, EP-7041, a parenteral inhibitor currently in clinical development¹⁵⁷ and ONO-5450598, an oral inhibitor¹⁵⁸. Allosteric inhibitors include sulfated pentagalloylglucoside, which binds charged residues on the catalytic domain of FXIa¹⁵⁹. Finally, also FXI-targeting aptamers have been developed¹⁶⁰.

Drugs based on ASOs, mAbs, and aptamers, in contrast with many small molecules, cannot be administered orally. Another disadvantage of ASOs is their delayed onset of action (up to 3-4 weeks to reach FXI levels within the therapeutic range¹⁶¹), which makes them unsuitable for the application in acute therapies¹⁴⁴. All the other mentioned formats, instead, present a fast onset of action. In addition, the prolonged half-life of mAbs and ASOs might be of concern in case of bleeding complications upon surgery or trauma¹²⁷. Finally, the renal clearance, less predictable PK profiles, and potential toxic metabolites of small molecules make them a riskier modality for clinical development. Thus, all molecules currently in development have strengths and weaknesses. As mentioned previously, the various indications where the application of an FXI-targeting anticoagulant could be beneficial can present different therapeutic requirements. Therefore, certain molecular formats might be more suitable for specific indications than others.

2 Aim of this work

Anticoagulants are a drug class used for the treatment and prevention of thrombosis. Although efficacious, they present a major limitation being the risk of severe bleeding, a life-threatening condition. Thus, there is a strong unmet need for safer agents. Coagulation factor XI (FXI) has been identified as a promising target, as several studies have shown that it is involved in the pathogenesis of thrombosis, while not playing an essential role in hemostasis. Many FXI-targeting molecules are currently in development but none of them is based on peptides. Peptides promise to be a suitable modality for targeting FXI as they combine high affinity and selectivity with tunable pharmacokinetic properties, a fast onset of action and absence of toxic metabolic products.

The general aim of my thesis was to develop cyclic peptide-based FXIa inhibitors for safer anticoagulation.

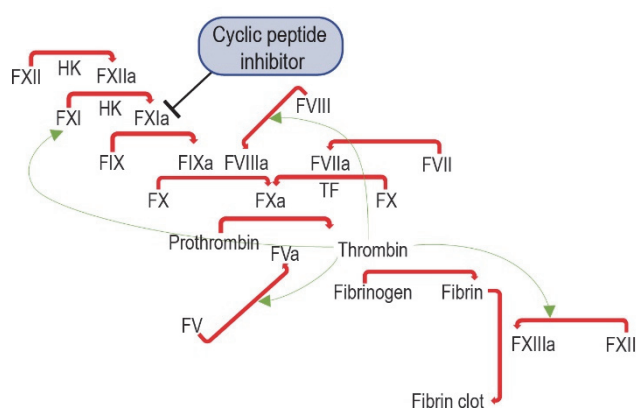


Figure 16. The aim of this thesis was the development of cyclic peptide inhibitors targeting FXIa.

I planned to generate molecules that fulfill specific requirements necessary for their application as anticoagulants, including high potency (in terms of inhibitory activity and anticoagulation effect), high selectivity, cross-reactivity with FXIa from model animals, and a

suitable pharmacokinetic profile. Towards this end, the first goal was to generate a phage display library of cyclic peptides that is larger and structurally more diverse than existing libraries. The new library should maximize the chance of identifying FXIa inhibitors with the desired properties. Subsequently, the library was planned to be screened against FXIa and the isolated binders characterized in terms of inhibitory activity and *ex vivo* anticoagulation effect. The pharmacological properties of the best hit(s) were intended to be improved, with a special focus on the extension of the elimination half-life and on stability, with the aim to confer drug-like properties to the cyclic peptide and to achieve a half-life of at least a day in humans. Finally, the optimized molecule was intended to be tested for anticoagulation efficacy *ex vivo* and *in vivo* in order to assess its therapeutic potential.

3 Generation and screening of a structurally diverse 100-billion cyclic peptide phage display library

This chapter is based on a manuscript that will be submitted for publication. I will be the only first author in this publication.

3.1 Abstract

Cyclic peptides generated by phage display offer attractive properties for drug development, including high binding affinity and selectivity, low inherent toxicity, good stability, and ease of production. The success of phage display selections depends critically on the size and structural diversity of the libraries. The generation of large libraries is currently hampered by various challenges in cloning library DNA and by the difficulty in transforming the DNA into bacterial cells. In this work, we have succeeded in generating a phage display library comprising 100 billion (bi)cyclic peptides which is > 10-fold larger than previously reported libraries. Building such a high diversity was achieved by generating library DNA by whole plasmid PCR as well as by using a small vector that facilitated bacterial transformation. The library is based on 273 different peptide backbones and thus has a skeletal diversity that is substantially larger than previously developed libraries. Panning of the peptide repertoire against a protein target led to the enrichment of peptides with specific backbone formats, long consensus sequences of more than 10 amino acids, and nanomolar binding affinities, demonstrating the benefits of screening larger and structurally highly diverse libraries.

3.2 Introduction

Cyclic peptides are an attractive modality for the development of therapeutics thanks to their ability to bind with high affinity and selectivity to protein targets, their low inherent toxicity, their relatively high stability, and their ease of production by solid-phase peptide synthesis. Currently, more than 40 cyclic peptides derived from nature or derivatives thereof are used as drugs, and more than 100 cyclic peptides are in pre-clinical or clinical development¹³. Several of the cyclic peptides in development were isolated by screening large combinatorial libraries of peptides by display techniques such as phage display or mRNA display^{26,28,162}. In phage display, the peptides are displayed on the surface of phage as fusion with a coat protein and are encoded by DNA packed in the phage particle. The efficient and correct coupling of pheno- and genotype achieved by phage display allows for identification of binders in only two or three iterative rounds of phage selection. The high stability of filamentous phage (high temperature, detergents, redox reagents, organic solvents) allows for the selection in presence of particular conditions, such as proteases (to eliminate unstable peptides). Protocols for phage library production and panning are robust and can be applied by non-specialists.

The most critical parameters in the phage display selection of cyclic peptides are the size and structural diversity of the library used. For easy targets such as proteins that bind to short, linear peptides (e.g. integrins to Arg-Gly-Asp peptides, streptavidin to His-Pro-Gln peptides), peptide ligands can be isolated from small libraries of a few thousands to a million different peptides. However, for the development of cyclic peptides to challenging targets, much larger libraries are needed. A large library size is also important for the selection of peptides that fulfill, in addition to binding to a target, additional qualities such as high stability or binding to multiple targets (e.g. binding to the human and mouse homologue of a protein). Since the innovation of phage display in the 1980's, several different cyclic peptide phage display libraries were reported, wherein the size and complexity has gradually increased. The first

libraries reported included peptides containing two flanking cysteines that cyclized upon disulfide bond formation^{43–47}. Later, linear peptides containing three cysteines were cyclized by reaction with chemical linkers containing three thiol-reactive groups, such as 1,3,5-tris(bromomethyl)benzene, to generate bicyclic peptides that could engage with targets through two peptide loops^{51,53,57}. Most recently, we reported bicyclic peptides by chemically bridging two pairs of cysteines in peptides containing four cysteines⁶⁰. The largest library of cyclic peptides contains 1×10^{10} peptides⁴⁶, the bicyclic peptide library 4×10^9 ⁵¹, and the largest library of double-bridged peptides comprises 8.5×10^9 different peptides (Kong *et al.*, unpublished data).

The difficulty in generating large phage display libraries is stemming from two experimental steps, the first one being the generation of phage DNA vectors coding for a large number of different peptides, and the second one being the transfer of vector DNA into many bacterial cells. Phage DNA coding for random peptides is typically cloned by cassette mutagenesis, ligating double-stranded DNA coding for the peptides into a phage vector opened by restriction enzymes. A challenge with this cloning strategy is the generation of fully opened vector and the correct ligation of vector and insert. We had recently adapted a strategy based on whole vector PCR for the efficient cloning of peptide phage display libraries (Kong *et al.*, unpublished data). With this approach, the entire phage vector is copied in a long PCR wherein the DNA coding for the peptide library is appended through a degenerated primer. Vector production through plasmid preparation is thus fully bypassed and the ligation is efficient as the vector needs only to be ligated at one site by "self-ligation". The second challenging step in the library construction, the transformation of vector DNA into bacterial cells, is difficult because the cell membrane needs to be broken sufficiently to allow entry, but not too excessively to ensure survival of the cells. Even with the most optimized transformation protocols, only a small fraction of the vector DNA is delivered into the cells. In this work, we set out to generate a cyclic peptide phage display library of unprecedented size, measured by the number of different peptide sequences it includes, and structural

diversity, given by the number of different cyclic peptide backbones. We speculated that a larger quantity of phage vector may be generated if we apply the recently adopted protocol for whole plasmid PCR to a phagemid vector, which is substantially smaller than a phage vector (around 5 kbases vs. around 9 kbases). Firstly, PCR amplification of a 5 kbase vector was expected to yield more and better-quality PCR product. Secondly, the circularization of a shorter linear DNA should be more efficient. Another advantage of using a smaller DNA vector is that it can be electroporated more efficiently into bacterial cells than a larger vector.

3.3 Results and discussion

3.3.1 Design of a cyclic peptide library with high backbone diversity

We designed a peptide library of the format $\text{XC(X)}_m\text{C(X)}_n\text{C(X)}_o\text{CX}$ (X = any amino acid, C = cysteine, $m + n + o = 12$), in which all peptides contain four cysteines and have a length of 18 amino acids (Fig. 17a). The first and last cysteines were kept in fixed positions (2nd and second last amino acid; red in Fig. 17) and the positions of the middle two cysteines (orange in Fig. 17) were varied in a combinatorial fashion. In this way, the four cysteines could be positioned in the peptides in 91 different ways (Fig. 17b). Upon bridging of two pairs of cysteines by disulfide formation or reaction with two chemical linkers, that is possible in three different ways (Fig. 17a), 273 different bicyclic peptide formats, characterized by different numbers m , n and o of random amino acids X in the three segments spaced by the four cysteines, could be generated. The skeletal diversity of this library was much larger than those of previously developed phage display peptide libraries (Fig. 17c). For example, it was 9 to 11-fold larger than in the two "double-bridged" peptide libraries reported before (3x3: 24 backbones; 4x4: 30 backbones)⁶⁰. Peptides in which the Cys1 and Cys2, and Cys3 and Cys4 are bridged can also be regarded as monocyclic peptides as the two macrocyclic rings are spaced by a linear peptide having a length of n amino acids. This would mean that each peptide can be cyclized to two bicyclic configurations and two monocyclic configurations, yielding four structures that can be sampled for binding to protein targets. We chose to display the peptides on filamentous phage as fusion of the coat protein 3 (pIII) as in most of the phage peptide libraries developed before^{42,54,163}. The peptide library and the pIII were spaced by a Gly-Ser-Gly linker.

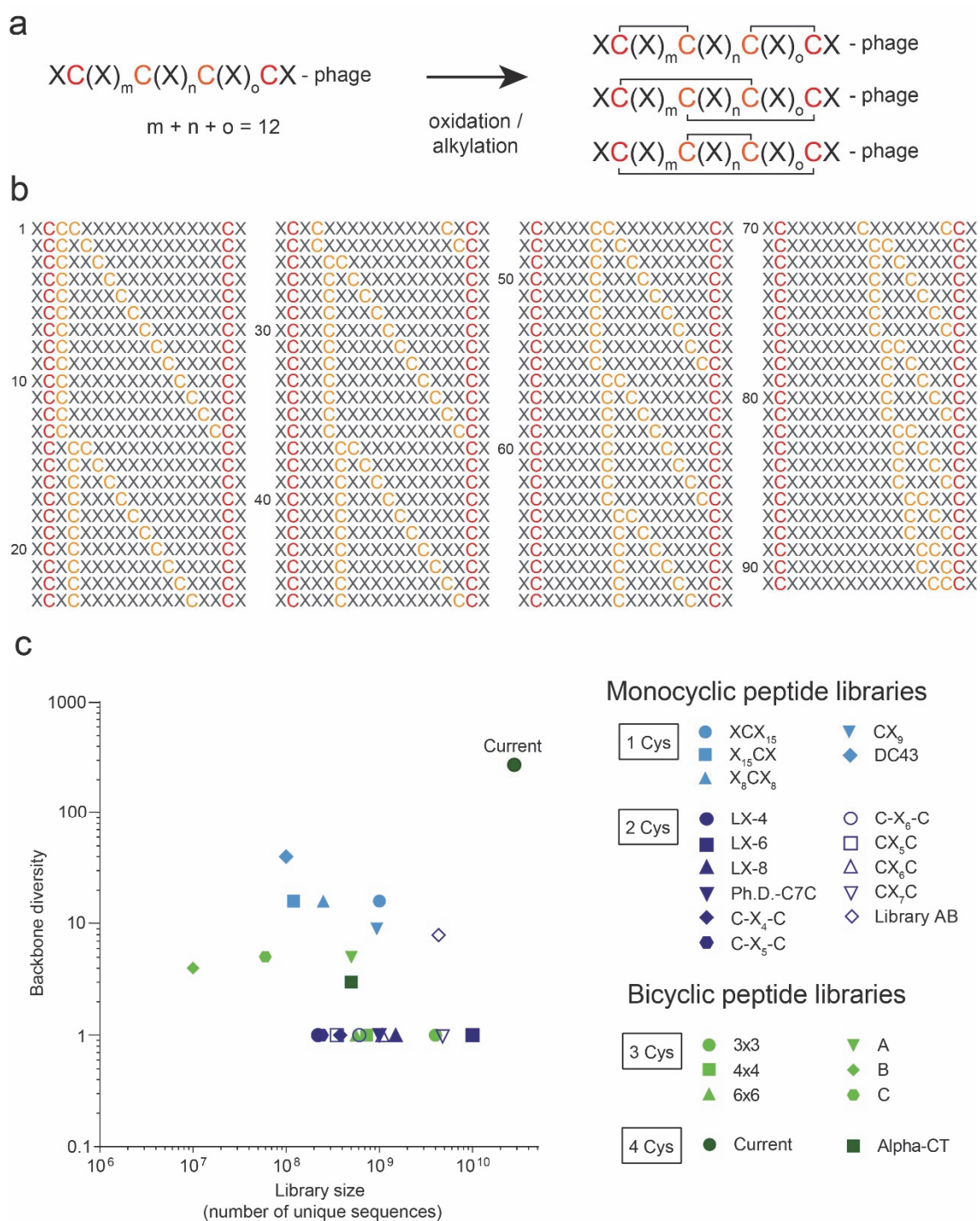


Figure 17. Cyclic peptide phage display library format and size comparison. a) Format of peptide library containing four cysteines (C) and 14 random amino acids (X). Bridging of two pairs of cysteines by disulfide bridges or chemical linkers yields bicyclic peptide formats. The first format shown can be suited to potentially identify ligands based on monocyclic peptides. b) Positions of the four cysteines in the peptide library. The two cysteines at the ends are kept in constant positions (in red) and the positions of the two middle cysteines (in orange) are varied to achieve 91 formats. c) Size and backbone diversity of previously reported cyclic peptide phage display libraries are compared to the new library.

3.3.2 Whole plasmid PCR of phagemid vector enables generation of large library

We inserted DNA encoding the random peptide sequences into a phagemid vector due to the around 2-fold smaller size (around 5 kbases) in comparison to a phage vector. As described above, this strategy promised a more efficient production and transformation of the DNA library. Phagemid vectors code for only the phage coat protein pIII, which means that bacterial cells need to be co-infected with a helper phage that codes for all other essential phage proteins to enable phage production³⁷. We cloned the DNA library by whole plasmid PCR as previously described (Kong *et al.*, unpublished). DNA coding for the random peptides was appended to the phagemid DNA of vector pSEX81 in a PCR reaction using forward degenerate primers that annealed at the start of the pIII gene (Fig. 18a). Both, the forward and the reverse primers contained an identical endonuclease restriction site (*NcoI*) that allowed for circularization of the vector by self-ligating sticky ends, to yield the library vector (Fig. 18b).

Linear vector synthesis by PCR of the 5 kbase DNA was much more efficient than the PCR amplification of a phage vector that needed optimization and use of a particularly performant DNA polymerase (Kong *et al.*, unpublished). For each one of the 91 degenerate primers used (Supplementary Table 1), we performed a separate PCR reaction and purified the products by agarose gel electrophoresis and DNA extraction. At this point, we combined the PCR products of multiple PCR reactions in 10 groups (Supplementary Table 2), digested the ends with *NcoI*, circularized the vector with T4 ligase and transformed the product into electrocompetent TG1 *E. coli* cells. The cells were plated on 2YT/ampicillin agar plates, grown overnight, resuspended, pooled and stored as a single glycerol stock. In parallel, samples of cells transformed with the 10 different DNA pools were serially diluted, plated, and the number of transformed cells calculated. The number of cells transformed with the 10 pools ranged from 1.47×10^9 to 4.25×10^9 (Supplementary Table 3) and the total number was 2.8×10^{10} . Assuming that all these transformed cells can produce phage with a different peptide, and that each peptide can be cyclized into two bicyclic peptides (double bridged) or two

monocyclic peptides (each singly bridged), the diversity of (bi)cyclic peptides generated is around 100 billion.

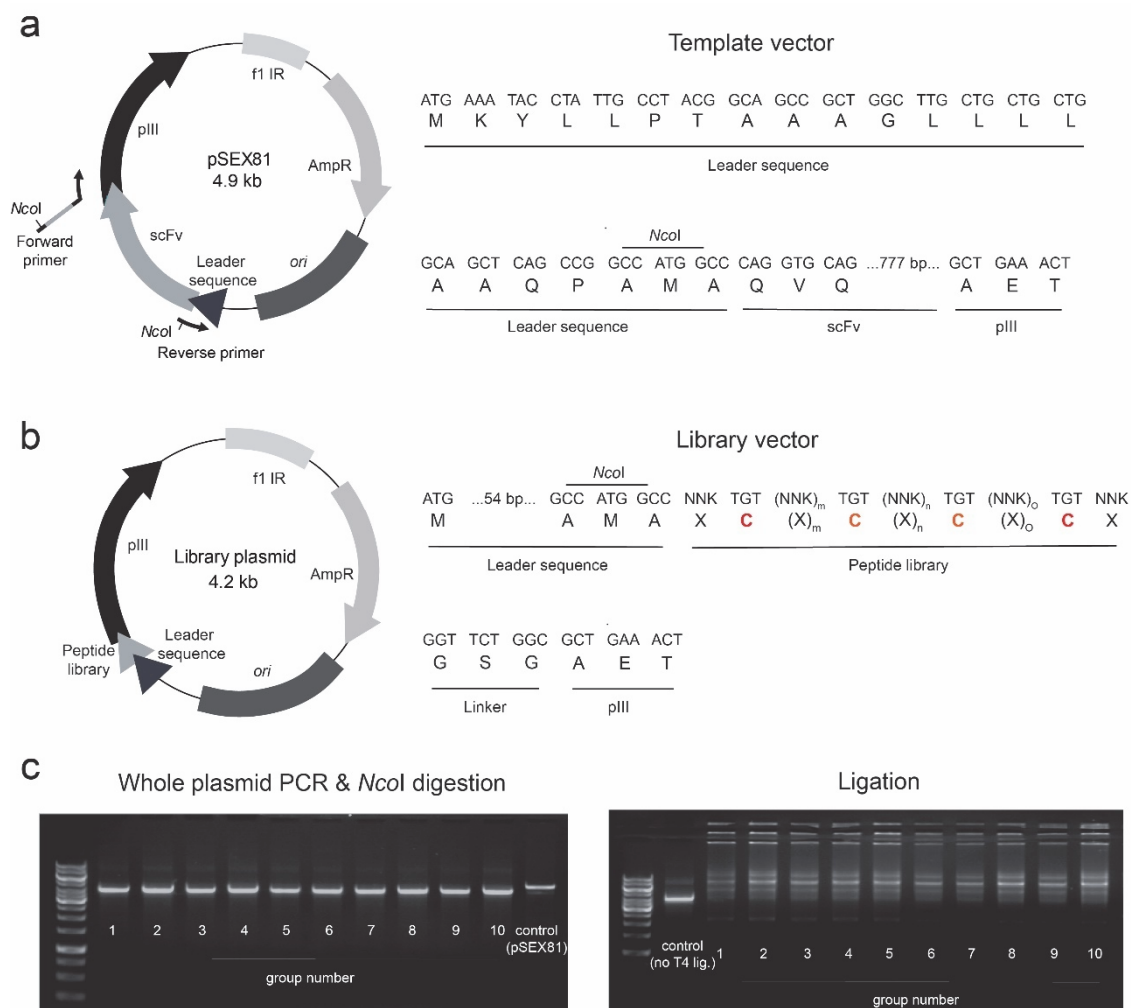


Figure 18. Cloning of the 100 billion cyclic peptide phage display library by whole plasmid PCR. a) Phagemid vector used as template for the whole plasmid PCR. The degenerated primer (forward) adding the random peptide sequences and the reverse primer, and their annealing sites are indicated. Both primers contain an *NcoI* cleavage site that allows for generation of sticky ends and efficient circularization by self-ligation. b) Library plasmid. c) PCR products obtained with the 91 different degenerated primers were purified by agarose electrophoresis, extracted, pooled in 10 groups, digested with *NcoI*, purified and analyzed before (left gel) and after ligation with T4 ligase (right gel).

Sequencing of 192 clones, and thus around 19 for each of the 10 transformed DNA pools, showed that most of the vectors contained DNA sequences that coded for the desired peptide formats (Supplementary Fig. 1). 56% of the library contained exactly four cysteines. 2 % of

the peptides contained four cysteines but a peptide format that was not foreseen in the library design but was generated due to random errors that occur in the synthesis of the degenerated DNA primers. This latter group of peptides increased additionally the structural diversity of the cyclic peptide library.

3.3.3 Phage need to be produced in large cultures to cover most of the library diversity

We produced phage in a large culture volume of one liter in order to ensure that most of the peptides encoded by the library were produced. The library glycerol stock was inoculated in the medium to reach an OD₆₀₀ of 0.1, yielding a total of 2.5×10^{10} viable cells, as determined by plating of 10-fold serial dilutions of the culture. This number was slightly below the library size of 2.8×10^{10} but was considered as just sufficient to represent the vast majority of the peptides in the library. We grew the cells, and at an OD₆₀₀ of 0.5 we infected them with 10^{12} hyperphage, a type of helper phage that does not code for the coat protein pIII and leads to production of phage that display multiple copies of the peptides⁴⁰. The number of cells infected with hyperphage was around 2.5×10^{10} , which was again at the lower limit that could be tolerated to cover a large fraction of peptides in the library.

3.3.4 Phage panning experiments reveal importance of the backbone diversity

Incubation of the culture overnight yielded around 10^{13} phage after PEG purification, which meant that each peptide was represented 400 times on average. We distributed the phage into two tubes and cyclized the peptides either by disulfide formation or by reaction with the alkylating reagent 2,6-bis(bromomethyl)pyridine (BBMP). The two phage libraries were individually subjected to three rounds of phage selection against coagulation factor XIa immobilized on magnetic streptavidin beads, a target that has received much interest due to its role in thrombosis^{127,128}. We performed in parallel selections on beads

without immobilized target, to assess if FXIa-specific phage peptide were enriched. Indeed, 35-fold and 7-fold more phage were isolated in the third rounds of selection with the library cyclized by disulfide bridges and chemical linker, respectively (Supplementary Fig. 2), indicating successful selection of FXIa-specific cyclic peptides. After the third round of selection, we sequenced 144 clones from each of the two libraries and analyzed, based on the positions of the cysteines, which peptide formats were enriched (Fig. 19a). In the selection with disulfide cyclized peptides, one of the 91 peptide formats was strongly enriched and in the selection with BBMP-cyclized peptides, two formats were strongly enriched. This finding showed that peptides with specific cysteine spacing patterns, and thus specific peptide backbones, were particularly suited to generate binders to the target. At the same time, this finding underscored the importance of incorporating a large skeletal diversity in the cyclic peptide libraries as it is not known a priori which format will eventually yield binders.

3.3.5 Isolated peptides display long consensus sequences

Comparison of the enriched peptides revealed strong consensus sequences (Fig. 19b). In the selection performed with the disulfide-cyclized peptide library, the peptides could be assigned to three slightly different consensus groups wherein the first two groups were rather similar (Fig. 19b, left). In the selection with BBMP-cyclized peptides, two consensus sequences were identified, that shared some similarity in the core sequences but differed in the positions of the two middle cysteines. Compared to phage selections with smaller peptide libraries^{53,164,165}, the identified consensus sequences were significantly longer. Most impressive was the first consensus sequence of the BBMP-cyclized peptides, in which several peptides shared identical amino acids in as many as 9 positions, not including the two cysteines in the middle for which the positions were varied too.

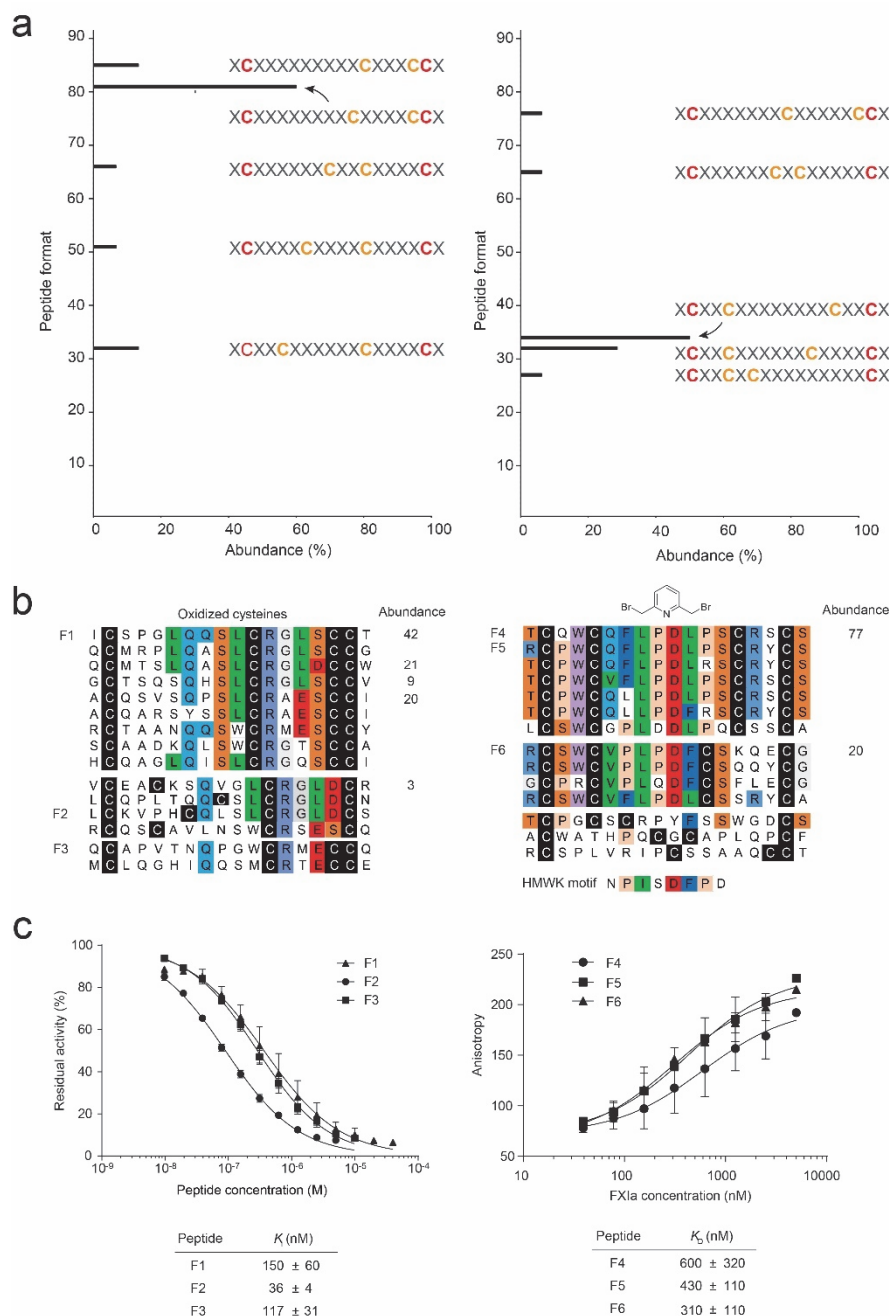


Figure 19. Cyclic peptides isolated in phage selections against coagulation factor XIa. a) Abundance of peptide formats after three rounds of phage selection. The left graph shows peptides isolated from a library that was cyclized by disulfide bridges and the right graph shows peptides isolated after cyclization with the chemical linker BBMP. The abundance was calculated by dividing the number of different peptides having the same cysteine positions by the total number of different peptides. b) Sequences of peptides isolated against FXIa. Peptides with similar sequences were aligned and identical amino acids are highlighted in color. The abundance of each peptide is indicated. c) Binding affinity and inhibitory activity of six peptides F1 to F6 shown in b). The peptides were chemically synthesized, cyclized by disulfide formation (left) or alkylation with BBMP (right), HPLC purified and their activity tested. The left graph shows inhibition of FXIa with a chromogenic substrate. The right graph shows binding of the fluorescein-labeled peptides measured by fluorescence polarization. Mean values and SD are shown and K_i and K_D values are indicated.

3.3.6 Bicyclic peptides bind FXIa with high affinity

We synthesized three peptides from each selection, purified them by HPLC and tested if they inhibit the catalytic domain of FXIa, being a trypsin-like serine protease. All three peptides of the selection with disulfide-cyclized library (F1, F2, F3) inhibited the protease, the best one being F2 with a K_i of 36 ± 4 nM (Fig. 19c, left panel). The three peptides pulled out of from the BBMB-cyclized library did not inhibit FXIa (results now shown) and we therefore tested if they bind to a site on FXIa that does not affect the proteolytic activity. Toward this end, we synthesized the peptides with fluorescein linked to the N-terminus and tested the binding to the coagulation factor. All three peptides were binding with affinities in the high nanomolar range (Fig. 19c, right panel). A comparison of the long consensus sequence with the amino acid sequence of the FXI binding protein high-molecular weight kininogen (HK or HMWK) revealed a striking similarity (Fig. 19b; amino acids 601-608 in HK uniprot entry “KNG1_HUMAN”), suggesting that our bicyclic peptides are binding to the same epitope on one of the apple domains of FXI.

3.4 Conclusions

We managed to generate a peptide phage display library that contains as many as 100 billion different mono- or bicyclic peptides. In previous work, we were never able to generate such a large library, despite enormous efforts in upscaling vector DNA production and electrocompetent cell production. Key for obtaining the around 10-fold larger library was twofold, namely the use of a different strategy for producing the library DNA by whole plasmid PCR, and the use of a smaller vector that facilitated the PCR-amplification of the DNA as well as the transformation of the DNA into cells. While we have applied this strategy for cloning peptide libraries, it might equally well be used for the production of antibody phage display libraries, wherein antibody genes are used as extra-long primers for the whole plasmid PCR.

In addition to increasing the size of the library, we have also achieved a substantial enlargement of the structural diversity by designing the library in a way that it codes for peptides in which the positions of the four cysteines are distributed in 91 different ways. Upon cyclization, this yields the large number of 273 different bicyclic peptide formats and thus a skeletal diversity that is substantially larger than that of previous libraries. In case that the two first and two last cysteines are connected by disulfide bridges or linkers, two monocyclic peptides separated by an amino acid linker are generated, allowing for the screening of monocyclic peptide libraries. In the present work, we have cyclized the peptides by forming two disulfide bridges or alkylation with one chemical linker that contains two thiol-reactive groups. Given the large number of commercial bis-electrophile reagents that can be used to connect pairs of cysteines, even larger libraries can be generated. For example by cyclizing the library with ten bis-electrophile reagents, a library comprising a diversity of a trillion (!) different cyclic peptides may be generated.

The advantages of a larger and structurally more diverse library became evident when we were panning the pool of (bi)cyclic peptides against a first target being coagulation factor XIa. Firstly, peptides with cysteines in specific positions, and thus specific backbones, were strongly enriched, which showed that it was important to cover a large skeletal diversity. Secondly, the consensus sequences identified were longer than those found in selections with smaller libraries. Such long sequences can only be obtained if a sufficiently large sequence diversity is present in the library. And thirdly, the isolated bicyclic peptides bound with nanomolar affinity to the protein target.

Given the record size of the library of around 100 billion bicyclic peptides, its enormous structural diversity, covering 273 different backbones, and the successful isolation of tight binders with long consensus sequences, it is likely that it will yield good binders to many more protein targets in the future.

3.5 Material and methods

Library generation

The primers used for library construction are shown in the Supplementary Information (Supplementary Tab. 1). The library was constructed by inserting DNA sequences encoding the peptides and a Gly-Ser-Gly linker in the phagemid pSEX81 (Progen). The peptide format was Xaa-Cys-(Xaa)_m-Cys-(Xaa)_n-Cys-(Xaa)_o-Cys-Xaa, with $m + n + o = 12$ amino acids and a total peptide length of 18 amino acids. The DNA sequences were incorporated upstream to the pIII gene through a whole vector PCR reaction. The DNA encoding the random peptides (in bold), the GSG linker (in italic) and the restriction site for the enzyme *NcoI* (underlined) were appended using forward primers with the following format:

5'-

AGCGCCATGGCCNNK**TGT(NNK)mTGT(NNK)nTGT(NNK)oTGTNNKGGTTCTGGCGCTGAA**ACTGTTGAA
AGTTGTTTAGC-3'.

The 3' end of forward primers annealed with the 5' end portion of the gene encoding for pIII. The reverse primer had the sequence

5'-CATGCCATGGCCGGCTGAGCTGCC-3'

and annealed to the pelB leader sequence on pSEX81, which includes a restriction site for the enzyme *NcoI* (underlined). 91 separate PCR reactions were performed (one for each forward primer). The total reaction volume was 30 µl and contained one of the forward primers each (600 nM), the reverse primer (600 nM), dNTP mix (200 µM) (Axon Lab AG), 30 ng of pSEX81 template (Progen), 6 µl of 5x Phusion buffer (ThermoFisher Scientific) and four units of Phusion polymerase (ThermoFisher Scientific). The following PCR program was used: 2 min at 95 °C, 30 cycles of 30 s at 95 °C, 50 s at 60 °C and 4 min at 72 °C, and final elongation for 7 min at 72 °C. The PCR reaction lead to the exclusion of the ScFv gene found on pSEX81 and the incorporation of the peptide library. The PCR products were purified by electrophoresis

on a 1% agarose gel in TAE buffer with 1 mM guanosine, gel extracted using a kit (QIAquick gel extraction kit, Qiagen) and the products were pooled in 10 separate groups. DNA from each group was then digested with *NcoI* as follows: 10 µg of the PCR product and 50 µl of 10X Tango buffer (ThermoFisher Scientific) were diluted to 490 µl with ddH₂O. *NcoI* was added (100 units, 10 µl) (ThermoFisher Scientific), the reaction was incubated for 3 h at 37° C in a water bath. The digested DNA was purified using a commercial kit (QIAquick gel extraction kit, Qiagen) and then self-ligated in a reaction with 50 µl 10X T4 DNA ligase buffer, 250 Weiss units of T4 ligase (ThermoFisher Scientific) and ddH₂O up to a final volume 500 µl. The reaction was incubated at 25° C for 4 h. Ligase inactivation was performed by incubating the tube at 65° C for 10 min. Subsequently, ligated DNA was purified using a commercial kit (QIAquick gel extraction kit, Qiagen) and eluted from the columns using ddH₂O. DNA was electroporated into commercial *E. coli* TG1 cells (Lucigen). 25 µL of cells were electroporated with 3 µg of DNA of each group separately. After electroporation, 2 ml pre-warmed commercial recovery medium (Lucigen) were added to the cells and finally incubated at 37° C for 1 h with shaking (200 rpm). Cells were plated on 20 large (20 cm diameter) 2YT/ampicillin (100 µg/ml) plates. Plates were incubated at 30°C overnight. The library size was determined by plating cell dilutions on 2xYT/ampicillin agar plates. Electroporation of the DNA into TG1 *E. coli* cells yielded 2.8×10^{10} colonies. Colonies were collected from the plates with 2YT medium/20% v/v glycerol and stored at -80° C. 192 library clones were sequenced by Sanger sequencing (Macrogen) to evaluate the library quality.

Phage production

Library glycerol stocks were inoculated to reach an OD₆₀₀=0.1 in 1 L 2YT/ampicillin (100 µg/ml) culture with 100 mM glucose. Serial dilutions of the starting culture were plated on 2YT/ampicillin (100 µg/ml) plates in order to assess the number of viable cells in the culture. The culture was grown at 37° C until it reached OD₆₀₀=0.5. Serial dilutions of the culture were plated on 2YT/ampicillin (100 µg/ml) plates. The culture was then infected with hyperphage

M13 K07ΔpIII (Progen Biotechnik GmbH) at a multiplicity of infection (MOI) of 10 and incubated for 20 min at 37° C (no shaking). The culture was then incubated at 37° C for 45 min with 200 rpm shaking. Serial dilutions of the infected culture were plated on 2YT/ampicillin (100 µg/ml) + kanamycin (50 µg/ml) plates in order to determine the fraction of infected cells. Cells were then pelleted at 2000 g for 20 min at 4° C and finally resuspended in 1 L of 2YT/ampicillin (100 µg/ml) + kanamycin (50 µg/ml) medium. The culture was then grown at 30° C overnight with shaking (250 rpm). Cultures were pelleted at 4500 g at 4° C for 20 min and the supernatant was kept. A supernatant sample was taken. Phage precipitation was performed by adding 250 ml (25% of the volume) of cold PEG/NaCl solution (20% PEG-6000 (w/v), 2.5 M NaCl) and inverting the bottle, followed by incubation for 45 min on ice. Phage were then centrifuged at 9000 g for 45 min at 4° C. The phage pellet was re-suspended in 20 ml degassed reaction buffer (20 mM NH₄HCO₃, 5 mM EDTA, pH 8.0). Phage precipitates and remaining cells were removed by centrifugation at 5000 g at 4° C for 15 min and the supernatant was kept. A sample was kept. The stored phage samples were used to determine phage titers by performing serial dilutions in 2YT medium and using them to infect 180 µL of E. coli TG1 cells (OD₆₀₀ = 0.5). 20 µL of cells infected with the different phage dilutions were plated on 2YT/ampicillin (100 µg/ml) plates and CFUs were counted. Phage titers were determined at all crucial steps of the process (before and after reduction, cyclization and panning).

Cyclization of cysteines on phage

The purified phage was split into two separate tubes. One of the samples was not further processed (oxidized cysteine residues), while in the other sample the cysteine residues of the peptides were reduced by adding 1 mM TCEP and incubating it for 30 min at 25° C. Phage precipitation was performed by PEG/NaCl precipitation (see above). The tube was incubated 15 min on ice and phage pelleted as described before. Phage were resuspended in 9 ml of reaction buffer. A sample was stored at 4° C for phage titer determination. The chemical

linker (2,6-bis(bromomethyl)pyridine) was added at 40 μ M (final conc.) and the reaction incubated at 30° C for 1 h. Phage were again precipitated and finally the phage pellet resuspended in 10 ml binding buffer containing BSA and Tween 20 (10 mM Tris-Cl, 150 mM NaCl, 10 mM MgCl₂, 1 mM CaCl₂, 0.1 % v/v Tween 20 and 1 % w/v BSA, pH 7.4) and stored at 4° C. A sample was stored for phage titer determination.

Biopanning

Human activated coagulation factor XI (FXIa) (Molecular Innovations) was biotinylated by incubating 0.2 mg of protein at 10 μ M with 100 μ M EZ-Link™ Sulfo-NHS-LC-Biotin (10-fold molar excess, ThermoFisher Scientific). The reaction was incubated at room temperature for 1 h. The protein was separated from the unreacted reagent using a PD-10 column (GE Healthcare). 5 μ g of biotinylated target protein were incubated with 50 μ L magnetic streptavidin beads (Dynabeads® M-280 Streptavidin, ThermoFisher Scientific, Waltham, MA, USA) in 500 μ L binding buffer for 10 minutes and non-immobilized protein was removed by washing three times. Beads were then resuspended in 300 μ L binding buffer with BSA and Tween 20 and incubated on a rotating wheel at room temperature for 30 min. Beads were then added to each modified phage and incubated 30 min at 10 rpm on a rotating wheel. Unbound phage were removed by washing the beads with binding buffer (10 times) and the tube was changed once in between the washes. Finally, beads were resuspended in 100 μ L of 20 mM glycine, pH 2.2, and incubated 5 min in order to elute the phage. The solution was neutralized by adding 100 μ L of 1 M Tris/HCl, pH 8.0 and added to 10 ml of *E. coli* TG1 cells at OD₆₀₀ = 0.5. After incubation at 37 °C for 30 min, the freshly infected bacteria were plated on 2YT/ampicillin (100 μ g/ml) plates and grown overnight at 37 °C. In addition, phage titers were also determined. Bacterial cells of the colonies grown overnight were recovered in 2YT medium and 20 % glycerol, flash-frozen and stored at -80 °C. Streptavidin- and neutravidin-coated magnetic beads were alternated in the rounds of selection in order to prevent the selection of bead coat protein binders. Neutravidin-coated beads were produced according to

the manufacturer's recommended protocol (Dynabeads M280 Tosylactivated, Invitrogen Dynal Biotech AS). After three rounds of phage selection, 144 clones per condition were sequenced by Sanger sequencing (Macrogen) and resulting sequences were grouped based on similarity into consensus sequences.

Chemical synthesis of peptides

Solid phase peptide synthesis (SPPS) was performed using Fmoc-chemistry, DMF as solvent and rink amide AM resin. Peptides were synthesized in a 30 μ mol scale. Amino acids were coupled twice (4 eq.), using HATU (4 eq.), and NMM (8 eq.) and each coupling was performed at RT for 45 minutes. After the coupling reaction, seven washing cycles with DMF were performed. N-terminal amines remained free after coupling were capped using acetic anhydride (5% v/v) and lutidine (6% v/v) at RT for 30 minutes. Seven washing cycles were again performed. Fmoc deprotection was performed using piperidine (20% v/v) at RT, 2 times for 5 min. Seven washing cycles were performed. Cleavage of peptides was performed with a standard cleavage cocktail (90% TFA, 2.5% thioanisole, 2.5% H₂O, 2.5% 1,2-ethanedithiol, 2.5% phenol). 10 ml of cleavage cocktail were added to each peptide and incubated for 3 h while shaking. Peptide-containing solution was collected by vacuum filtration and peptides were then initially purified by cold ether precipitation. 50 ml of ice-cold diethyl ether were added to the peptides, incubated 30 min at -20 °C and then centrifuged at 2700 g for 5 min. Peptide pellets were washed another time with 35 ml of diethyl ether and centrifuged again to remove remaining diethyl ether.

Peptide purification by HPLC

Peptides were resuspended in DMF (0.5 ml), acetonitrile/0.1% TFA v/v (1.5 ml) and ddH₂O/0.1% TFA v/v and purified by RP-HPLC (Prep LC 2535 HPLC, Waters) on a C18 column (Sunfire prep C18 TM ODB, 10 μ m, 100 Å, 19 × 250 mm, Waters) at 20 ml/min flow rate, using ddH₂O/0.1% TFA v/v (solvent A) and acetonitrile/0.1% TFA v/v (solvent B) as

solvents and a linear gradient of solvent B over solvent A. The mass of peptides contained in the collected fractions was analyzed by ESI-MS on a single quadrupole LCMS (LCMS-2020, Shimadzu) in positive ion mode. Peptides were then lyophilized.

Peptide cyclization

For cyclization with the alkylating reagent, linear peptides were dissolved in 8 ml reaction buffer (60 mM NH_4HCO_3 , pH 8.0) and 2 ml acetonitrile to obtain a concentration of 1 mM. Linker was added to a final concentration of 4 mM and the reaction was incubated for 1 hr at 30°C. The reaction was monitored by ESI-MS as described above and stopped by adding 2% v/v formic acid (final conc.). For cyclization by formation of disulfide bridges, peptides were dissolved in 8 ml of reaction buffer and 2 ml of DMSO. Cyclization reaction was monitored by ESI-MS. The cyclized peptides were purified by RP-HPLC as described above and fractions with pure peptides lyophilized. Peptides were dissolved in ddH₂O at a concentration of 2 mM. Purity was characterized by running the peptide solutions on an analytical HPLC (1260 HPLC system, Agilent), with a C18 column (ZORBAX 300SB-C18, 5 μm , 300 Å, 4.6 × 250 mm, Agilent). A 0–100% gradient of acetonitrile, 0.1% TFA v/v (solvent B) in ddH₂O, 5% acetonitrile v/v, 0.1% TFA v/v (solvent A) in 30 minutes was applied.

Inhibitory activity determination

Inhibitory constants (K_i) of peptides were determined by measuring the residual enzymatic activities of coagulation factor XIa incubated with inhibitor at different concentrations (30 μM to 9 nM final conc.) with the substrate Pyr-Pro-Arg-pNA (Bachem). Activities were measured at 25°C in an activity assay buffer (10 mM Tris-Cl, 150 mM NaCl, 10 mM MgCl_2 , 1 mM CaCl_2 , 0.1% (w/v) BSA and 0.01% (v/v) Triton-X100, pH 7.4). Reactions were started by adding the substrate (400 μM final conc.) to 0.5 nM FXIa in presence or absence of bicyclic peptides. Substrate hydrolysis led to the release of p-nitroaniline (pNA), which was recorded over at least 20 min using an absorbance microtiter plate reader (Infinite M200 Pro, Tecan)

by measuring the absorbance at 405 nm every minute. The rate of increase in absorbance is a measure of enzyme activity. The following equation was applied to determine the IC₅₀ values (using Prism 5 (GraphPad)):

$$y = \frac{100}{1 + 10^{(\log IC_{50} - x)p}}$$

Wherein y corresponds to the residual activity (%) of protease, x is the logarithm of bicyclic peptide concentration, IC₅₀ is the inhibitor concentration necessary to achieve 50% inhibition, and p is the Hill coefficient. The following equation was applied to calculate the K_i values:

$$K_i = \frac{IC_{50}}{1 + \frac{[S]_0}{K_m}}$$

Where [S]₀ is the initial concentration of substrate, and K_m is the substrate Michaelis constant. The K_m of FXIa for Pyr-Pro-Arg-pNA was determined to be 255 ± 14 μM.

Fluorescence polarization for measurement of binding affinity

FXIa was diluted serially in PBS with 0.01% v/v Tween-20. 15 μL were added to 15 μL of peptide-fluorescein conjugate (25 nM final concentration) in 96-well microtiter plates (black, half-area). An absorption microwell plate reader (Infinite M200Pro, Tecan) was used to measure fluorescence anisotropy, with a filter for excitation at 485 nm and an at 535 nm for emission. Dissociation constants (K_D) were calculated using the following equation (using Prism 5 (GraphPad)):

$$A = A_f + (A_b - A_f) \times \left\{ \frac{[L]_T + K_D + [P]_T - \sqrt{([L]_T + K_D + [P]_T)^2 - 4[L]_T[P]_T}}{2[L]_T} \right\}$$

Where A is anisotropy. A_f and A_b are the anisotropy values for free (A_f) and bound (A_b) ligand. $[L]_T$ is the concentration of total fluorescent ligand and $[P]_T$ the concentration of protein.

3.6 Supplementary information

Supplementary Table 1. Degenerated DNA primers used for whole plasmid PCR.

Nr	Primer sequence
1	AGCGCCATGGCCNNKTGTTGTTGTNNKNNKNNKNNKNNKNNKNNKNNKNNKNNKNNKNNKNNKTGT NNKGGTTCTGGCGCTGAAACTGTTGAAAGTTGTTTAGC
2	AGCGCCATGGCCNNKTGTTGTNNKTGTNNKNNKNNKNNKNNKNNKNNKNNKNNKNNKNNKNNKNNKTGT NNKGGTTCTGGCGCTGAAACTGTTGAAAGTTGTTTAGC
3	AGCGCCATGGCCNNKTGTTGTNNKNNKTGTNNKNNKNNKNNKNNKNNKNNKNNKNNKNNKNNKNNKNNKTGT NNKGGTTCTGGCGCTGAAACTGTTGAAAGTTGTTTAGC
4	AGCGCCATGGCCNNKTGTTGTNNKNNKNNKTGTNNKNNKNNKNNKNNKNNKNNKNNKNNKNNKNNKNNKNNKTGT NNKGGTTCTGGCGCTGAAACTGTTGAAAGTTGTTTAGC
5	AGCGCCATGGCCNNKTGTTGTNNKNNKNNKNNKNNKTGTNNKNNKNNKNNKNNKNNKNNKNNKNNKNNKNNKNNKNNKTGT NNKGGTTCTGGCGCTGAAACTGTTGAAAGTTGTTTAGC
6	AGCGCCATGGCCNNKTGTTGTNNKNNKNNKNNKNNKNNKTGTNNKNNKNNKNNKNNKNNKNNKNNKNNKNNKNNKNNKNNKTGT NNKGGTTCTGGCGCTGAAACTGTTGAAAGTTGTTTAGC
7	AGCGCCATGGCCNNKTGTTGTNNKNNKNNKNNKNNKNNKTGTNNKNNKNNKNNKNNKNNKNNKNNKNNKNNKNNKNNKNNKTGT NNKGGTTCTGGCGCTGAAACTGTTGAAAGTTGTTTAGC
8	AGCGCCATGGCCNNKTGTTGTNNKNNKNNKNNKNNKNNKNNKTGTNNKNNKNNKNNKNNKNNKNNKNNKNNKNNKNNKNNKNNKTGT NNKGGTTCTGGCGCTGAAACTGTTGAAAGTTGTTTAGC
9	AGCGCCATGGCCNNKTGTTGTNNKNNKNNKNNKNNKNNKNNKTGTNNKNNKNNKNNKNNKNNKNNKNNKNNKNNKNNKNNKNNKTGT NNKGGTTCTGGCGCTGAAACTGTTGAAAGTTGTTTAGC
10	AGCGCCATGGCCNNKTGTTGTNNKTGT NNKGGTTCTGGCGCTGAAACTGTTGAAAGTTGTTTAGC
11	AGCGCCATGGCCNNKTGTTGTNNKTGT NNKGGTTCTGGCGCTGAAACTGTTGAAAGTTGTTTAGC
12	AGCGCCATGGCCNNKTGTTGTNNKTGT NNKGGTTCTGGCGCTGAAACTGTTGAAAGTTGTTTAGC
13	AGCGCCATGGCCNNKTGTTGTNNKTGT NNKGGTTCTGGCGCTGAAACTGTTGAAAGTTGTTTAGC
14	AGCGCCATGGCCNNKTGTNNKTGTTGTNNKTGT NNKGGTTCTGGCGCTGAAACTGTTGAAAGTTGTTTAGC
15	AGCGCCATGGCCNNKTGTNNKTGTNNKTGTNNKNNKNNKNNKNNKNNKNNKNNKNNKNNKNNKNNKNNKNNKNNKNNKNNKNNKNNKTGT NNKGGTTCTGGCGCTGAAACTGTTGAAAGTTGTTTAGC
16	AGCGCCATGGCCNNKTGTNNKTGTNNKNNKTGTNNKNNKNNKNNKNNKNNKNNKNNKNNKNNKNNKNNKNNKNNKNNKNNKNNKNNKNNKTGT NNKGGTTCTGGCGCTGAAACTGTTGAAAGTTGTTTAGC
17	AGCGCCATGGCCNNKTGTNNKTGTNNKNNKNNKNNKTGTNNKNNKNNKNNKNNKNNKNNKNNKNNKNNKNNKNNKNNKNNKNNKTGT NNKGGTTCTGGCGCTGAAACTGTTGAAAGTTGTTTAGC
18	AGCGCCATGGCCNNKTGTNNKTGTNNKNNKNNKNNKNNKTGTNNKNNKNNKNNKNNKNNKNNKNNKNNKNNKNNKNNKNNKNNKNNKTGT NNKGGTTCTGGCGCTGAAACTGTTGAAAGTTGTTTAGC
19	AGCGCCATGGCCNNKTGTNNKTGTNNKNNKNNKNNKNNKNNKTGTNNKNNKNNKNNKNNKNNKNNKNNKNNKNNKNNKNNKNNKNNKNNKTGT NNKGGTTCTGGCGCTGAAACTGTTGAAAGTTGTTTAGC
20	AGCGCCATGGCCNNKTGTNNKTGTNNKNNKNNKNNKNNKNNKNNKTGTNNKNNKNNKNNKNNKNNKNNKNNKNNKNNKNNKNNKNNKNNKNNKTGT NNKGGTTCTGGCGCTGAAACTGTTGAAAGTTGTTTAGC
21	AGCGCCATGGCCNNKTGTNNKTGTNNKTGT NNKGGTTCTGGCGCTGAAACTGTTGAAAGTTGTTTAGC
22	AGCGCCATGGCCNNKTGTNNKTGTNNKTGT NNKGGTTCTGGCGCTGAAACTGTTGAAAGTTGTTTAGC

23	AGCGCCATGGCCNNKTGTNNKTGTNNKNNKNNKNNKNNKNNKNNKNNKTGTNNKNNKTGT NNKGGTCTGGCGCTGAAACTGTTGAAAGTTGTTTAGC
24	AGCGCCATGGCCNNKTGTNNKTGTNNKNNKNNKNNKNNKNNKNNKNNKTGTNNKTGT NNKGGTCTGGCGCTGAAACTGTTGAAAGTTGTTTAGC
25	AGCGCCATGGCCNNKTGTNNKTGTNNKNNKNNKNNKNNKNNKNNKNNKTGTGT NNKGGTCTGGCGCTGAAACTGTTGAAAGTTGTTTAGC
26	AGCGCCATGGCCNNKTGTNNKNNKTGTGTNNKNNKNNKNNKNNKNNKNNKNNKTGT NNKGGTCTGGCGCTGAAACTGTTGAAAGTTGTTTAGC
27	AGCGCCATGGCCNNKTGTNNKNNKTGTNNKTGTNNKNNKNNKNNKNNKNNKNNKNNKTGT NNKGGTCTGGCGCTGAAACTGTTGAAAGTTGTTTAGC
28	AGCGCCATGGCCNNKTGTNNKNNKTGTNNKNNKTGTNNKNNKNNKNNKNNKNNKNNKNNKTGT NNKGGTCTGGCGCTGAAACTGTTGAAAGTTGTTTAGC
29	AGCGCCATGGCCNNKTGTNNKNNKTGTNNKNNKNNKTGTNNKNNKNNKNNKNNKNNKNNKTGT NNKGGTCTGGCGCTGAAACTGTTGAAAGTTGTTTAGC
30	AGCGCCATGGCCNNKTGTNNKNNKTGTNNKNNKNNKNNKTGTNNKNNKNNKNNKNNKNNKTGT NNKGGTCTGGCGCTGAAACTGTTGAAAGTTGTTTAGC
31	AGCGCCATGGCCNNKTGTNNKNNKTGTNNKNNKNNKNNKNNKNNKTGTNNKNNKNNKNNKNNKTGT NNKGGTCTGGCGCTGAAACTGTTGAAAGTTGTTTAGC
32	AGCGCCATGGCCNNKTGTNNKNNKTGTNNKNNKNNKNNKNNKNNKTGTNNKNNKNNKNNKNNKTGT NNKGGTCTGGCGCTGAAACTGTTGAAAGTTGTTTAGC
33	AGCGCCATGGCCNNKTGTNNKNNKTGTNNKNNKNNKNNKNNKNNKTGTNNKNNKNNKNNKTGT NNKGGTCTGGCGCTGAAACTGTTGAAAGTTGTTTAGC
34	AGCGCCATGGCCNNKTGTNNKNNKTGTNNKNNKNNKNNKNNKNNKTGTNNKNNKNNKTGT NNKGGTCTGGCGCTGAAACTGTTGAAAGTTGTTTAGC
35	AGCGCCATGGCCNNKTGTNNKNNKTGTNNKNNKNNKNNKNNKNNKTGTNNKNNKNNKTGT NNKGGTCTGGCGCTGAAACTGTTGAAAGTTGTTTAGC
36	AGCGCCATGGCCNNKTGTNNKNNKTGTNNKNNKNNKNNKNNKNNKTGTNNKNNKNNKTGTGT NNKGGTCTGGCGCTGAAACTGTTGAAAGTTGTTTAGC
37	AGCGCCATGGCCNNKTGTNNKNNKNNKTGTTGTNNKNNKNNKNNKNNKNNKNNKNNKNNKNNKTGT NNKGGTCTGGCGCTGAAACTGTTGAAAGTTGTTTAGC
38	AGCGCCATGGCCNNKTGTNNKNNKNNKTGTNNKTGTNNKNNKNNKNNKNNKNNKNNKNNKNNKTGT NNKGGTCTGGCGCTGAAACTGTTGAAAGTTGTTTAGC
39	AGCGCCATGGCCNNKTGTNNKNNKNNKTGTNNKNNKTGTNNKNNKNNKNNKNNKNNKNNKNNKTGT NNKGGTCTGGCGCTGAAACTGTTGAAAGTTGTTTAGC
40	AGCGCCATGGCCNNKTGTNNKNNKNNKTGTNNKNNKNNKNNKTGTNNKNNKNNKNNKNNKNNKTGT NNKGGTCTGGCGCTGAAACTGTTGAAAGTTGTTTAGC
41	AGCGCCATGGCCNNKTGTNNKNNKNNKTGTNNKNNKNNKNNKTGTNNKNNKNNKNNKNNKNNKTGT NNKGGTCTGGCGCTGAAACTGTTGAAAGTTGTTTAGC
42	AGCGCCATGGCCNNKTGTNNKNNKNNKTGTNNKNNKNNKNNKNNKNNKTGTNNKNNKNNKNNKTGT NNKGGTCTGGCGCTGAAACTGTTGAAAGTTGTTTAGC
43	AGCGCCATGGCCNNKTGTNNKNNKNNKTGTNNKNNKNNKNNKNNKNNKTGTNNKNNKNNKTGT NNKGGTCTGGCGCTGAAACTGTTGAAAGTTGTTTAGC
44	AGCGCCATGGCCNNKTGTNNKNNKNNKTGTNNKNNKNNKNNKNNKNNKNNKNNKTGTNNKNNKTGT NNKGGTCTGGCGCTGAAACTGTTGAAAGTTGTTTAGC
45	AGCGCCATGGCCNNKTGTNNKNNKNNKTGTNNKNNKNNKNNKNNKNNKNNKNNKNNKNNKNNKTGT NNKGGTCTGGCGCTGAAACTGTTGAAAGTTGTTTAGC
46	AGCGCCATGGCCNNKTGTNNKNNKNNKTGTNNKNNKNNKNNKNNKNNKNNKNNKNNKNNKNNKTGTGT NNKGGTCTGGCGCTGAAACTGTTGAAAGTTGTTTAGC
47	AGCGCCATGGCCNNKTGTNNKNNKNNKNNKTGTTGTNNKNNKNNKNNKNNKNNKNNKNNKNNKNNKTGT NNKGGTCTGGCGCTGAAACTGTTGAAAGTTGTTTAGC
48	AGCGCCATGGCCNNKTGTNNKNNKNNKNNKTGTNNKTGTNNKNNKNNKNNKNNKNNKNNKNNKNNKTGT NNKGGTCTGGCGCTGAAACTGTTGAAAGTTGTTTAGC

49	AGCGCCATGGCCNNKTGTNNKNNKNNKNNKTGTNNKNNKTGTNNKNNKNNKNNKNNKNNKTGT NNKGGTTCTGGCGCTGAAACTGTTGAAAGTTGTTTAGC
50	AGCGCCATGGCCNNKTGTNNKNNKNNKNNKTGTNNKNNKNNKTGTNNKNNKNNKNNKNNKNNKTGT NNKGGTTCTGGCGCTGAAACTGTTGAAAGTTGTTTAGC
51	AGCGCCATGGCCNNKTGTNNKNNKNNKNNKTGTNNKNNKNNKNNKTGTNNKNNKNNKNNKNNKTGT NNKGGTTCTGGCGCTGAAACTGTTGAAAGTTGTTTAGC
52	AGCGCCATGGCCNNKTGTNNKNNKNNKNNKTGTNNKNNKNNKNNKNNKNNKTGTNNKNNKNNKTGT NNKGGTTCTGGCGCTGAAACTGTTGAAAGTTGTTTAGC
53	AGCGCCATGGCCNNKTGTNNKNNKNNKNNKTGTNNKNNKNNKNNKNNKNNKTGTNNKNNKNNKTGT NNKGGTTCTGGCGCTGAAACTGTTGAAAGTTGTTTAGC
54	AGCGCCATGGCCNNKTGTNNKNNKNNKNNKTGTNNKNNKNNKNNKNNKNNKNNKNNKTGTNNKTGT NNKGGTTCTGGCGCTGAAACTGTTGAAAGTTGTTTAGC
55	AGCGCCATGGCCNNKTGTNNKNNKNNKNNKTGTNNKNNKNNKNNKNNKNNKNNKNNKNNKTGTGT NNKGGTTCTGGCGCTGAAACTGTTGAAAGTTGTTTAGC
56	AGCGCCATGGCCNNKTGTNNKNNKNNKNNKNNKTGTTGTNNKNNKNNKNNKNNKNNKNNKNNKTGT NNKGGTTCTGGCGCTGAAACTGTTGAAAGTTGTTTAGC
57	AGCGCCATGGCCNNKTGTNNKNNKNNKNNKNNKTGTNNKTGTNNKNNKNNKNNKNNKNNKNNKTGT NNKGGTTCTGGCGCTGAAACTGTTGAAAGTTGTTTAGC
58	AGCGCCATGGCCNNKTGTNNKNNKNNKNNKNNKTGTNNKNNKTGTNNKNNKNNKNNKNNKNNKTGT NNKGGTTCTGGCGCTGAAACTGTTGAAAGTTGTTTAGC
59	AGCGCCATGGCCNNKTGTNNKNNKNNKNNKNNKTGTNNKNNKNNKTGTNNKNNKNNKNNKNNKTGT NNKGGTTCTGGCGCTGAAACTGTTGAAAGTTGTTTAGC
60	AGCGCCATGGCCNNKTGTNNKNNKNNKNNKNNKTGTNNKNNKNNKNNKNNKTGTNNKNNKNNKTGT NNKGGTTCTGGCGCTGAAACTGTTGAAAGTTGTTTAGC
61	AGCGCCATGGCCNNKTGTNNKNNKNNKNNKNNKTGTNNKNNKNNKNNKNNKNNKTGTNNKNNKTGT NNKGGTTCTGGCGCTGAAACTGTTGAAAGTTGTTTAGC
62	AGCGCCATGGCCNNKTGTNNKNNKNNKNNKNNKTGTNNKNNKNNKNNKNNKNNKNNKTGTNNKTGT NNKGGTTCTGGCGCTGAAACTGTTGAAAGTTGTTTAGC
63	AGCGCCATGGCCNNKTGTNNKNNKNNKNNKNNKTGTNNKNNKNNKNNKNNKNNKNNKNNKTGTGT NNKGGTTCTGGCGCTGAAACTGTTGAAAGTTGTTTAGC
64	AGCGCCATGGCCNNKTGTNNKNNKNNKNNKNNKNNKNNKTGTTGTNNKNNKNNKNNKNNKNNKTGT NNKGGTTCTGGCGCTGAAACTGTTGAAAGTTGTTTAGC
65	AGCGCCATGGCCNNKTGTNNKNNKNNKNNKNNKNNKNNKTGTNNKTGTNNKNNKNNKNNKNNKTGT NNKGGTTCTGGCGCTGAAACTGTTGAAAGTTGTTTAGC
66	AGCGCCATGGCCNNKTGTNNKNNKNNKNNKNNKNNKNNKTGTNNKNNKTGTNNKNNKNNKNNKTGT NNKGGTTCTGGCGCTGAAACTGTTGAAAGTTGTTTAGC
67	AGCGCCATGGCCNNKTGTNNKNNKNNKNNKNNKNNKNNKTGTNNKNNKNNKTGTNNKNNKNNKTGT NNKGGTTCTGGCGCTGAAACTGTTGAAAGTTGTTTAGC
68	AGCGCCATGGCCNNKTGTNNKNNKNNKNNKNNKNNKNNKTGTNNKNNKNNKNNKNNKTGTNNKNNKTGT NNKGGTTCTGGCGCTGAAACTGTTGAAAGTTGTTTAGC
69	AGCGCCATGGCCNNKTGTNNKNNKNNKNNKNNKNNKNNKTGTNNKNNKNNKNNKNNKNNKTGTNNKTGT NNKGGTTCTGGCGCTGAAACTGTTGAAAGTTGTTTAGC
70	AGCGCCATGGCCNNKTGTNNKNNKNNKNNKNNKNNKNNKTGTNNKNNKNNKNNKNNKNNKNNKTGTGT NNKGGTTCTGGCGCTGAAACTGTTGAAAGTTGTTTAGC
71	AGCGCCATGGCCNNKTGTNNKNNKNNKNNKNNKNNKNNKTGTTGTNNKNNKNNKNNKNNKNNKTGT NNKGGTTCTGGCGCTGAAACTGTTGAAAGTTGTTTAGC
72	AGCGCCATGGCCNNKTGTNNKNNKNNKNNKNNKNNKNNKTGTNNKTGTNNKNNKNNKNNKNNKTGT NNKGGTTCTGGCGCTGAAACTGTTGAAAGTTGTTTAGC
73	AGCGCCATGGCCNNKTGTNNKNNKNNKNNKNNKNNKNNKTGTNNKNNKTGTNNKNNKNNKNNKTGT NNKGGTTCTGGCGCTGAAACTGTTGAAAGTTGTTTAGC
74	AGCGCCATGGCCNNKTGTNNKNNKNNKNNKNNKNNKNNKTGTNNKNNKNNKTGTNNKNNKNNKTGT NNKGGTTCTGGCGCTGAAACTGTTGAAAGTTGTTTAGC

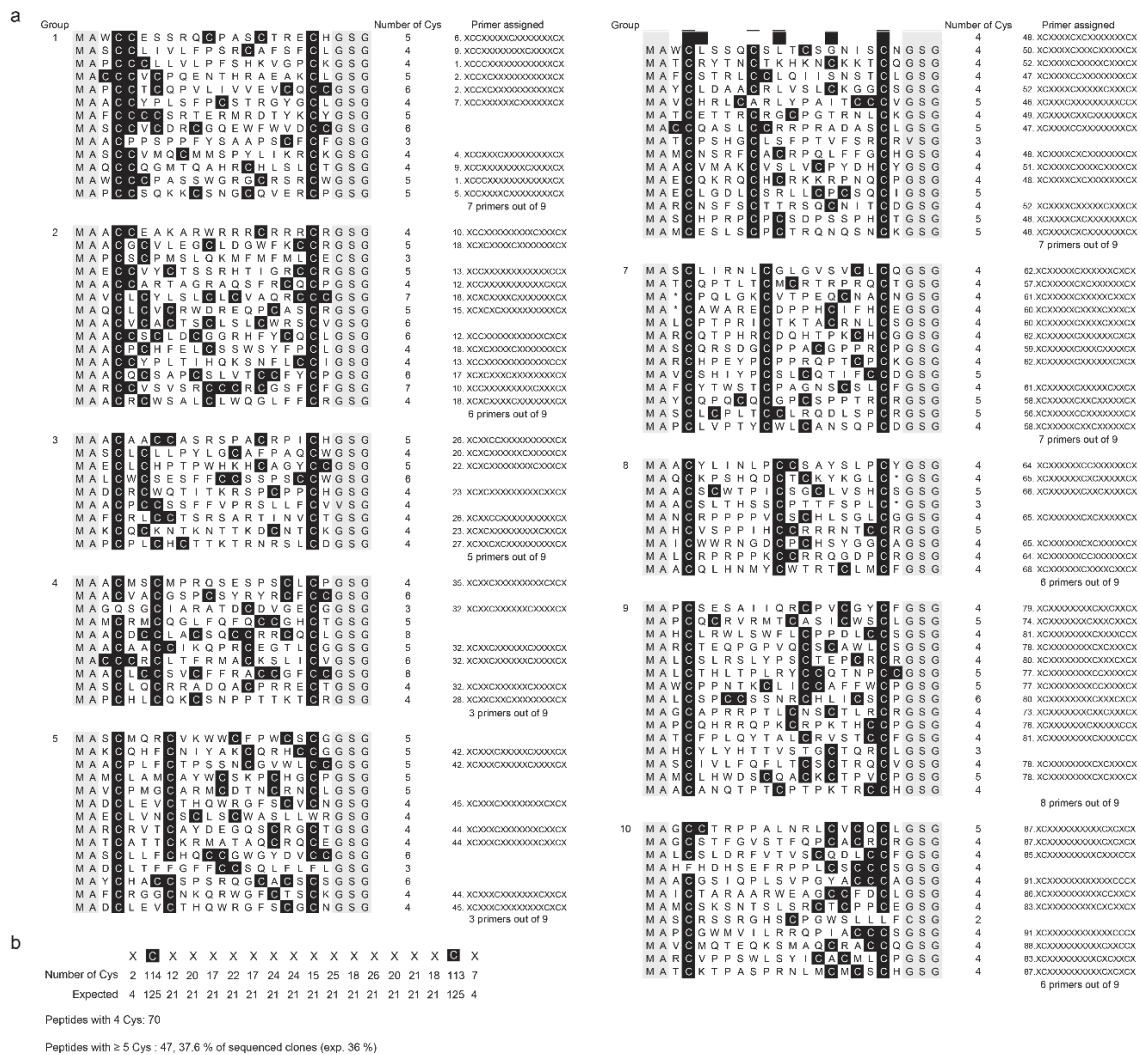
75	AGCGCCATGGCCNNKTGTNNKNNKNNKNNKNNKNNKNNKTGTNNKNNKNNKNNKTGTNNKTGT NNKGGTTCGGCGCTGAAACTGTTGAAAGTTGTTTAGC
76	AGCGCCATGGCCNNKTGTNNKNNKNNKNNKNNKNNKNNKTGTNNKNNKNNKNNKTGTGT NNKGGTTCGGCGCTGAAACTGTTGAAAGTTGTTTAGC
77	AGCGCCATGGCCNNKTGTNNKNNKNNKNNKNNKNNKNNKTGTTGTNNKNNKNNKNNKTGT NNKGGTTCGGCGCTGAAACTGTTGAAAGTTGTTTAGC
78	AGCGCCATGGCCNNKTGTNNKNNKNNKNNKNNKNNKNNKTGTNNKTGTNNKNNKNNKTGT NNKGGTTCGGCGCTGAAACTGTTGAAAGTTGTTTAGC
79	AGCGCCATGGCCNNKTGTNNKNNKNNKNNKNNKNNKNNKTGTNNKNNKTGTNNKNNKTGT NNKGGTTCGGCGCTGAAACTGTTGAAAGTTGTTTAGC
80	AGCGCCATGGCCNNKTGTNNKNNKNNKNNKNNKNNKNNKTGTNNKNNKNNKTGTNNKTGT NNKGGTTCGGCGCTGAAACTGTTGAAAGTTGTTTAGC
81	AGCGCCATGGCCNNKTGTNNKNNKNNKNNKNNKNNKNNKTGTNNKNNKNNKNNKTGTTGT NNKGGTTCGGCGCTGAAACTGTTGAAAGTTGTTTAGC
82	AGCGCCATGGCCNNKTGTNNKNNKNNKNNKNNKNNKNNKTGTTGTNNKNNKNNKTGT NNKGGTTCGGCGCTGAAACTGTTGAAAGTTGTTTAGC
83	AGCGCCATGGCCNNKTGTNNKNNKNNKNNKNNKNNKNNKTGTNNKTGTNNKNNKTGT NNKGGTTCGGCGCTGAAACTGTTGAAAGTTGTTTAGC
84	AGCGCCATGGCCNNKTGTNNKNNKNNKNNKNNKNNKNNKTGTNNKNNKTGTNNKTGT NNKGGTTCGGCGCTGAAACTGTTGAAAGTTGTTTAGC
85	AGCGCCATGGCCNNKTGTNNKNNKNNKNNKNNKNNKNNKTGTNNKNNKNNKTGTTGT NNKGGTTCGGCGCTGAAACTGTTGAAAGTTGTTTAGC
86	AGCGCCATGGCCNNKTGTNNKNNKNNKNNKNNKNNKNNKTGTTGTNNKNNKTGT NNKGGTTCGGCGCTGAAACTGTTGAAAGTTGTTTAGC
87	AGCGCCATGGCCNNKTGTNNKNNKNNKNNKNNKNNKNNKTGTNNKTGTNNKTGT NNKGGTTCGGCGCTGAAACTGTTGAAAGTTGTTTAGC
88	AGCGCCATGGCCNNKTGTNNKNNKNNKNNKNNKNNKNNKTGTNNKNNKTGTTGT NNKGGTTCGGCGCTGAAACTGTTGAAAGTTGTTTAGC
89	AGCGCCATGGCCNNKTGTNNKNNKNNKNNKNNKNNKNNKTGTTGTNNKTGT NNKGGTTCGGCGCTGAAACTGTTGAAAGTTGTTTAGC
90	AGCGCCATGGCCNNKTGTNNKNNKNNKNNKNNKNNKNNKTGTNNKTGTTGT NNKGGTTCGGCGCTGAAACTGTTGAAAGTTGTTTAGC
91	AGCGCCATGGCCNNKTGTNNKNNKNNKNNKNNKNNKNNKTGTTGTTGT NNKGGTTCGGCGCTGAAACTGTTGAAAGTTGTTTAGC

Supplementary Table 2. PCR reactions pooled after purification by electrophoresis and extraction from agarose gel.

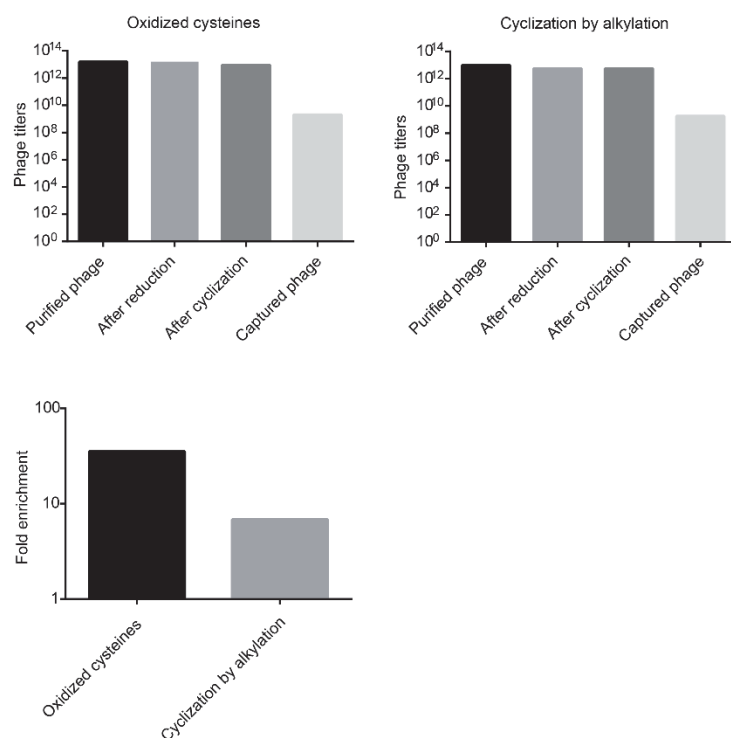
Group number	Forward primers	DNA concentration (ng/μl)	Total volume (μl)
1	1 - 9	40	200
2	10 - 18	45	200
3	19 - 27	43	200
4	28 - 36	43	200
5	37 - 45	42	200
6	46 - 54	37	200
7	55 - 63	37	200
8	64 - 72	36	200
9	73 - 81	37	200
10	82 - 91	57	200

Supplementary Table 3. Number of bacterial cells transformed with library vector. Determined in duplicate by plating dilutions of transformed cells on selective agar plates.

Group number	Titer 1	Titer 2	Average in total volume
1	1.80E+07	1.00E+07	1.47E+09
2	1.70E+07	2.00E+07	1.94E+09
3	2.00E+07	2.00E+07	2.10E+09
4	2.60E+07	2.00E+07	2.42E+09
5	1.90E+07	1.00E+07	1.52E+09
6	2.00E+07	3.00E+07	2.63E+09
7	4.20E+07	3.00E+07	3.78E+09
8	3.80E+07	4.00E+07	4.10E+09
9	2.30E+07	5.00E+07	3.83E+09
10	3.10E+07	5.00E+07	4.25E+09



Supplementary Figure 1. Sequences of peptides in phage library. From each of the 10 pools, around 19 clones were sequenced.



Supplementary Figure 2. Phage titers at different stages of phage selection. After PEG purification, after reduction, after cyclization and captured phage after biopanning (top). On the bottom figure, enrichment factors (defined as the ratio of captured phage titer in each condition and titer in the negative control) in the third round of selection.

4 Development of selective FXIa inhibitors based on cyclic peptides and their application for safe anticoagulation

This chapter is based on a manuscript that will be submitted for publication. I will be the only first author in this publication.

4.1 Abstract

Coagulation factor XI (FXI) has emerged as a promising target for safe anticoagulation due to its role in the pathogenesis of thrombosis while being not essential for homeostasis. Herein, we report the first peptide-based FXIa inhibitor that selectively and potently inhibits activated FXI (FXIa) in human and animal blood and suppresses blood coagulation ($K_i = 3 \pm 0.2$ nM). A comparison to the reference anticoagulant heparin showed that the cyclic peptide achieves anticoagulation effects that are obtained with a therapeutic heparin dose (0.3 - 0.7 IU/ml), while having a substantially broader therapeutic range. PEGylation of the cyclic peptides allowed for prolongation of the plasma half-life and inhibition of FXIa over extended periods *in vivo* (rabbits) and in an experimental model of hemodialysis performed with human blood. Our work shows that FXI can efficiently and selectively be targeted with peptides and provides a promising candidate for the development of a safe anticoagulation therapy.

4.2 Introduction

Hemostasis is a complex physiological process responsible for limiting hemorrhage caused by vascular injury. It is achieved through a tightly regulated process, which leads to the formation of a local fibrin-rich platelet plug closing off the blood vessel. In parallel, normal blood flow is maintained in the rest of the vascular system. The dysregulation of this mechanism can lead to the formation of clots that obstruct the blood flow in vessels, causing thrombotic diseases, one of the primary causes of morbidity and mortality worldwide¹⁶⁶. Anticoagulants are the drugs used for the treatment and prevention of thrombosis. Although efficacious, all drugs currently available also interfere with hemostasis, and thus increase the risk of severe bleeding, a life-threatening condition. This safety issue can lead to events of inappropriate treatment with suboptimal doses of anticoagulants, as physicians fear the risk of bleeding^{122,123}.

A novel strategy that could allow the development of safer anticoagulants with limited risk of severe bleeding involves targeting coagulation factor XI (FXI). FXI is a protease of the intrinsic pathway of coagulation that can be activated by coagulation factors XIIa (FXIIa) and thrombin and by autoactivation. Activated FXI (FXIa) is responsible for the activation of coagulation factor XI (FXI). Deficiency of FXI (hemophilia C) causes a mild bleeding disorder, rarely associated with spontaneous bleeding, while excessive bleeding can sometimes occur with surgery or trauma to tissues characterized by high levels of fibrinolysis^{125,126}. Epidemiological data and studies with animal models have shown an involvement of FXI in thrombosis. A strong dose-dependency between FXI levels and risk of venous thrombosis was observed. Patients with FXI plasma levels in the highest fraction of the normal distribution (> 90th percentile) had two times higher risk to develop venous thromboembolism than the population with lower values¹³⁸. Other studies have linked FXI levels and the risk of ischemic stroke and myocardial infarction^{139,140}. In addition, severe FXI deficiency leads to protection against cardiovascular events (myocardial infarction, stroke,

and transient ischemic attack) and venous thromboembolism¹⁴¹. In parallel, studies in mice, rabbits and baboons targeting FXI have also demonstrated its importance in thrombosis with limited contribution to hemostasis^{145,155,167–169}.

Several indications where FXI-targeted therapies could potentially be beneficial have been identified, including primary VTE prophylaxis, thrombosis prevention in end-stage renal disease and atrial fibrillation patients, anticoagulation in extracorporeal circuits and in patients undergoing hemodialysis¹²⁷. FXI-targeting molecules currently in development include small molecule inhibitors^{143,156,170,171}, antisense oligonucleotides^{142,169} and proteins such as monoclonal antibodies^{172,173}. No peptide-based FXI inhibitor drug development program has so far been reported, despite the suitability of peptides as a modality for this target, including the good binding properties (affinity and selectivity), the absence of toxic metabolic products, the ease of manufacturing by synthesis, and the tunable pharmacokinetic properties. The reasons for the lack of FXI peptide inhibitor programs might be the rather challenging nature of the target, as experienced in previous work in our lab. While we could recently generate inhibitors with single-digit nM K_i s to FXIa, they bound only human FXIa but not animal homologs, which hindered their evaluation *in vivo* and further development (Kong *et al.*, unpublished).

In this work, we screened a new phage display library of an enormous size and structural diversity, comprising more than 500 billion (5×10^{11}) different cyclic peptides, in order to identify peptides that inhibit human FXIa with high affinity and selectivity, that block also FXIa of animals, and that are stable and active in blood. We identified peptides that fulfill all requirements and we extended the plasma half-life of one of them to several hours in rabbits through PEGylation and showed anticoagulation properties *in vivo* in rabbits and in a human *ex vivo* model of hemodialysis.

4.3 Results and discussion

4.3.1 Screening a 500-billion cyclic peptide library for FXIa inhibitors

We generated a peptide phage display library of the form shown in Fig. 20a, comprising more than 500 billion different cyclic or bicyclic peptides, and thus being larger and structurally more diverse than any previously reported library. The library was generated by cyclizing random peptides of the form $XC(X)_mC(X)_nC(X)_oCX$ (C = cysteine, X = any amino acid, $m + n + o = 12$) through reacting pairs of two cysteines with eight bis-electrophile reagents⁶⁰ shown in Fig. 20b. Phage displaying the large number of 30 billion different linear peptides could recently be obtained with a new cloning procedure based on whole-vector PCR (Kong *et al.*, unpublished) and by using a phagemid system that allowed efficient production and bacterial transformation of circular DNA (chapter 3). The four cysteines of the linear peptides are connected by two linkers in three different ways and give rise to three bicyclic peptide formats (Fig. 20a). While bicyclic peptides are formed, the library is also suited to screen for monocyclic peptides; for example, the first format shown in Fig. 20a displays two monocyclic peptide rings that can independently engage with the target protein. The combinatorial variation of the number of random amino acids m , n and o in the three segments spaced by cysteines yielded 182 bicyclic peptide backbones, as well as 12 different monocyclic backbones.

We performed three rounds of phage selection in which we iteratively produced phage, cyclized peptides on the tip of phage with the eight different linkers (in parallel reactions), panned the sub-libraries against immobilized human FXIa (5 μ g in round 1 and 2, 0.5 μ g in round 3), and propagated phage by bacterial infection. In a previous attempt to generate peptide FXIa inhibitors, phage selections had enriched binders to the apple domain of FXIa that were not inhibitors (chapter 3).

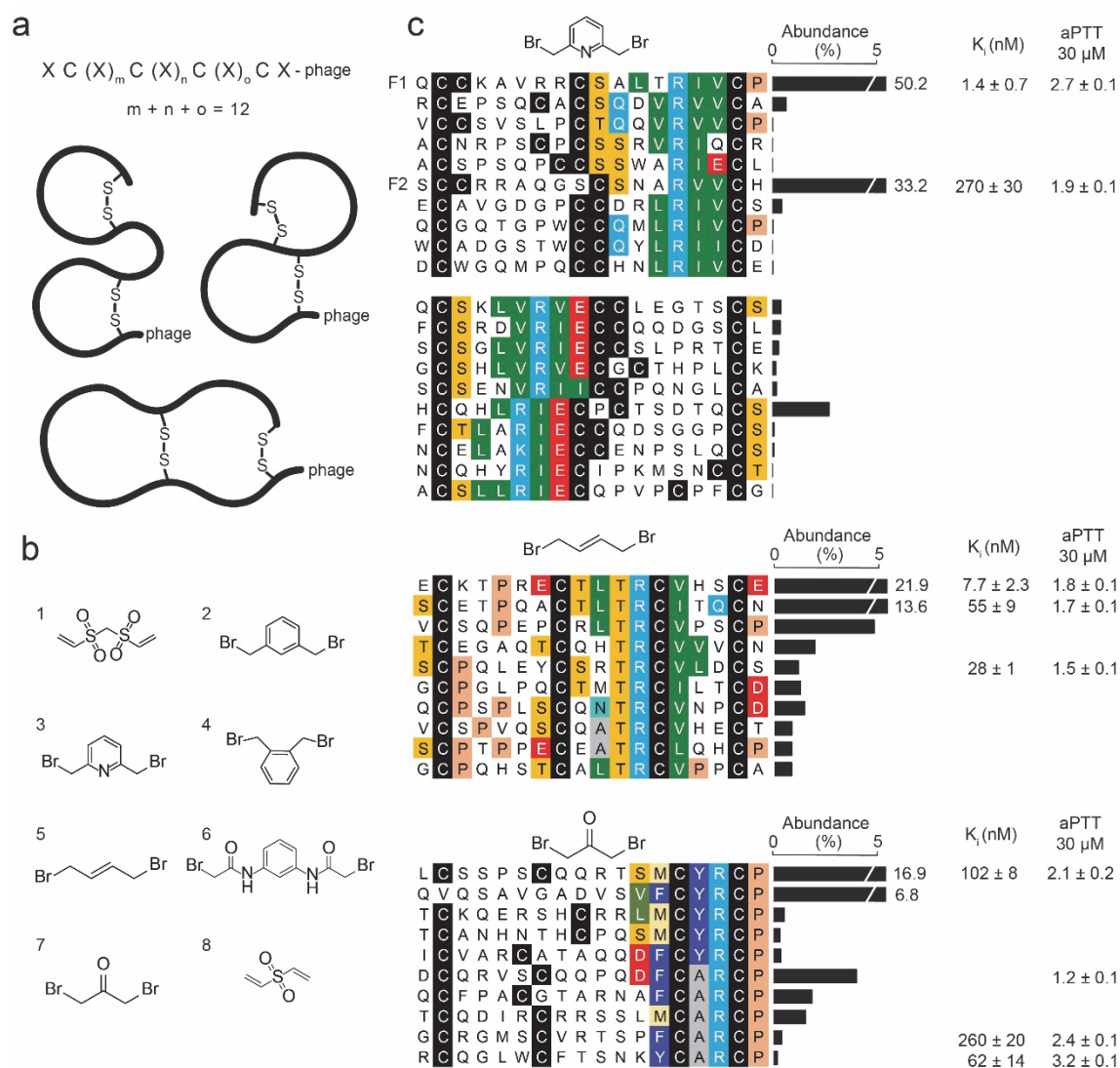


Figure 20. Phage display selection of cyclic peptide against FXIa. a) Library format. b) Bis-electrophile cyclization reagents. c) Sequences of peptides enriched after three rounds of phage selection against FXIa. Selections with eight sub-libraries, generated by cyclizing the linear peptides with reagents 1-8, were performed in parallel. Peptides isolated in selections with reagents 3, 5 and 7 converged to consensus groups and are shown. For each consensus group, the 10 most abundant peptides are shown in the figure and the remaining ones are shown in Supplementary Fig. 4. Sequence similarities are highlighted by color. K_i values and prolongation of aPTT at 30 μ M are indicated for the most active isomer of the characterized peptides. Values are means and SD of three measurements.

In order to isolate inhibitory peptides binding to the catalytic domain of FXIa, we eluted phage by addition of the covalent active site FXIa inhibitor PPACK (D-phenylalanyl-prolyl-arginyl chloromethyl ketone). In the third round of selection, the number of captured phage was increased more than 100-fold compared to the first round in the selections with the cyclization reagents 3, 4, 5, 7 and 8, suggesting that target selective binders were enriched

(Supplementary Fig. 3). High-throughput sequencing and comparison of the sequences with an alignment tool¹⁷⁴ identified strong consensus sequences for the selections with the chemical linkers **3**, **5** and **7**, wherein completely different consensus sequences were found for different linkers (Fig. 20c and Supplementary Fig. 4). Most of the consensus sequences occurred in one of the three randomized peptide segments [C(X)_mC, C(X)_nC or C(X)_oC] instead of spreading over two or three segments. Some of the consensus sequences occurred in different segments, suggesting that the enriched sequences bind to FXIa as monocyclic peptides.

4.3.2 Cyclic peptide inhibits FXIa with high affinity and selectivity

We synthesized a few peptides of each consensus sequence, reacted the linear peptides with reagents **3**, **5** or **7**, purified the three regioisomer products by HPLC, and assessed the inhibitory activity in activity assays with a chromogenic FXIa substrate as well as the prolongation of the activated partial thromboplastin time (aPTT) in human plasma, a parameter that indicates inhibition of the intrinsic pathway of coagulation (Fig. 20c). The most active peptide in terms of both, inhibition constant K_i and aPTT prolongation, was isomer 1 of F1 ($K_i = 1.4 \pm 0.7$ nM; 2.7-fold prolongation of aPTT at 30 μ M; Fig. 20c and Supplementary Fig. 5). A peptide sharing the same consensus sequence, F2, showed a 200-fold weaker K_i , but prolonged aPTT also efficiently (1.9-fold at 30 μ M; Fig. 20c and Supplementary Fig. 6).

Before further analysis of the structure-activity relationship of F1 isomer 1 (named F1 in the following), we assessed if the peptide fulfills the key requirements such as inhibition of the intrinsic coagulation pathway, selectivity, activity in blood, stability, and inhibition of animal homologues. F1 prolonged the aPTT in human plasma in a dose-dependent manner and at low micromolar concentrations ($EC_{2x} = 3.8 \pm 0.4$ μ M; Fig. 21b), indicating efficient inhibition of the intrinsic pathway.

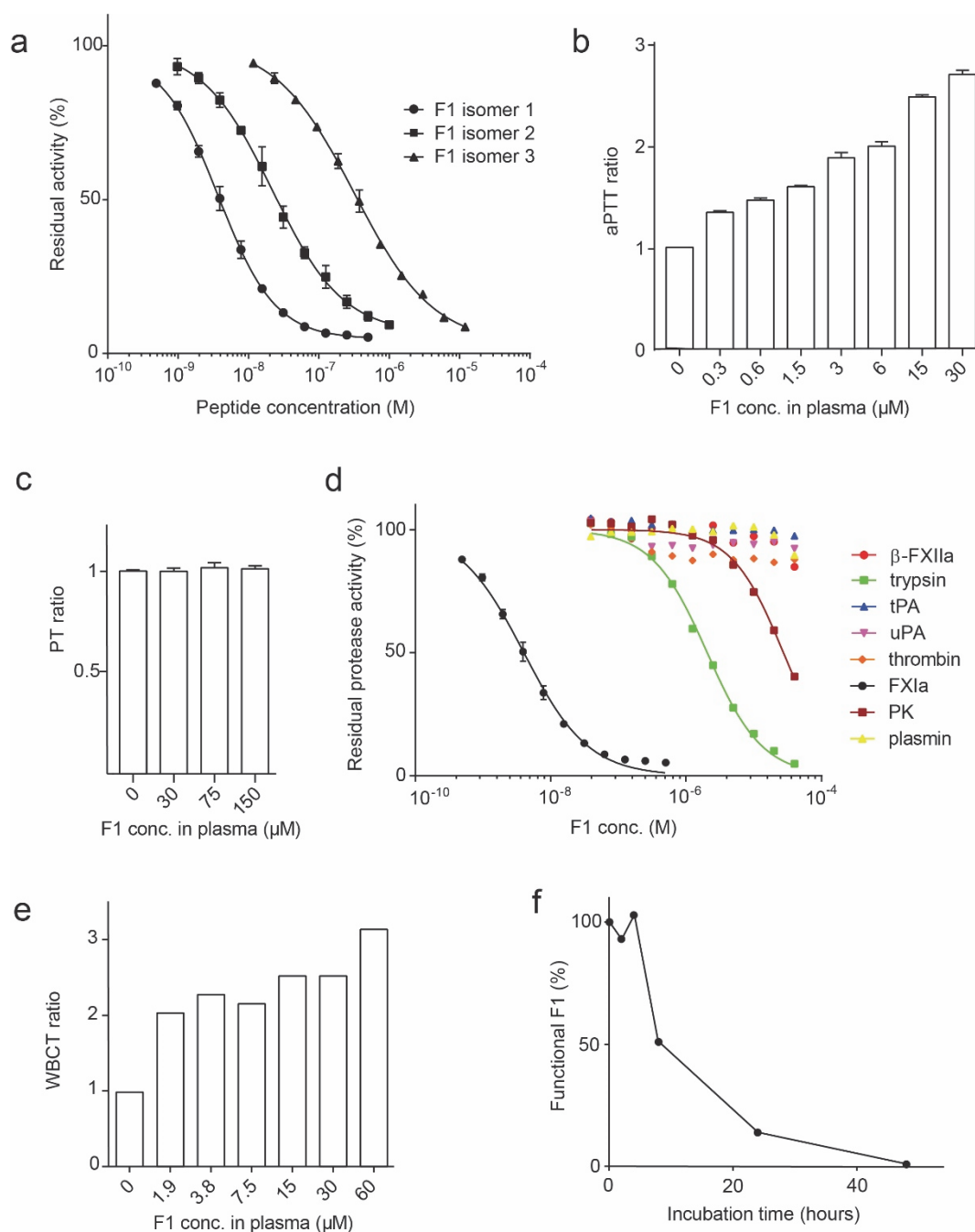


Figure 21. Activity, selectivity and stability of double-bridged peptide F1. a) Inhibition of human FXIa by three regioisomers of F1. b) Prolongation of aPTT by F1 in human plasma. c) Prolongation of PT by F1 in human plasma. Mean values and SD of three measurements are shown. d) Inhibition of homologous serine proteases. e) Prolongation of clotting time of F1 in human blood. f) Stability of F1 in human plasma at 37 °C. The amount of F1 remaining functional was quantified in a FXIa inhibition assay.

At the same time, the peptide did not affect the prothrombin time, even at a high concentration of 150 μ M (PT; Fig. 21c), showing that other serine proteases of the extrinsic

and common pathway were not inhibited and thus suggesting a high target selectivity. Indeed, a specificity profiling of F1 with a panel of seven homologous trypsin-like serine proteases revealed a high selectivity for the peptide (> 1000 -fold), with trypsin being the only protease inhibited at low micromolar concentrations (Fig. 21d). Assessment of the whole blood clotting time (WBCT), an assay used to characterize intrinsic pathway-driven coagulation in whole blood, showed that F1 was also active in this more complex environment ($EC_{2x} = 1.9 \mu M$; Fig. 21e), which was important as blood is the medium in which the inhibitor will need to act as an anticoagulant. The plasma stability was tested by incubating the peptide in human plasma at $37^\circ C$ and quantifying the residual FXIa inhibitory activity over time as a measure of stability and showed that most F1 remained functional for several hours ($t_{1/2} = 10.7$ hrs; Fig. 21f). Finally, we tested if F1 inhibits FXIa homologues of experimental animals. While F1 did not inhibit mouse FXIa, it prolonged aPTT in rabbit plasma ($EC_{2x} = 2 \pm 0.07 \mu M$), providing a suitable model for *in vivo* studies.

4.3.3 Peptide engineering affords inhibitor with long plasma half-life

We next aimed at reducing the synthetic complexity of the peptide and prolonging its half-life *in vivo*, that was expected to be short due to the typically rapid renal filtration of small molecules such as peptides¹⁷⁵. We chose to PEGylate the peptide as this offered to prolong the plasma half-life to hours or days, depending on the size of the PEG^{70,176}, and thus to flexibly tailor the pharmacokinetic properties to the specific medical application. In a first step, we tested if the chemical bridge connecting Cys2 and Cys3 in F1 was essential for its activity, or if a monocyclic peptide with the same sequence would inhibit FXIa with a similar affinity. Peptide F3 having the modifications Cys2 \rightarrow Ser and Cys3 \rightarrow Ser had a K_i and activity in plasma and whole blood comparable to F1 (Fig. 22a and Supplementary Fig. 7), which was pleasing as the synthesis of a monocyclic peptide was somewhat easier. Conjugation of PEG polymers to the peptide promised to be easiest if they could be conjugated via the peptide's N-terminal amine. In order to enable this strategy, we had to eliminate Lys4 that would react

and get PEGylated too. Mutation of Lys4 to arginine conserved the peptide's activity (F4; Fig. 22a and Supplementary Fig. 7). In addition, we found that deletion of the first three amino acids, yielding peptide F5, did not reduce the activity either (Fig. 22a and Supplementary Fig. 8).

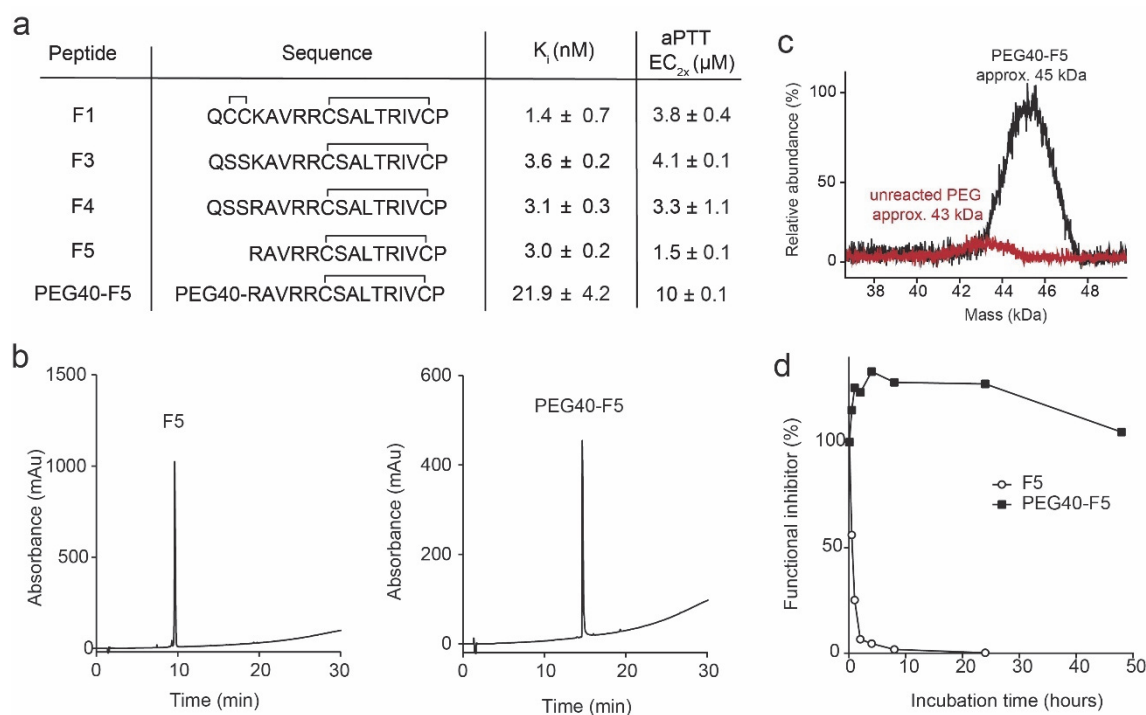


Figure 22. PEGylated cyclic peptide FXIa inhibitor. a) Structure and activity of cyclic peptide variants based on F1. Mean values and SD of three measurements are shown. b) Analytical HPLC traces of cyclic peptide F5 and PEGylated derivative. c) MALDI-TOF analysis of PEGylated peptide compared to PEG alone. d) Stability of F5 before and after PEGylation. Peptides were incubated in human plasma at 37 °C and the residual fraction of functional inhibitor assessed in FXIa inhibition assays.

We conjugated a linear 40 kDa PEG polymer with N-hydroxysuccinimide ester functionalization (PEG40-NHS) to F5 by reacting the peptide with a 2-fold molar excess of PEG40-NHS. Purification of the PEG40-F5 conjugate was facilitated by the high net positive charge of F5 (+4) that allowed for separation of PEG40-F5 from unreacted PEG by cation exchange chromatography. A subsequent desalting step removed salts used for elution in the cation exchange and allowed for separation of PEG40-F5 and unconjugated peptide (Fig. 22b and 22c). PEG40-F5 inhibited FXIa with a K_i of 22 ± 4.2 nM and doubled aPTT with an EC_{2x} of 10 ± 0.1 μ M, which corresponded to an approximately 7-fold lower potency in comparison

to unconjugated F5 peptide (Fig. 22a and Supplementary Fig. 8). While PEGylation reduced the activity of the inhibitor, it improved substantially the peptide's stability, the conjugate retaining 100% of its initial activity after the longest incubation time of 48 hours in human plasma (Fig. 22d). The higher stability was important as PEGylated polypeptides typically have half-lives in the order of days in human.

4.3.4 Cyclic peptide has a 100-fold wider therapeutic range than heparin

We next compared the activity of F5 and PEG40-F5 with unfractionated heparin (UFH), the golden standard in many anticoagulation therapies, and estimated the therapeutic range for the cyclic peptide FXIa inhibitor. The main challenge in the use of heparin is the narrow therapeutic range that is 0.3 – 0.7 IU/ml (factor = 2.3;^{109,177}). Higher doses cannot be applied due to risk of bleeding and lower doses will not suppress pathologic coagulation. It is likely that many patients treated with heparin are not optimally anticoagulated, at least not over the entire time period targeted^{123,127}. We assessed the concentration of F5 required to achieve the same prolongation of aPTT as with 0.3 - 0.7 IU/ml UFH (Fig. 23a; dotted lines). A 1.6-fold prolonged aPTT, obtained with 0.3 IU/ml UFH, was achieved at 0.2 μ M of F5, and a 5.1-fold prolonged aPTT, obtained with 0.7 IU/ml UFH, was achieved at 60 μ M of F5 (Fig. 23b; dotted lines). The F5 concentration range suited for therapeutic anticoagulation was thus estimated to be between 0.2 to 60 μ M, which is more than 100-fold broader than the therapeutic range for UFH. The minimal concentration of PEG40-F5 required to reach a 1.6-fold prolongation of the aPTT, and thus estimated to be required for therapeutic anticoagulation, was 0.9 μ M (Fig. 23b).

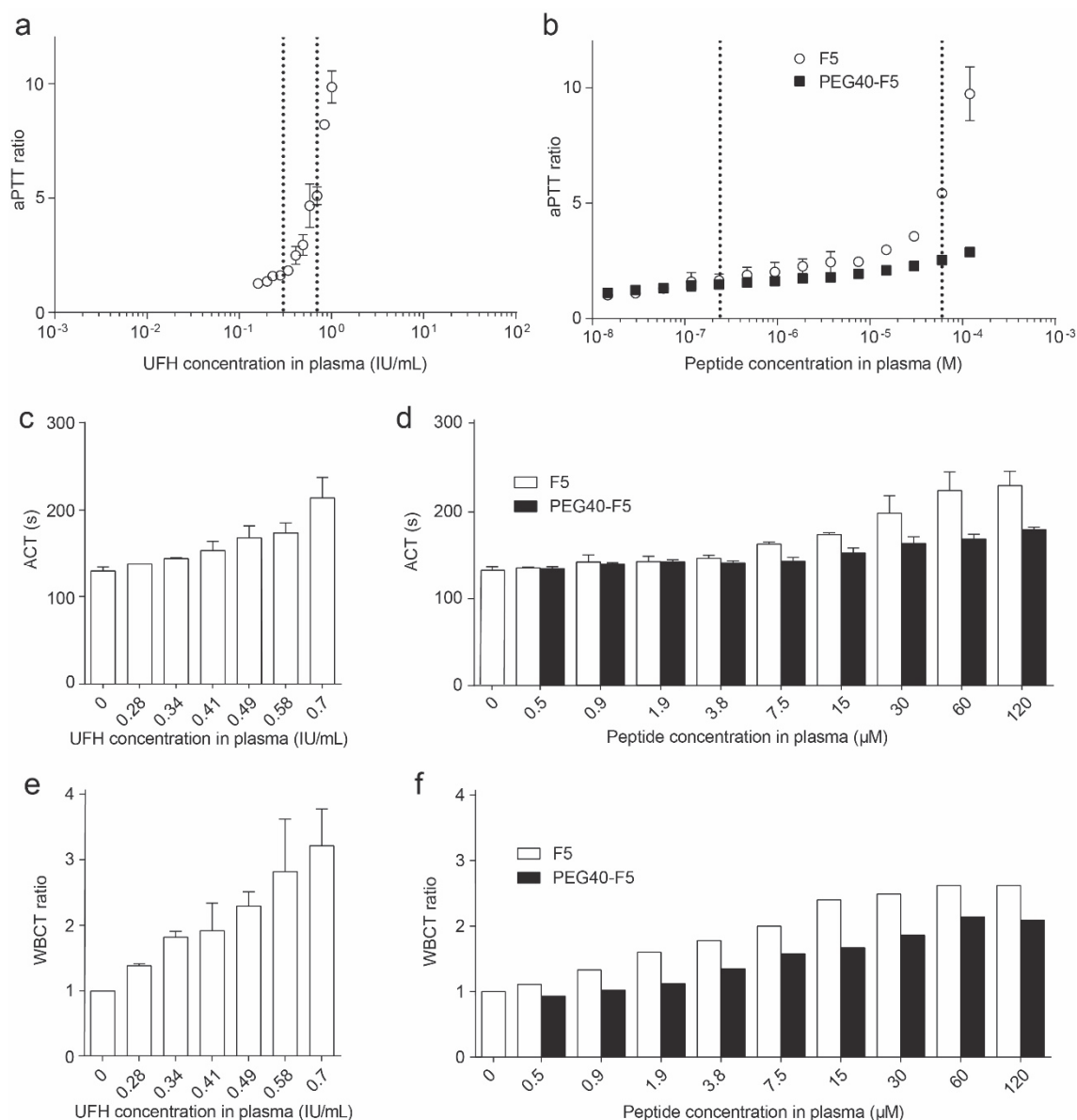


Figure 23. Comparison of cyclic peptide inhibitor with heparin and estimation of therapeutic range. a) Prolongation of aPTT by different UFH concentrations in human plasma. The dotted lines indicate the therapeutic range of 0.3 to 0.7 IU/ml. b) Prolongation of aPTT by different cyclic peptide concentrations. The dotted lines indicate the F5 concentrations at which the same aPTT prolongations are achieved as with 0.3 and 0.7 IU/ml UFH. (c and d) ACT at different concentrations of UFH c) and cyclic peptide d) in human blood. (e and f) Prolongation of WBCT at different concentrations of UFH e) and cyclic peptide f) measured with human blood.

We further estimated the minimal concentration required for therapeutic anticoagulation by testing the inhibitors in whole blood *ex vivo*. Activated clotting time (ACT) is a parameter commonly measured in the clinic for assessing anticoagulation in whole blood triggered via the intrinsic pathway of coagulation. ACT is prolonged 1.1-fold at the lower end of the

therapeutic range of UFH (0.3 IU/ml; Fig. 23c). F5 and PEG40-F5 concentrations of 0.9 and 1.9 μ M, respectively, were required to prolong the ACT to the same extent (Fig. 23d). WBCT is the time that it takes for whole blood to coagulate if left in a tube without adding a coagulation trigger, unlike in ACT. In this assay, the coagulation is initiated by contact of the blood component with the plastic surface of the tube and the assay thus represents closely a clinical situation of hemodialysis or extracorporeal membrane oxygenation (ECMO), in which coagulation may be triggered through contact of blood with plastic tubes and membranes. WBCT was prolonged 1.5-fold at 0.3 IU/ml UFH (Fig. 23e) and the same prolongation was achieved with 1.5 μ M F5 or 6.3 μ M PEG40-F5 (Fig. 23f).

4.3.5 Inhibition of the intrinsic coagulation pathway in rabbits for hours

PEG40-F5 prolonged aPTT in rabbit plasma in a dose dependent manner and an EC_{2x} of 7.3 ± 0.3 μ M (Fig. 24a). In order to assess the pharmacokinetic properties of the inhibitor and to test the activity after circulation *in vivo*, we administered PEG40-F5 to New Zealand White rabbits (n = 3) at a dose of 60 mg/kg and determined the aPTT of plasma samples at different time points (Fig. 24b). The inhibitor prolonged aPTT 1.7 to 2.5-fold over the first eight hours and showed activity even at the last time point tested (24 hrs, 1.2-fold). The anticoagulation activities measured in the first hours correspond to plasma concentrations of 4.6 – 11.8 μ M. Based on the activity reduction over time, a half-life of around one day was estimated for PEG40-F5 in rabbits.

4.3.6 Cyclic peptide suppresses coagulation in a hemodialysis model

The efficient anticoagulation activity observed in the whole blood assays (ACT, WBCT) suggested that PEG40-F5 may be used for safe anticoagulation in hemodialysis, an important and widely applied medical procedure for purifying blood of patients with impaired kidney function¹⁷⁸. A challenge in hemodialysis is the suppression of coagulation

induced by contact of blood with the tubing and the filtration membranes. Heparin is used as efficient anticoagulant in hemodialysis, but it can cause bleeding complications^{179,180}. We tested PEG40-F5 in a previously established *ex vivo* hemodialysis model¹⁸¹, in which citrated human whole blood from healthy donors is recirculated in a dialysis circuit until total clotting occurs. We used tubing and filter materials designed for infants in order to minimize the blood volume (230 ml blood per experiment) and to run the blood once every 1.5 minutes through the device. Citrate was efficiently removed after one passage of blood through the dialyzer and thus in less than around two minutes, as verified by measuring free ionized calcium levels (1.08 – 1.29 mM).

In a preliminary experiment, we tested if the PEG-F5 remained in the circulation as expected based on the large size and hydrodynamic radius of PEG40, or if it was cleared through the filter. We applied the peptide together with a high dose of UFH (3.5 IU/ml) that prevented coagulation, took samples and determined the concentration of PEG40-F5 by measuring FXIa inhibition. Control experiments showed that UFH did not interfere with the FXIa inhibition assay (Supplementary Fig. 9). PEG40-F5 was detected at similar concentrations (15.3 μ M to 22.2 μ M) over one hour of hemodialysis, showing that the inhibitor was efficiently retained in the system (Fig. 24c).

For testing the anticoagulation effect of PEG40-F5, blood from 460 ml blood bags (single donors) was split into two, and the two bags were run in parallel on two hemodialysis devices. One bag was used as negative control (saline; n = 6) and the other was injected with PEG40-F5 as a bolus to reach a plasma concentration of 30 μ M (n = 6). Blood without inhibitor clotted after 4.7 ± 2.7 minutes. Blood supplemented with PEG40-F5 clotted after 13.7 ± 4.5 min and thus 2.9-fold later, showing a strong anticoagulation effect of the cyclic peptide (Fig. 24d). For comparing the inhibitor with heparin, the same experiment was performed three times (n = 3) wherein one of the bags served again as a negative control (saline) and one was injected with UFH to reach a plasma concentration of 0.7 IU/ml, which is the concentration at the higher end of the therapeutic range. UFH delayed the coagulation 3.9-fold, which was

comparable to the time of the cyclic peptide, suggesting that the new peptidic inhibitor reached the same anticoagulation activity as the standard heparin (Fig. 24e).

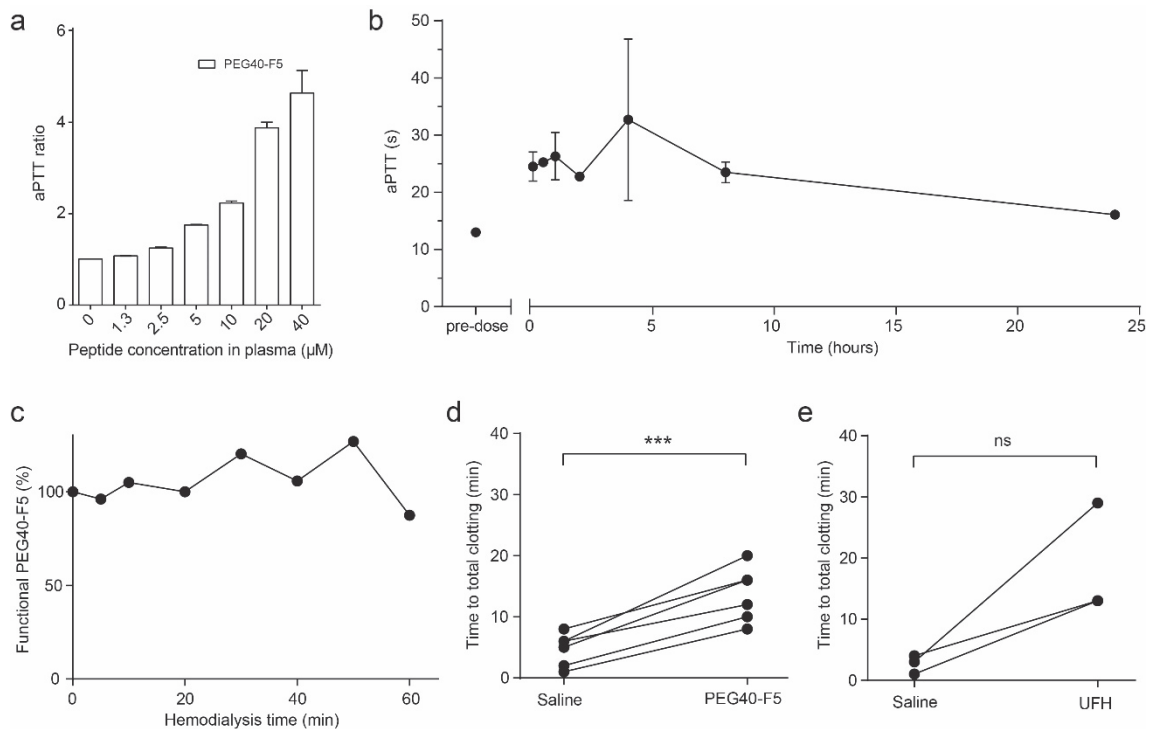


Figure 24. Inhibition of FXIa in rabbits and in a human *ex vivo* hemodialysis model. a) Prolongation of aPTT by PEG40-F5 in rabbit plasma. Mean values and SD of three measurements are shown. b) Prolongation of aPTT in plasma samples taken from New Zealand White rabbits (n = 3) injected IV with 60 mg/kg PEG40-F5 at time = 0. The aPTT of each sample was measured in triplicate and SD are indicated. c) Residual amount of functional PEG40-F5 in hemodialysis circuit at different time points. The inhibitor concentration in blood samples was determined in a FXIa inhibition assay. Blood coagulation was suppressed by co-application of a high dose of UFH. d) Prolongation of the time to total clotting within the hemodialysis circuit by PEG40-F5 (n = 6) and UFH (n = 3) compared to saline controls. For each hemodialysis experiment, blood units of a single donor were divided into two bags of 230 ml to which either inhibitor or saline was added. Statistical analyses were performed using the paired t test to compare the results within the different series (PEG40-F5 vs. saline and UFH vs. saline). *** = p < 0.001, ns = not significant.

4.4 Conclusions

We have identified a cyclic peptide that inhibits the coagulation FXIa with single-digit nanomolar affinity and high selectivity over homologous proteases. While previously developed peptide-based FXIa inhibitors - also in our laboratory - were not inhibiting efficiently FXIa homologs of animals and could not be tested *in vivo*, the newly generated peptide F5 inhibits rabbit FXIa, which is key for *in vivo* evaluation and preclinical development. Importantly, the peptide F5 is active in plasma and whole blood, which is a further requirement for its development towards a therapeutic. Key for the identification of the peptide inhibitor was most likely the screening of a new combinatorial cyclic peptide library that is larger and structurally much more diverse than any previously reported peptide repertoire. Our work showed that peptide-based inhibitors can be developed to FXIa. A small structure-activity relationship study including only a few variants of the phage-selected peptide F1 showed that a monocyclic peptide is sufficient for binding and inhibition. The latter finding was of interest because monocyclic peptides are easier to manufacture than double-bridged peptides, that need to be synthesized by step-wise bridging of two pairs of cysteines and that depend on a synthesis strategy with orthogonal cysteine protecting groups.

We found that the half-life of the cyclic peptide F5 can be modulated by PEGylation, which offers the possibility of tailoring its pharmacokinetic properties. A conjugate of the peptide with a 40 kDa PEG chain had a half-life of several hours in rabbits, which corresponds to more than one day or even several days in human. Depending on the specific therapeutic application, smaller PEG chains may be used to achieve shorter half-lives. For example, for the suppression of contact activation in extracorporeal circulation or in hemodialysis, procedures that usually do not take longer than a few hours, a smaller PEG chain could yield a shorter half-life. Conversely, for preventing thrombosis on several days after surgery, a longer exposure is desired and an inhibitor with a longer PEG chain may be used.

With the potent and specific FXIa inhibitor in hand, we could address the question whether FXIa inhibition by a peptide leads to efficient anticoagulation, and if the FXIa inhibition rivals anticoagulation activities of established anticoagulants such as heparin. Specifically, we asked the question if contact activation occurring by exposure of human blood to plastic tubes and membranes, used in medical devices for extracorporeal circulation, can efficiently be suppressed by the peptide FXIa inhibitor. We found that the cyclic peptide can delay the clotting of whole blood incubated in polypropylene tubes by the same extent as heparin (UFH) applied at a therapeutic dose. The absolute concentrations of the peptide required to reach the effects achieved with the minimal therapeutic dose of UFH were 1.5 μM for the peptide F5 and 6.3 μM for the PEGylated peptide PEG40-F5. These concentrations are relatively high for therapeutic application, but the potency of the inhibitor may be improved by increasing the binding affinity for FXIa. It is worth to mention that the peptide F5 was not matured in terms of affinity or stability, as usually done for *in vitro* evolved peptides. The potency may be improved by optimizing the amino acid sequence using natural or unnatural amino acids, a strategy that we are applying routinely to improve phage-selected peptides^{58,59,182}.

We were pleased to see that the PEGylated peptide remained functional 24 hours after IV administration to rabbits, showing that the peptide is not deactivated by proteases or other mechanisms *in vivo*. A potential application of the inhibitor could be the suppression of contact activation in hemodialysis. Inhibition of FXIa could potentially prevent coagulation as efficiently as heparin but is expected to have a smaller bleeding risk. In addition, some hemodialysis patients cannot be anticoagulated by heparin due to heparin induced thrombocytopenia (HIT). We found that the PEG40-F5 efficiently delayed blood clotting in an *ex vivo* model of hemodialysis to a similar extent as heparin applied at the maximal recommended dose of 0.7 IU/ml for the standard anticoagulant.

In summary, we present the development of a first peptide-based FXIa inhibitor that shows good affinity, selectivity and plasma stability, and that inhibits also FXIa of an experimental animal, enabling *in vivo* evaluation. We show that the pharmacokinetics of the peptide can be modulated by PEGylation, enabling inhibition of FXIa for 24 hours in rabbits, which corresponds potentially to days in human. We furthermore found that the peptidic inhibitor suppresses contact activation in blood as well as heparin applied at its therapeutic dose, and we show that it works as well as heparin in an *ex vivo* hemodialysis model. The properties of this molecule make it a good candidate for indications of thrombosis prevention such as hemodialysis and post-operative anticoagulation, where there is a clear unmet need for safer anticoagulation strategies.

4.5 Material and methods

Phage selections

The library used for phage selection was described previously (chapter 3). Phage selections were performed as previously reported (chapter 3), with a few modifications. Library glycerol stocks were inoculated to reach an $OD_{600}=0.1$ in 1 L 2YT/ampicillin (100 $\mu\text{g/ml}$) culture with 100 mM glucose. Serial dilutions of the starting culture were plated on 2YT/ampicillin (100 $\mu\text{g/ml}$). The culture was grown at 37° C until it reached $OD_{600}=0.5$. Serial dilutions of the culture were plated on 2YT/ampicillin (100 $\mu\text{g/ml}$) plates. The culture was then infected with hyperphage M13 K07 Δ pIII (Progen Biotechnik GmbH) as described before. Serial dilutions of the culture were plated on 2YT/ampicillin (100 $\mu\text{g/ml}$) + kanamycin (50 $\mu\text{g/ml}$) plates in order to determine the fraction of infected cells. Cells were then pelleted and resuspended in 1 L of 2YT/ampicillin (100 $\mu\text{g/ml}$) + kanamycin (50 $\mu\text{g/ml}$) medium. The culture was then grown at 30° C overnight with shaking (250 rpm). Cultures were pelleted, and the supernatant was kept. A supernatant sample was stored at 4° C. Phage precipitation with PEG/NaCl was performed as described before. The phage pellet was re-suspended in 20 ml degassed reaction buffer. Phage precipitates and remaining cells were removed by centrifugation and the supernatant was kept. 40 μl phage sample was used to determine phage titers by performing serial dilutions in 2YT medium and using them to infect 180 μl of *E. coli* TG1 cells ($OD_{600} = 0.5$). 20 μl of cells infected with the different phage dilutions were plated on 2YT/ampicillin (100 $\mu\text{g/ml}$) plates and CFUs were counted. Phage titers were determined at all crucial steps of the process (before and after reduction, cyclization and panning).

The cysteine residues of the peptides on phage were reduced as described before. The phage was subsequently precipitated with PEG/NaCl as described before. Phage were resuspended in 72 ml of reaction buffer. A sample was stored at 4° C for phage titer determination. Chemical linkers were added at 40 μM (final conc., 1 mL of each linker to 9 mL of phage) and

the reaction incubated at 30° C for 1 h. Phage were again precipitated and finally the phage pellet resuspended in 10 ml binding buffer containing BSA and Tween 20 and stored at 4° C. A sample was stored for phage titer determination.

FXIa (Molecular Innovations) was biotinylated as explained before (chapter 3). 5 µg of biotinylated target protein were incubated with 50 µl magnetic streptavidin beads (Dynabeads® M-280 Streptavidin, ThermoFisher Scientific, Waltham, MA, USA) in 500 µl binding buffer for 10 minutes and non-immobilized protein was removed by washing three times. Beads were then resuspended in 300 µl binding buffer containing BSA and Tween 20 and incubated on a rotating wheel at room temperature for 30 min. Beads were added to modified phage and incubated 30 min at 10 rpm on a rotating wheel. Beads were then washed as described previously. Active site binders were selectively eluted by incubating beads with 100 µl of 1 mM PPACK (D-phenylalanyl-prolyl-arginyl chloromethyl ketone) for 30 min on the rotating wheel. Supernatant was kept, and beads were then resuspended in 100 µl of 20 mM glycine as described before in order to elute the remaining phage. The acid pH of the solution was neutralized with 100 µl of 1 M Tris/HCl, pH 8.0. Both PPACK and glycine-eluted phage were added to 10 ml of TG1 *E. coli* cells ($OD_{600} = 0.5$). After 30 min incubation at 37 °C, bacteria were plated on 2YT/ampicillin (100 µg/ml) plates and grown overnight at 37 °C. Phage titers were also determined. Bacterial cells of the colonies were recovered in 2YT medium with 20 %, flash frozen in liquid nitrogen and stored at -80 °C. Neutraavidin and streptavidin beads were alternated as described before. In the third (the last) selection round 0.5 µg of biotinylated target protein were immobilized on beads in order to enrich potent binders.

Next Generation Sequencing (NGS)

The DNA from the phage selected in the third round was isolated with a kit for plasmid purification (Macherey-Nagel). The DNA sequences encoding the peptides were amplified in a first PCR using a mixture (equimolar) of 5 forward primers and 5 reverse primers:

NGS forward hyper 1-5

5' -TCGTCGGCAGCGTCAGATGTGTATAAGAGACAG(N)_xCTGCTGGCAGCTCAGC-3'
x= 0 to 4

NGS reverse hyper 1-5

5'-GTCTCGTGGGCTCGGAGATGTGTATAAGAGACAGG(N)_xCAGTTTCAGCGCCAGAACC-3'
x= 0 to 4

For the reaction, primers (40 nM each, final conc.), dNTP mix (250 μM each, final conc.), 100 ng of phagemid DNA as template, 0.9 μl DMSO, 6 μl of 5x HF buffer and 0.6 units of Phusion High fidelity Polymerase (New England Biolabs) were used in a 30 μl PCR reaction. 25 PCR cycles were performed (initial denaturation at 98° C for 2 min, then 25 cycles of 98° C for 15 sec, 55° C for 30 sec, and 72° C for 15 sec and final elongation at 72° C for 5 min). The products were analyzed by agarose (UltraPure agarose, Invitrogen) gel electrophoresis (2.5 % agarose gel). A second PCR was performed with primers containing the adapter and index sequences. The following primers were used:

NGS 2nd Forward S505

5'- AATGATACGGCGACCAACGAGATCTACACGTAAGGAGTCGTCGGCAGCGTC-3'

NGS 2nd Reverse N706

5'-CAAGCAGAAGACGGCATAACGAGATCATGCCTAGTCTCGTGGGCTCGG-3'

A PCR reaction with total volume of 60 μl was set up, which contained primers (400 nM, final conc.), dNTP mix (250 μM each, final conc.), 2 μl of PCR 1 product, 1.8 μl DMSO, 12 μl of 5x HF buffer and 1.2 units of Phusion High fidelity Polymerase (New England Biolabs). The PCR was performed applying the same program as described above. PCR products were run on a agarose gel (2.5 %, UltraPure agarose, Invitrogen). A kit for gel extraction (QIAquick Gel Extraction Kit, Qiagen) was applied to purify them. Sequencing was performed as described previously¹⁸³. Results from sequencing were analyzed with MatLab scripts developed in our group as previously described¹⁷⁴.

Chemical synthesis of cyclic peptides

Peptides synthesis was performed as described before (chapter 3) in 50 μmol scale, using SPPS, Fmoc chemistry, rink amide AM resin and DMF as solvent. Cleavage of peptide was

performed with a cocktail containing 90% TFA, 2.5% thioanisole, 2.5% H₂O, 2.5% 1,2-ethanedithiol, 2.5% phenol, followed by ether precipitation. Peptides were purified by RP-HPLC (Prep LC 2535 HPLC, Waters) on a C18 column (Sunfire prep C18 TM ODB, 10 μ m, 100 Å, 19 \times 250 mm, Waters) at 20 ml/min flow rate, using ddH₂O/0.1% TFA and acetonitrile/0.1% TFA as solvents. Fractions containing pure peptides were lyophilized. For cyclization, peptides were dissolved in 8.5 ml 60 mM NH₄HCO₃, pH 8.0 and 1.5 ml acetonitrile at 1 mM, and reacted with 2 mM linker (monocyclic peptides) or 4 mM linker (double-bridged peptides) for 1 hr at 30°C. The reaction was stopped by adding formic acid to 2% (v/v) of total volume. The chemically modified peptide was purified by RP-HPLC and pure fractions were lyophilized. Peptide purity was analyzed by running the peptide solutions on the analytical HPLC (1260 HPLC system, Agilent) equipped with a C18 column (ZORBAX 300SB-C18, 5 μ m, 300 Å, 4.6 \times 250 mm, Agilent). Peptide masses were confirmed by ESI-MS on a single quadrupole LCMS (LCMS-2020, Shimadzu) in positive ion mode.

PEGylation of cyclic peptides and purification

A 40 kDa linear PEG-NHS (SUNBRIGHT ME-400HS, NOF Europe) was conjugated through an NHS-ester reaction to the peptide via the N-terminal amine group. The reaction was performed in aqueous solution containing 15 mM HEPES, pH 7, with peptide at a concentration of 800 μ M and PEG at 1.6 mM and was incubated for 2 h at RT. The reaction was monitored by analytical RP-HPLC (1260 HPLC system, Agilent), with a C8 column (Aeris™ 3.6 μ m WIDEPORE XB-C8 200 Å, 150 \times 2.1 mm, Phenomenex), with a 0-100% gradient of solvent B (acetonitrile, 0.1% TFA v/v) in solvent A (ddH₂O, 5% acetonitrile v/v, 0.1% TFA v/v) in 30 minutes. The conjugate was then separated from unreacted PEG and peptide via cation exchange chromatography, using a 100 ml column packed with Capto SP ImpRes resin (GE Healthcare) and 15 mM HEPES and 1 M NaCl as solvents (linear gradient). The mass of the conjugate was checked with a MALDI-TOF mass spectrometer (AutoFlex Speed, Bruker). Subsequently, a desalting step with a HiPrep desalting column (GE

Healthcare) was added to remove salts from previous purification step and to remove remaining unreacted peptide. Pure fractions were lyophilized and dissolved in ddH₂O at a concentration of 1 mM. Purity was characterized by analytical HPLC as described above.

Assessment of inhibitory activity of selected peptides

For the K_i determination of peptides, the residual enzymatic activities of coagulation factor XIa incubated with serial dilutions of inhibitor (10 μ M to 900 pM final conc.) were assessed with the substrate Pyr-Pro-Arg-pNA (Bachem). Activity curves were determined as described before (chapter 3) at 25°C in an activity assay buffer. Reactions were started by adding the substrate (400 μ M final concentration) to 0.5 nM FXIa in presence or absence of bicyclic peptides. The release of pNA (p-nitroaniline), following hydrolysis of the substrate, was monitored over at least 20 min by measuring the increase in absorbance per minute at 405 nm using an absorbance microtiter plate reader (Infinite M200 Pro, Tecan). The rate of substrate cleavage is proportional to enzymatic activity. The IC_{50} values were determined by applying the following equation:

$$y = \frac{100}{1 + 10^{(\log IC_{50} - x)p}}$$

Wherein y is the residual activity (%) of protease, x is the logarithm of peptide concentration, IC_{50} is the inhibitor concentration necessary to achieve 50% inhibition, and p is the Hill coefficient. The K_i values were obtained applying the equation:

$$K_i = \frac{IC_{50}}{1 + \frac{[S]_0}{K_m}}$$

Wherein $[S]_0$ is the initial substrate concentration, and K_m is the substrate Michaelis constant. The K_m of FXIa for Pyr-Pro-Arg-pNA was determined to be $255 \pm 14 \mu$ M.

For specificity profiling, the residual activities of several serine proteases homologous to FXIa were determined similarly as described above. The final concentrations of the proteases were: 2 nM β -FXIIa, 0.1 nM trypsin, 7.5 nM tPA, 1.5 nM uPA, 2 nM thrombin, 0.25 nM plasma kallikrein, 2.5 nM plasmin (all from Molecular Innovations, PK from Innovative research). Fluorogenic substrates (Bachem) were used at 50 μ M: Z-Phe-Arg-AMC for PK, Z-Gly-Gly-Arg-AMC for thrombin, trypsin, tPA and uPA, H-D-Val-Leu-Lys-AMC for plasmin. Fluorescence (AMC ex. 368 nm, em. 467 nm) was measured at 25 °C over time using a fluorescence microtiter plate reader (Infinite M200Pro, Tecan).

Plasma stability assays

Plasma stability assays were performed as described previously⁵⁸. Briefly, 18 μ L of peptide solution were added to 892 μ L of human citrated plasma (Innovative Research) to a final concentration of 40 μ M. Samples were incubated at 37 °C and 30 μ L samples were taken at 0, 0.5, 1, 2, 4, 8, 24, and 48 h, diluted to 400 μ L with activity assay buffer without BSA, and incubated for 20 min at 65 °C. Samples were then centrifuged for 5 min at 16 000 g to remove proteins and serially diluted, obtaining peptide concentrations within 1 μ M to 900 pM. Finally, the residual activity of FXIa was measured. Residual inhibitory activity was calculated as a fraction of the activity at time = 0.

aPTT and PT coagulation activity measurements

aPTT and PT coagulation assays were performed in order to characterize the anticoagulation activity of the peptide and were assessed plasma from human or New Zealand white rabbit using a STAGO STart4 machine (Diagnostica Stago). For PT, 50 μ L of citrated human single donor plasma (with or without peptide dilutions) were incubated for 2 min at 37 °C. 100 μ L of Innovin (activator of the extrinsic pathway; Dade Behring/Siemens) were then added with the instrument's pipette. The movement (induced electromagnetically) of a ball made out of steel in plasma was recorded by the instrument. The coagulation time was defined as the time

after addition of Innovin until the ball stopped moving. For aPTT with citrated human single donor plasma, 100 μ L of plasma (with or without peptide dilutions) were added to 100 μ L of Pathromtin SL or Dade Actin activated cephaloplastin (for experiments for the determination of the therapeutic range) (Activator of the intrinsic pathway; Siemens) and incubated for 2 min at 37 °C. 100 μ L of CaCl_2 solution (25 mM, Siemens) were added with the dedicated pipette, which triggered coagulation and movement of the steel ball was monitored as described above. For aPTT with citrated rabbit single donor plasma, the same procedure was followed, except for the use of Dade Actin activated cephaloplastin and 3 min incubation time.

Whole blood clotting time (WBCT)

WBCT tests were performed to characterize the anticoagulation activity of peptides in whole blood. 472.5 μ L of freshly drawn citrated human single donor whole blood (Cambridge Bioscience) were incubated with 7.5 μ L of peptide (final plasma conc. ranging from 0.5 to 120 μ M), or unfractionated heparin (final plasma conc. ranging from 0.3 to 0.7 IU/ml) or PBS (negative control) at 37°C for 10 min. 20 μ L of 0.5 M CaCl_2 (final conc. 20 μ M) were then added to in order to allow for the activity of calcium-dependent serine proteases of the coagulation cascade. The coagulation status was checked every 30 s by inverting the tubes. Total clotting was defined as the ability to hold the sample tube upside-down without causing the sample to fall. Time to total clotting from the addition of CaCl_2 was recorded as clotting time.

Activated clotting time

ACT tests were performed to characterize the anticoagulation activity of peptides in whole blood. Briefly, 7 μ L of peptide (final plasma concentration ranging from 0.5 to 120 μ M), or unfractionated heparin (final plasma conc. ranging from 0.3 to 0.7 IU/ml) or PBS (negative control) were added to 213 μ L of freshly drawn citrated human single donor whole blood

(Cambridge Bioscience). 200 μ L of sample were added into Recalcified Activated Clotting Time (RACT) cartridges (Medtronic), containing 100 μ L of 2.2% kaolin and 50 μ M CaCl_2 in HEPES buffer and sodium azide and the ACT clotting time was recorded using the automated ACT Plus machine (Medtronic).

Ex vivo hemodialysis study

20 *ex vivo* hemodialysis experiments were performed in total (10 parallel series, n=20 hemodialysis). Freshly drawn blood from 10 donors (400 ml whole blood per donor) collected in CPD bags was used (Cambridge Bioscience). Blood from each bag was split equally in two bags and two hemodialysis circuits were built. Two Fresenius 4008 S dialysis machines (Fresenius Medical Care) were run in parallel with two FX50 Cordiax dialyzers (Fresenius Medical Care). The composition of the dialysis solution was: potassium at a final concentration of 4 mM, calcium at 1.25 mM, glucose at 1 g/L, sodium at 138 mM, magnesium at 0.5 mM, chlorine at 110.5 mM and bicarbonate at 32 mM. The flow of the dialysate was 500 ml/min. Peptide (final plasma conc. 30 μ M), unfractionated heparin (final plasma conc. 0.7 IU/ml) or saline were injected into the blood bag. In each series either peptide or heparin-containing blood was dialyzed in parallel with saline-containing blood (negative control). The circuits were primed with 0.5 L of saline (0.9 % NaCl) and then both the arterial and the venous side were connected to the blood bag and blood was recirculated at 150 ml/min and dialyzed until total clotting. Blood samples were drawn at different time points (at 0, 5, 10, 20, 30 min after dialysis start) and ACT was measured. In addition, blood was also processed to plasma by centrifugation in vacutainer tubes (BD) at 2000 g for 15 min for subsequent analyses and to assess the concentration of ionized calcium, used to estimate the time taken by the dialyzer to remove sodium citrate. When total clotting within the circuit occurred, blood recirculation had to be discontinued because of high pressure in the hemodialysis machine. Time until total clotting was recorded. Statistical analyses were performed using a paired t test to compare the results within the different series. In addition, in one experiment

(used to evaluate the extent of peptide elimination from the system), the peptide was injected at a plasma concentration of 30 μ M, together with 3.5 IU/ml of UFH. The hemodialysis run was performed as described above. Samples of blood were taken at 5, 10, 20, 30, 40, 50 and 60 min and processed to plasma. Residual FXIa inhibitory activity of the peptide was tested as described previously (section plasma stability assays). In parallel, control experiments were run in order to evaluate the possible effect of 3.5 IU/ml UFH on FXIa inhibition.

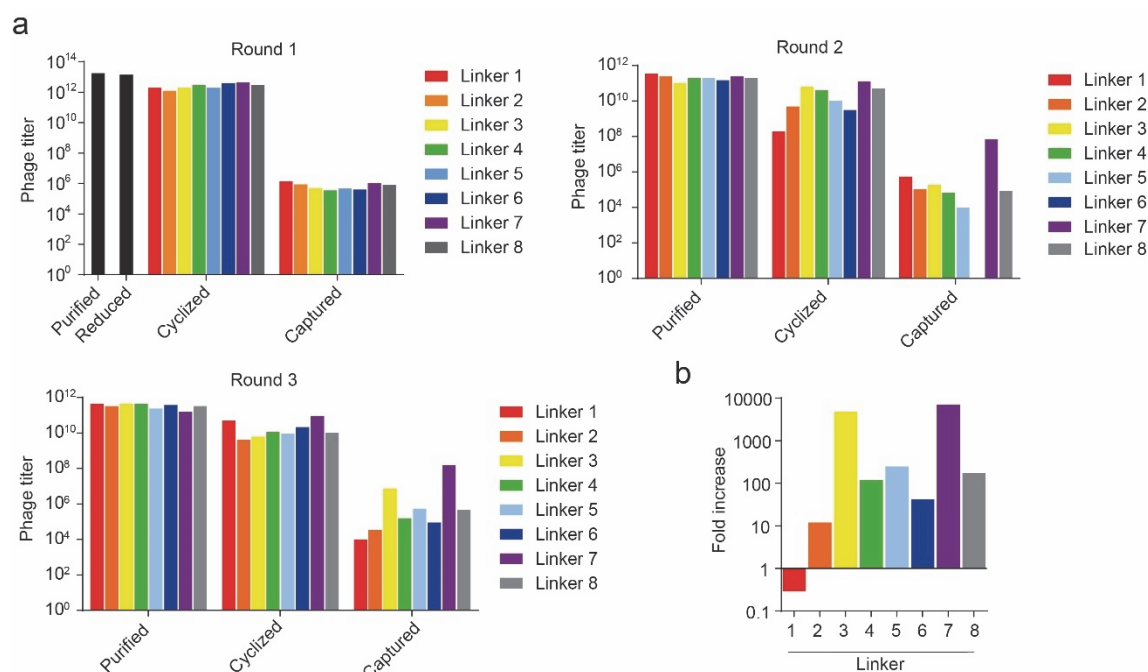
PK study in rabbits

The study was performed in 3 New Zealand white (NZW) rabbits (female, 2-3 kg). Test peptide was administered to the animals by IV injection in the marginal ear vein. 4.2 ml of peptide solution in PBS were injected at a dose of 60 mg/kg, reaching a plasma concentration of around 40 μ M. Blood samples were collected via the auricular artery in sodium citrate Vacutainer tubes (BD) according to the following schedule: pre-dose, 5, 30, 60, 120, 240, 480, 1440 min. Blood samples were immediately processed to plasma by centrifugation at 2000 g for 15 minutes at 4°C and frozen immediately. aPTT of the collected samples was then tested in order to determine the anticoagulation activity of the peptide *in vivo* over time.

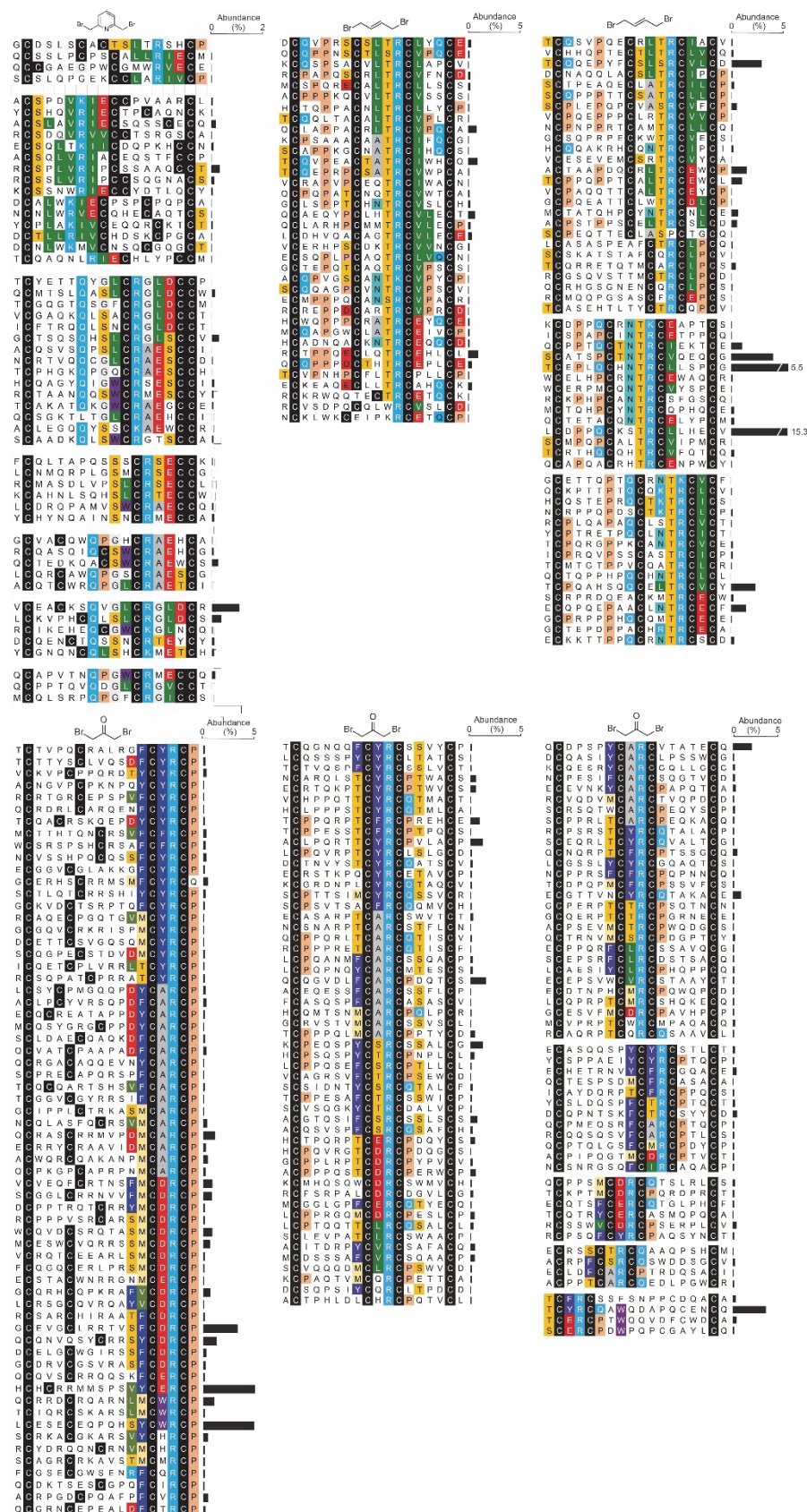
Statistical analysis

Statistical analysis of the results of the *ex vivo* hemodialysis study was performed with a two-tailed paired t-test using the software Prism 5 (GraphPad). Significance threshold was defined as $p < 0.05$.

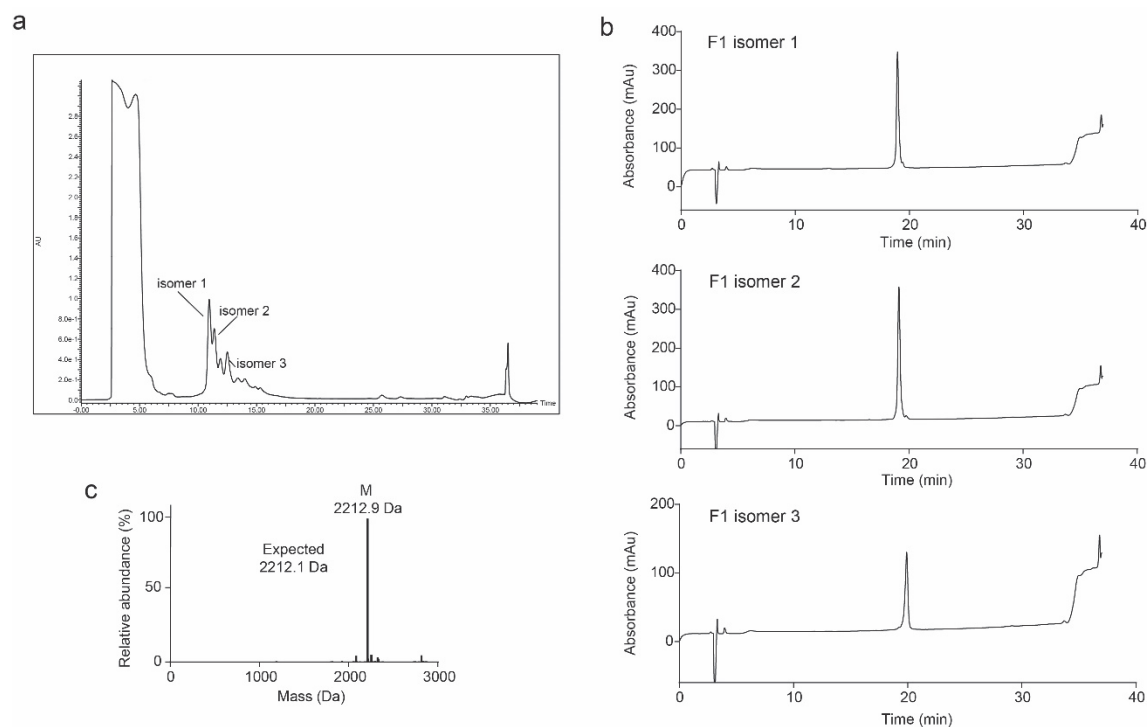
4.6 Supplementary information



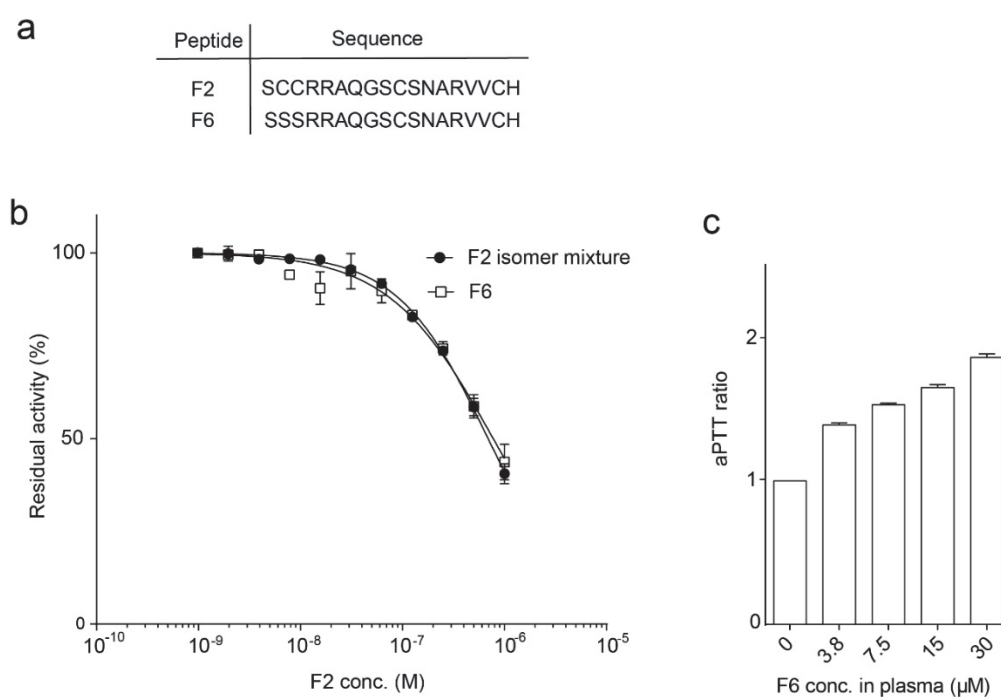
Supplementary Figure 3. Phage titers indicative for the enrichment of target-specific peptides.



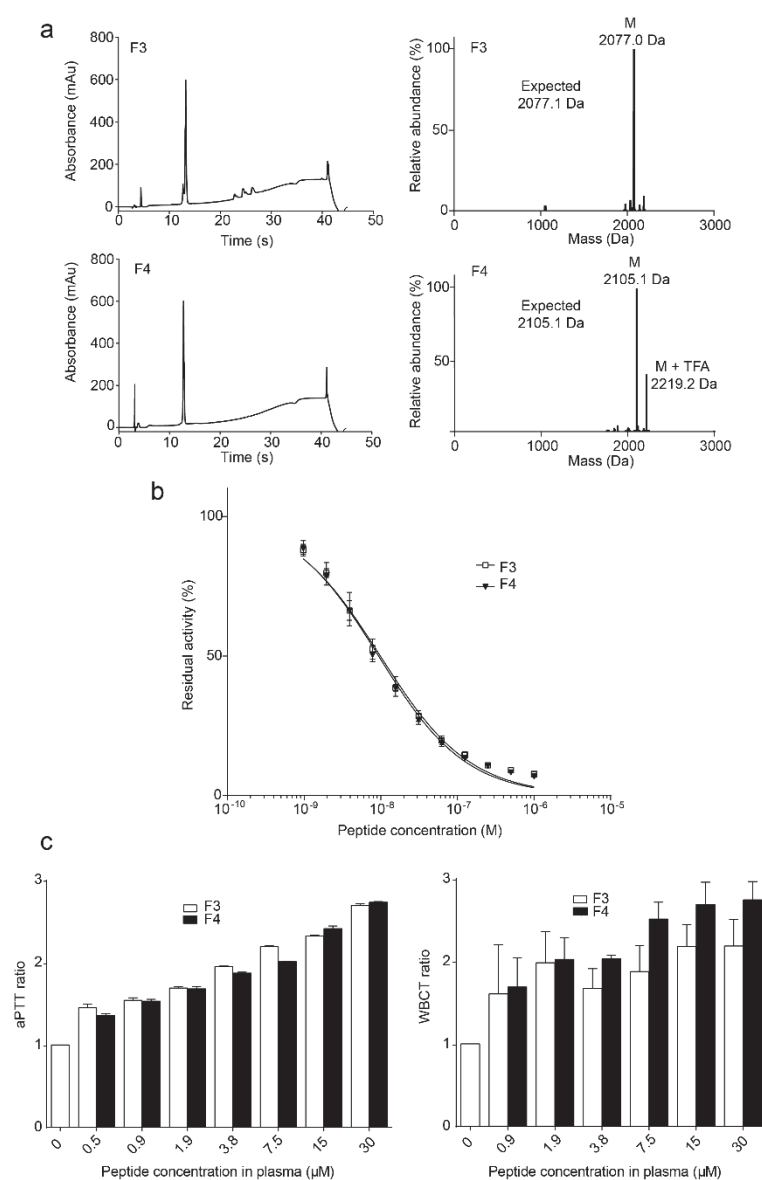
Supplementary Figure 4. Peptides isolated in round 3 sharing consensus sequences. Peptides shown do not include the ten most abundant sequences shown in Fig. 1c. Sequence similarities are highlighted in color and the relative abundance of each sequence is indicated.



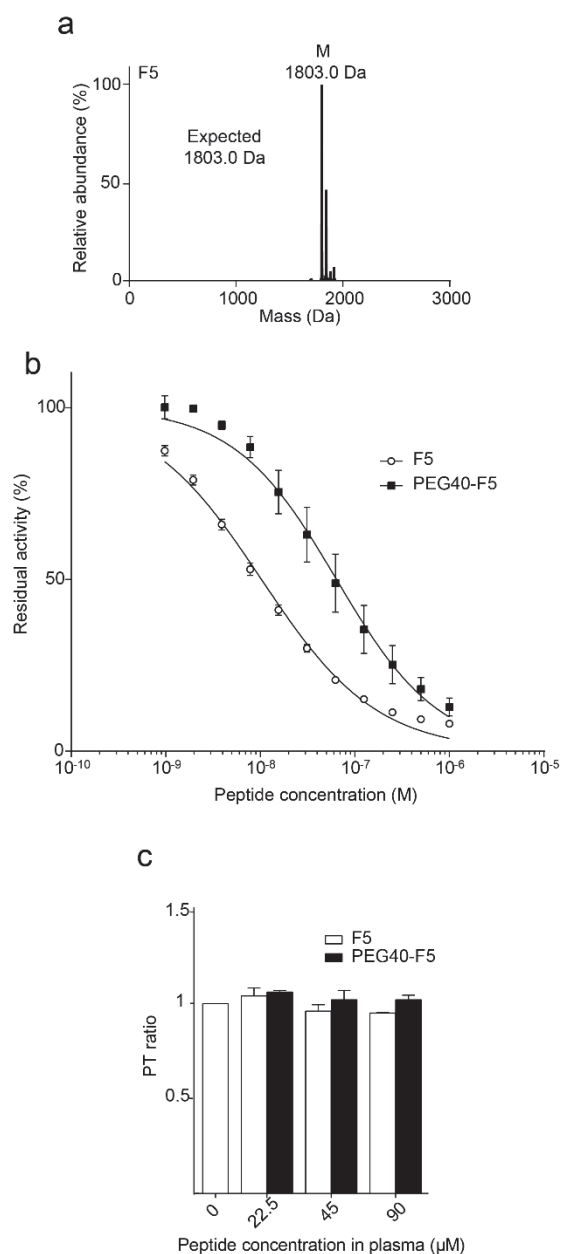
Supplementary Figure 5. Purification of peptide isomers of F1 by HPLC. a) Preparative HPLC chromatogram. The three major peaks were collected and showed all the expected mass of 2212.1 Da. b) Analytical HPLC chromatograms of the three isolated fractions. c) Mass spectrometric analysis of the isomer 3.



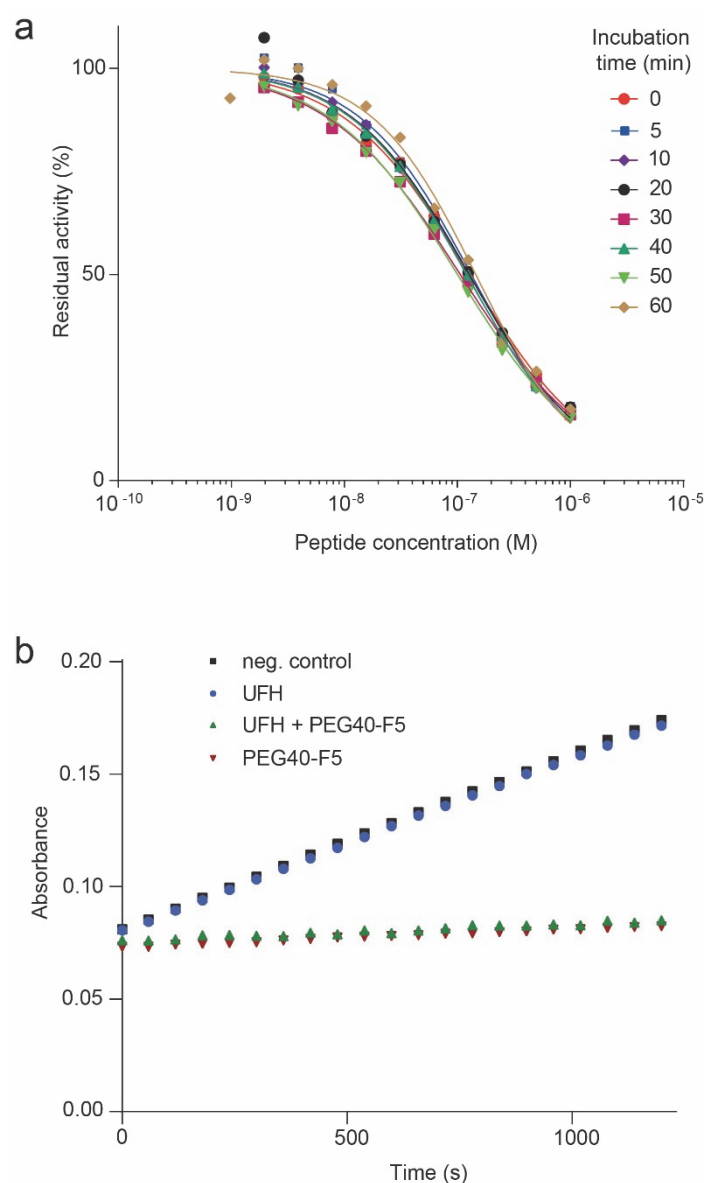
Supplementary Figure 6. Characterization of bicyclic peptide F2. a) Sequence of F2 and the monocyclic analogue F6. b) Inhibition of human FXIa by the peptides F2 and F6. Mean values and SD of three measurements are shown. c) Prolongation of aPTT by F6 in human plasma. Mean values and SD of three measurements are shown.



Supplementary Figure 7. Characterization of monocyclic and mutated peptides F3 and F4. a) Analytical HPLC chromatograms and mass spectra. b) Inhibition of human FXIa by F3 and F4. Mean values and SD of three measurements are shown. c) Prolongation of aPTT in human plasma and WBCT in human blood. Mean values and SD of three measurements are shown.



Supplementary Figure 8. Characterization of peptide F5 before and after PEGylation. a) Mass spectrum of F5. b) Inhibition of human FXIa by F5 and PEG40-F5. Mean values and SD of three measurements are shown. c) Prolongation of PT by F5 and PEG40-F5 in human plasma. Mean values and SD of three measurements are shown.



Supplementary Figure 9. Concentration of PEG40-F5 in blood bag during hemodialysis. a) Inhibition of FXIa by blood samples taken at different time points of circulation in the hemodialysis circuit. b) Effect of UFH (3.5 IU/ml) on FXIa inhibition in presence/absence of PEG40-F5 (30 μ M) measured by a chromogenic substrate of FXIa. The increase in absorbance at 405 nm is proportional to the residual enzymatic activity.

5 Fast binding kinetics of a coagulation factor inhibitor are key for strong anticoagulation

This chapter is based on a manuscript that will be submitted for publication. I will be the only first author in this publication.

5.1 Abstract

Coagulation factor XIa (FXIa) is an attractive therapeutic target due to its role in thrombosis while being not essential for hemostasis. We have recently developed FXIa inhibitors based on cyclic peptides using phage display and observed that the anticoagulation activity (prolongation of clotting in plasma) of several of the inhibitors did not directly correlate with the strength of FXIa inhibition (K_i). In this work, we characterized four of the inhibitors in detail to understand the underlying molecular basis for the variable anticoagulation activities. An alanine scan of a cyclic peptide FXIa inhibitor having a particularly strong anticoagulation activity but rather weak K_i identified a lysine residue that is key for the peptide's anticoagulation activity and pointed to an electrostatic interaction. Analysis of the peptides' binding kinetics revealed that the peptide with lysine has a more than 10-fold faster on-rate than all other peptides, most likely due to the electrostatic attraction of the lysine. Our results underscore that rapid target binding can be important to block fast biological processes such as the activation of the coagulation cascade, and recommend the introduction of electrostatic interactions in the development of coagulation inhibitors.

5.2 Introduction

Blood coagulation is an essential physiological process that is activated upon vascular injury to stop bleeding. The coagulation cascade can be divided into extrinsic and intrinsic pathway, that converge into a common pathway, which ultimately leads to the formation of a fibrin plug. Inappropriate activation of the coagulation cascade leads to thrombosis, a major cause of morbidity and mortality worldwide⁹⁵. It involves the abnormal formation of a clot that can occlude blood vessels in the arterial and venous circulation and might lead to infarction of tissues. Prophylaxis of many of these conditions involves the use of anticoagulants that inhibit factors of the coagulation cascade. Anticoagulants currently in clinical use block one or multiple factors of the extrinsic coagulation pathway, which is essential for hemostasis, and they thus all bring a risk of bleeding^{105,111,144}.

Towards the development of safer anticoagulants, coagulation factor XI has received much attention due to its role in thrombosis while being not essential for homeostasis. Several inhibitors based on small molecules, antibodies and antisense oligonucleotides have been developed and are at various stages of clinical development^{121,127,144}. Our laboratory has recently developed FXIa inhibitors based on cyclic peptides. The peptides were isolated from large combinatorial libraries of cyclic or bicyclic peptides using phage display. One of the peptides was further characterized and proved to be efficient at inhibiting blood coagulation in tubes *ex vivo*, stable and active *in vivo* (rabbits) and to suppress coagulation in a hemodialysis model using human blood (chapter 4).

When comparing the anticoagulation activities of the phage-selected peptides with their FXIa inhibitory activities (K_i s), we observed that the two parameters did not correlate for most of the inhibitors analyzed. The anticoagulation activities were assessed by measuring the prolongation of activated partial thromboplastin time (aPTT) in human plasma at an inhibitor concentration of 30 μ M (chapter 4). The aPTT is the time needed for blood plasma

to coagulate upon addition of a reagent that triggers the intrinsic coagulation pathway. The inhibition of FXIa was determined by measuring the residual activity of purified FXIa using a chromogenic protease substrate and calculating the inhibitory constant K_i . In this study, we investigated the molecular basis for this discrepancy of anticoagulation activity and inhibition activity. Towards this end, we characterized four of the inhibitors in more detail. For one inhibitor with a strong anticoagulation activity and a comparatively weak K_i , we performed an alanine scan and found that a lysine residue was contributing much to the anticoagulation affinity and to a lesser extent to the binding affinity, which hinted at an electrostatic interaction and a potentially fast binding kinetic. We indeed found that the peptide has a particularly fast binding kinetics and identified this as the reason for the strong anticoagulation activity. Our finding may encourage the incorporation of charges in the development of coagulation factor inhibitors or in agents interfering with other fast biological events such as coagulation.

5.3 Results and Discussion

5.3.1 Anticoagulation activity and K_i do not correlate

We chose four of nine phage-selected bicyclic peptides that we had characterized so far only roughly by measuring their K_i and determining their aPTT value at a peptide concentration of 30 μ M (Fig. 25a and 25b) and characterized them in more detail. The four peptides included peptide **4**, for which we observed a particularly large disconnection between inhibitory activity and anticoagulation activity (indicated with an asterisk in Fig. 25a). We assessed the anticoagulation activity of the peptides by measuring the effect on the aPTT at different inhibitor concentrations and calculated the concentration at which the aPTT increased by 50% ($EC_{1.5x}$) (Fig. 25c). Plotting of the $EC_{1.5x}$ values of the peptides versus their K_i values confirmed the large disconnection between the two parameters (Fig. 25d). In particular, peptide **4** showed a strong effect on the aPTT, while having the worst inhibitory activity. In contrast, peptide **3** had the weakest anticoagulation effect while showing high binding affinity.

5.3.2 Efficient anticoagulation is not based on multi-target inhibition

The efficient anticoagulation activity of peptide **4** could potentially result from the inhibition of additional coagulation factors, as several of them are also trypsin-like serine proteases that have a similar structure and substrate specificity as FXIa. In a first experiment, we tested if the prothrombin time (PT) is prolonged by peptides **1** to **4**. PT is the coagulation time of blood plasma upon addition of an activator of the extrinsic coagulation pathway and it is expected to be prolonged in the case that a peptide inhibits a protease of the extrinsic or common coagulation pathway. Even at the highest peptide concentration tested (150 μ M), none of peptides prolonged the PT, suggesting a high target selectivity (Fig. 25e).

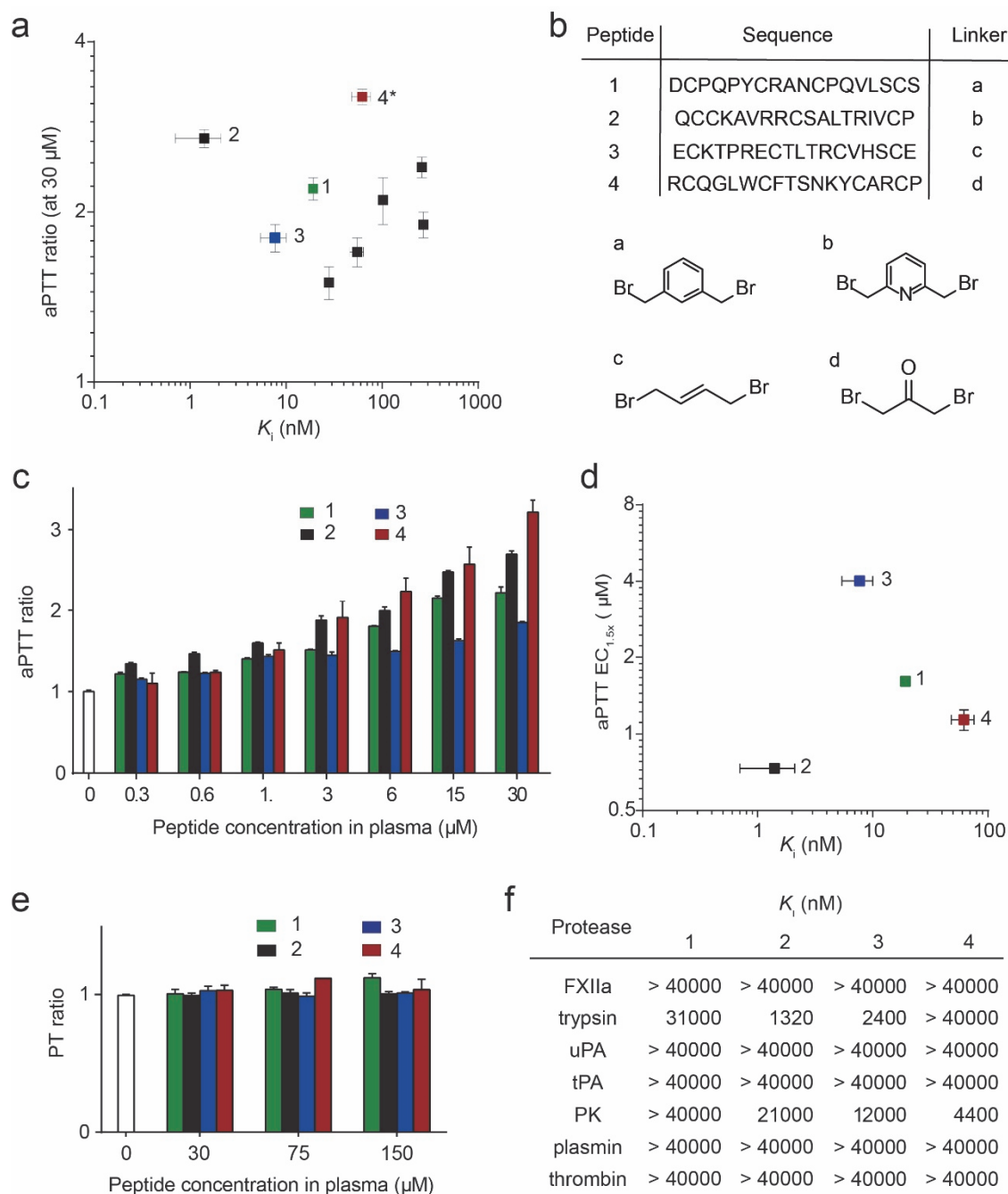


Figure 25. Inhibitory activity, anticoagulation activity and specificity of cyclic peptide FXIIa inhibitors.

a) Correlation of anticoagulation activity and K_i for nine phage-selected cyclic peptides. The anticoagulation activity was assessed by measuring the aPTT in human plasma at an inhibitor concentration of 30 μ M. b) Four peptides that were characterized in more detail. The peptides are doubly-cyclized via the four cysteines by the indicated linkers a-d. c) Prolongation of the aPTT in human plasma relative to a control without inhibitor. Mean values and SDs are shown for three measurements. d) Correlation of aPTT and K_i for the four peptides. $EC_{1.5x}$ is the concentration of inhibitor needed to prolong the aPTT 1.5-fold. Mean values and SDs are shown for three measurements. e) PT in human plasma. Mean values and SDs are shown for three measurements. f) Specificity profiling of inhibitors. Raw data is shown in Supporting information.

In a second experiment, we tested the inhibition of a panel of purified trypsin-like serine proteases. All four peptides showed > 1000-fold selectivity for FXIa, with the only proteases inhibited at low micromolar concentrations being trypsin (by peptides **2** and **3**) and plasma kallikrein (by peptide **4**) (Fig. 25f and Supplementary Fig. 10). The high target selectivity found in both assays for peptide **4** suggested that its efficient anticoagulation activity (indicated by the prolongation of the aPTT) is not based on the inhibition of multiple targets but must have another reason.

5.3.3 Alanine scan identifies key role for a lysine residue in peptide **4**

We next aimed at studying the structure-activity relationship (SAR) of peptide **4** and at improving its activity (Fig. 26a). We were particularly interested in peptide **4** because it had a high anticoagulation activity in the aPTT assay while having a moderate K_i that we speculated could more easily be improved than that of a high affinity binder. We performed an alanine scan by synthesizing variants of peptide **4** in which each amino acid (except the cysteine residues that are necessary for cyclization) was individually changed to alanine (Supplementary Fig. 12; Ala was mutated to Gly) and determined the inhibition constants (Fig. 26b and Supplementary Fig. 13). The SAR study showed that the C-terminal region of the peptide was most important for binding, as could be expected based on the sequence similarity in this region of peptides that were phage-selected in parallel (chapter 4). Tyr13 and Arg16 were most important for the binding as shown by a > 100-fold loss of binding affinity upon mutation to alanine, the latter one most likely binding with its side chain into the S1 sub-site of FXI's substrate binding region. Substitution of Ala15 and Pro18 to glycine or alanine reduced their activity by 15 and 20-fold, respectively, indicating a substantial contribution of these two residues.

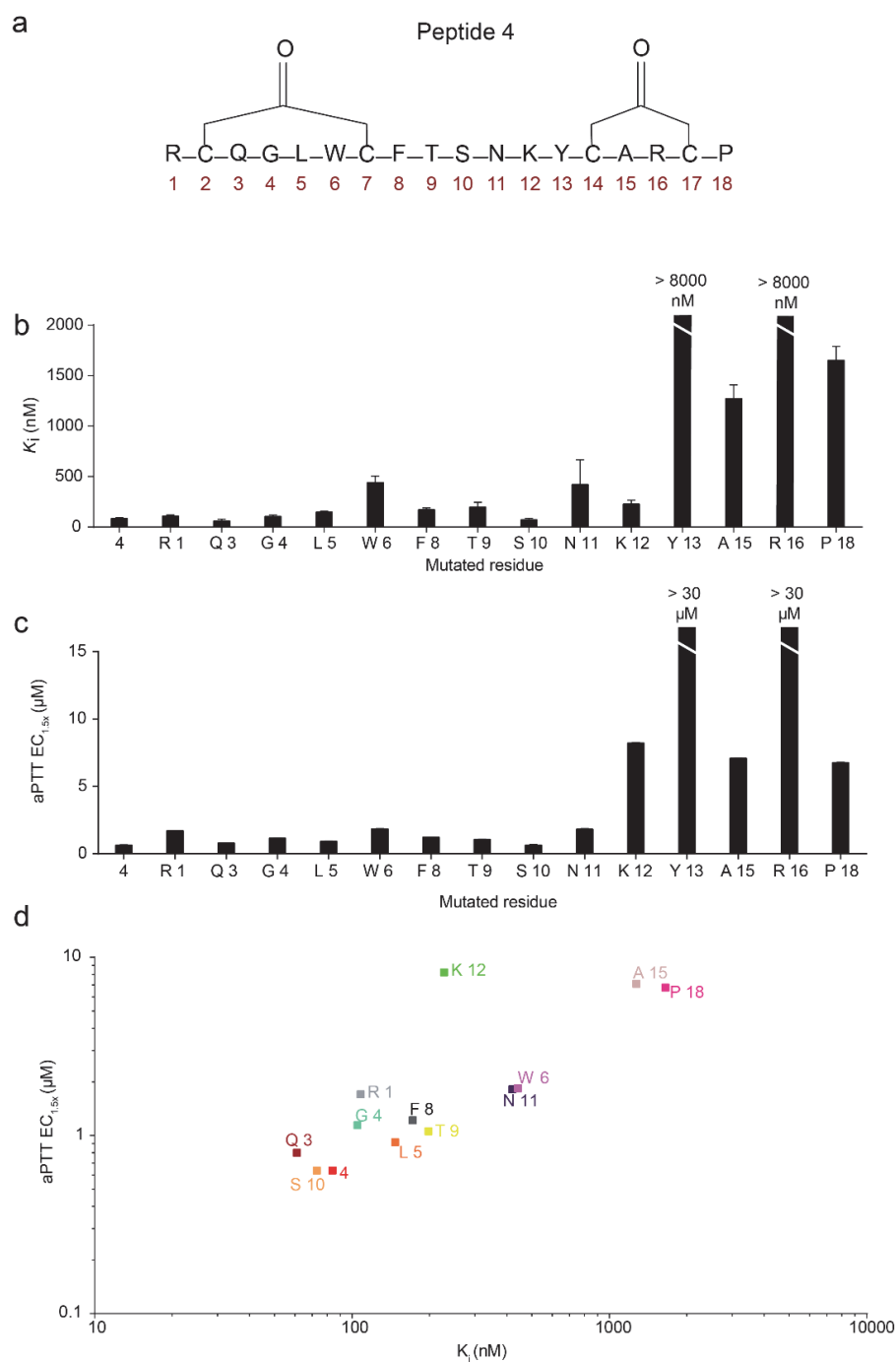


Figure 26. Alanine scan of peptide 4 and role of Lys12. a) Schematic representation of peptide 4. b) Inhibitory constants of the alanine scan peptides. Mutation of Tyr13 and Arg16 to alanine led to K_i values > 8000 nM. Mean values and SDs are shown for three measurements. c) Effect on the aPTT (represented as $EC_{1.5x}$ values) of the alanine scan peptides. Mutation of Tyr13 and Arg16 to alanine led to $EC_{1.5x}$ values > 30 μ M. Mean values and SDs are shown for three measurements. d) K_i versus $EC_{1.5x}$ values for the different peptides.

In addition to the K_i s, we assessed the effects of the alanine mutations onto the anticoagulation activity by determining the concentrations at which the aPTT increased by 50% ($EC_{1.5x}$; Fig. 26c and Supplementary Fig. 14). The increase of the $EC_{1.5x}$ values was proportional to the increase of the K_i s, except for one alanine mutant, the one at Lys12. The Lys12 to alanine substitution reduced the inhibition constant K_i by a relatively small factor ($K_i = 230 \pm 38$ nM; 2.7-fold higher) but reduced substantially the anticoagulation activity ($EC_{1.5x} = 8.2 \pm 0.02$ μ M; 13-fold higher) (Fig. 26d). We hypothesized that the positive charge provided by Lys12 could be important to achieve a good anticoagulation activity, but the mechanism remained unclear at this point.

5.3.4 Reducing the complexity of the inhibitor structure

Given the limited contribution of the N-terminal region of peptide **4** to the binding, we speculated that the structural complexity might be reduced by truncating the peptide from this end. This was only possible in case the cysteines in the N-terminal end were not bridged to those in the C-terminal region. As we did not know which cysteine pairs were bridged in peptide **4**, we synthesized the three possible regioisomers using orthogonal cysteine protecting groups as described previously⁶⁰, and tested their K_i s for FXIa (Supplementary Fig. 15). The isomer with Cys2/Cys7 and Cys14/Cys17 bridged showed a K_i of 60 nM and thus the same activity as the peptide **4** that we had previously synthesized by randomly connecting the four cysteines and HPLC separation of the isomers. This cysteine connectivity allowed us to easily reduce the size of the peptide by eliminating the first 10 amino acids that did not contribute much to the binding affinity. The shorter, monocyclic peptide **5** had a K_i of 290 ± 45 nM.

In order to improve the potency of peptide **5** and to study its SAR, we synthesized 40 variants in which we substituted one amino acid at a time to analogs and tested the inhibitory activity (Fig. 27).

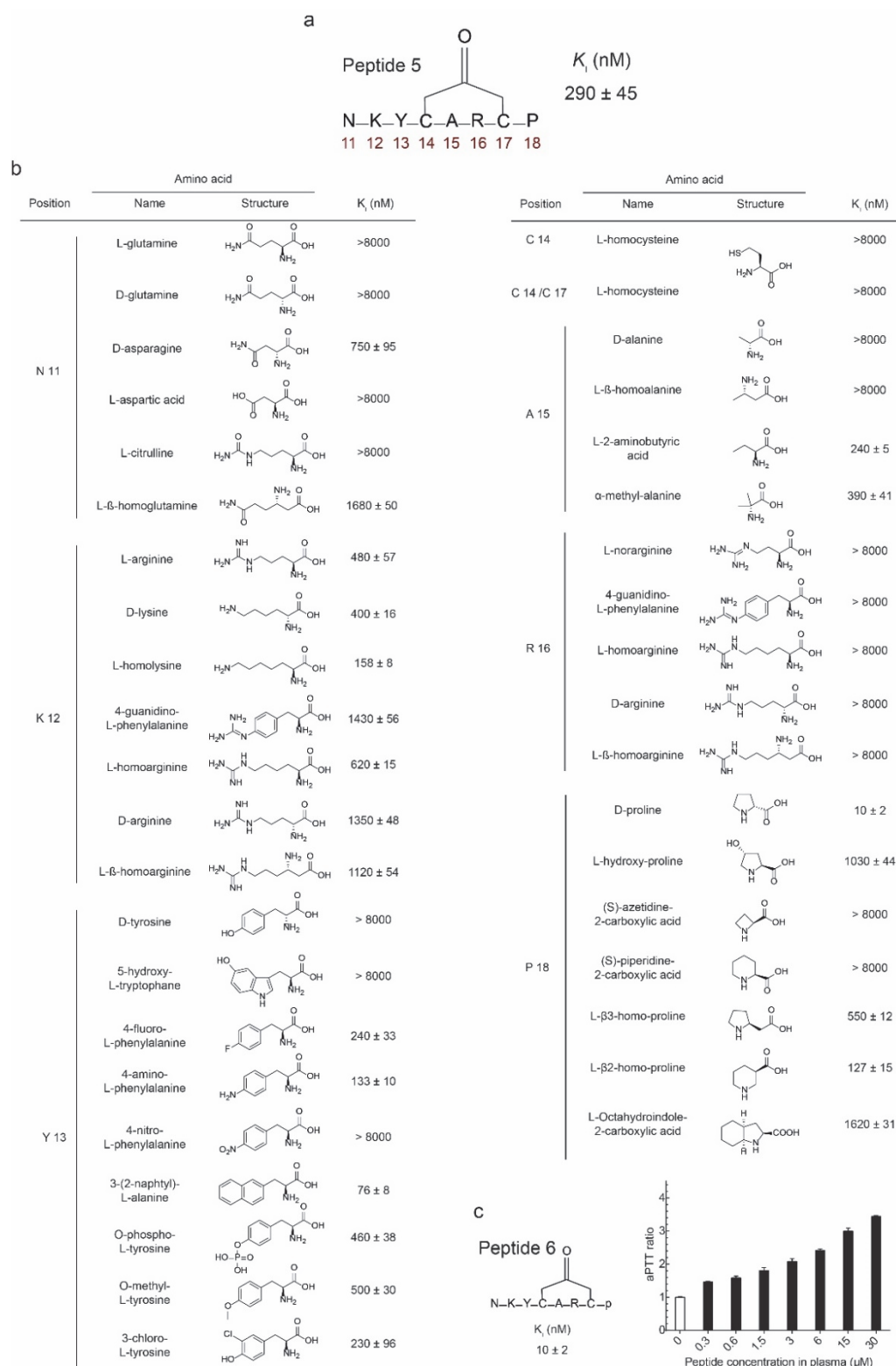


Figure 27. Structure-activity relationship study of peptide 5. a) Schematic representation of peptide 5. b) List of the mutated positions with residues used for substitution and inhibitory constants of the resulting peptides. c) Peptide 6 was the most potent peptide resulting from the SAR study. Mean values and SDs are shown for three measurements.

Most modifications reduced the activity or rendered the inhibitor completely inactive (Fig. 27, Supplementary Fig. 16). One mutation, Pro18 to D-Pro, resulted in a large improvement of around 30-fold and yielded an inhibitor with a K_i of 10 ± 2 (peptide **6**). Modification of the Lys12 to seven different positively charged amino acids with various side chain lengths and shapes altered the K_i s at maximum 5-fold. Substitution to homolysine improved the affinity 2-fold ($K_i = 158 \pm 8$ nM). The tolerance of amino acids with different side chain lengths and shapes at this position, that had all in common the positive charge, suggested that this residue formed mainly an electrostatic interaction. This was further confirmed by assessing the effect of these peptides on the aPTT at a concentration of 30 μ M. Substitution of Lys12 with other charged residues did not largely affect the aPTT effect, with the worst peptide showing aPTT prolongation of 1.5-fold (compared to 1.9-fold prolongation achieved with peptide **5**) (Supplementary Fig. 17).

5.3.5 Determination of the peptide binding on-rate

We speculated that the good anticoagulation activity observed for peptide **4** could potentially be based on a particularly fast binding on-rate resulting from an electrostatic interaction of Lys12 with FXIa. Rapid blockade of freshly generated FXIa could efficiently limit amplification of the coagulation cascade by activated downstream proteases and thus hinder formation of fibrin and thus blood clotting. FXI is activated to FXIa either by self-activation, by coagulation factor XIIa (FXIa) following activation of the intrinsic coagulation pathway, or by thrombin as an amplification mechanism of either pathway^{126,129}. We hypothesized that differences in binding kinetics could be responsible for the lack of correlation between inhibitory activity and potency in the aPTT. Inhibitors having a similar binding affinity (K_d) may differ substantially in their binding kinetics. For example, an inhibitor A could have a faster on-rate and faster off-rate than inhibitor B, but have the same K_d .

We tested the binding kinetics of peptides **1** – **4** using the following strategy and assay. FXIa (1 nM) was incubated with a chromogenic peptide substrate (260 μ M) and the activity of FXIa monitored over time by measuring absorption of the para-nitroaniline cleavage product. After starting the assay, the inhibitors **1** – **4** were added at concentrations ranging from 9.4 to 150 nM and the effect on FXI-mediated substrate cleavage monitored by measuring the pNA absorption using an absorption microwell plate reader. Without inhibitor, the absorption curves were linear, and the rate of cleavage was thus constant over time. With inhibitor, the curves were bent initially and became straight over time when an equilibrium for the interaction of FXIa and inhibitor was reached. Based on the curvature of the curves, we calculated the rate of peptide substrate cleavage based on the pNA absorption change for each time point.

The plots in Fig. 28a show the kinetic data obtained for peptides **2**, **3** and **4**. It is apparent that the peptide **4** binds much faster than the peptides **2** and **3**. The on-rate values for **2** and **3** are $1.3 \times 10^5 \pm 0.06 \text{ M}^{-1} \text{ s}^{-1}$ and $1.6 \times 10^5 \pm 0.05 \text{ M}^{-1} \text{ s}^{-1}$, respectively. For peptide **4**, the on-rate could not be determined with the absorption microwell plate reader as an equilibrium in binding of FXIa and the inhibitor was reached after a few seconds already. In order to determine the on-rate of peptide **4**, we used a stopped-flow spectrometer in which the FXIa/substrate is mixed with inhibitor within milliseconds (Fig. 28b). The k_{on} for peptide **4** determined with this method was around 10-fold faster than for the peptides **2** and **3** (and thus in the order of $10^6 \text{ M}^{-1} \text{ s}^{-1}$). The much faster binding rate observed for peptide **4** suggested that the difference in the binding kinetics are responsible for the better anticoagulation activity observed in the aPTT assay.

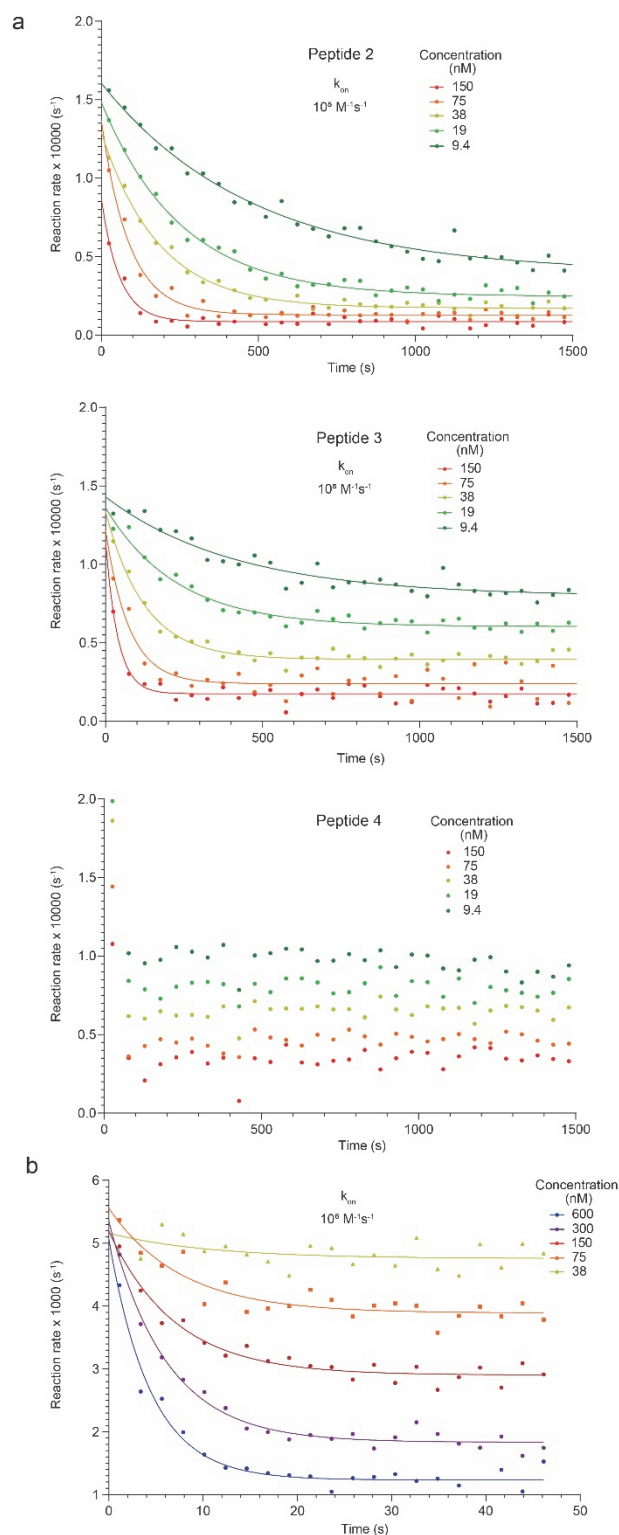


Figure 28. Binding kinetics of bicyclic peptide FXIa inhibitors. a) Kinetic curves of reaction rate versus time for peptides 2, 3 and 4. Binding was measured with an absorption microwell plate reader. b) Kinetic curves of reaction rate versus time for peptide 4. Binding was measured with a stopped-flow spectrometer. Curves were fitted with an exponential decay equation to derive the k_{obs} .

5.4 Conclusions

We have deciphered the molecular basis for the strong anticoagulation activity of a phage-selected cyclic peptide inhibitor that showed a relatively weak affinity for its target, coagulation factor XIa. After excluding that the strong anticoagulation was based on the inhibition of multiple proteases in the coagulation pathway, we performed a SAR study and observed that a lysine residue is key for the high activity, and we found that the positive charge of the lysine provides the peptide with a particularly fast binding rate, which translates into a strong anticoagulation activity. Inspection of the inhibitor-binding region of FXIa showed regions with negative charges to which the lysine possibly binds. Our finding suggests that FXIa inhibitors might be best developed by including positive charges. Insertion of a positive charge is easy to achieve with peptides, as shown in our work, and also with protein-based inhibitors such as antibodies. It may be more challenging to incorporate a positive charge into a small molecule drug as it would likely impair oral delivery, unless the charge is shielded by a removable group.

The correlation of strong anticoagulation activity and fast binding kinetics underscores how important rapid binding kinetics are for the inhibition of the blood coagulation cascade. Many coagulation protease inhibitors, including the peptides in our work, bind only to the activated proteases but not to the zymogens. This means that they can bind only once a coagulation protease gets activated. At the moment of zymogen activation, it is very important that inhibitors bind fast in order to prevent the activation of the next coagulation factor in the cascade. We show the importance of fast inhibitor binding in experiments in which we triggered the activation of the intrinsic coagulation pathway in blood plasma *ex vivo*, but it is likely that a fast binding is also beneficial *in vivo*, for example for the prevention of thrombosis. While we show in our work that a fast binding constant k_{on} is important for blocking blood coagulation, it is probable that rapid binding is critical also in many other fast

biological processes. For the development of inhibitors of such processes, it might be worth to also include charges in order to promote a fast binding through electrostatic interactions.

5.5 Material and methods

Chemical synthesis of cyclic peptides

Peptides synthesis was performed by SPPS as described before (chapter 3), in 30 μ mol scale using amino acids with N-terminal Fmoc protecting group, rink amide AM resin and DMF as solvent. Cleavage of peptide was performed with a cocktail containing 90% TFA, 2.5% thioanisole, 2.5% H₂O, 2.5% 1,2-ethanedithiol, 2.5% phenol, followed by ether precipitation. The crude peptide was purified by HPLC (Prep LC 2535 HPLC, Waters) on a C18 column (Sunfire prep C18 TM ODB, 10 μ m, 100 Å, 19 \times 250 mm, Waters) at 20 ml/min flow rate, using ddH₂O/0.1% TFA and acetonitrile/0.1% TFA as solvents. Fractions containing pure peptides were lyophilized. For cyclization, peptides were dissolved in 8.5 ml 60 mM NH₄HCO₃, pH 8.0 and 1.5 ml acetonitrile at 1 mM, and reacted with 2 mM linker (monocyclic peptides) or 4 mM linker (bicyclic peptides) for 1 hr at 30°C. The reaction was quenched by adding formic acid to 2% (v/v) of total volume. The chemically modified peptide was purified by HPLC and pure fractions were lyophilized. Peptide purity was analyzed by analytical HPLC as described before. When analyzing purity of isomers, a 0-50% gradient of solvent B in solvent A in 30 minutes was applied. When analyzing purity of other peptides, a 0-50% gradient in 15 minutes was applied. Peptide masses were confirmed by ESI-MS on a single quadrupole LCMS (LCMS-2020, Shimadzu) in positive ion mode.

Synthesis of individual regioisomers

Regioisomers with selected cysteines linked by chemical linkers were synthesized as described previously¹⁷ with a few modifications. Peptides synthesis on Rink amide resin was performed as described above, but the Fmoc group at the N-terminus was not deprotected. One pair of cysteines carried the side chain-protecting group Mmt and the other pair Dpm. Deprotection of the Mmt groups was performed using 5 ml of TFA:TIS:DCM (1:5:94) and the resin was

incubated for 3 min while shaking. This step was repeated 10 times. Resins were washed three times with DCM and then DMF and then cyclization was performed by adding 1.5 equivalents of chemical linker in 2 ml DMF and 3 equivalents of DIPEA in 2 ml of DMF. The reaction was incubated at room temperature for 1 hour with shaking. A test cleavage with TIS:TFA:H₂O (1:97:2) of a small amount of the resin was performed. The resin was then washed 3 times with DMF (5 ml) and Fmoc deprotection was performed twice by adding 2.5 ml of 20% piperidine and incubating for 5 min with shaking. The resin was again washed with DMF and DCM and then deprotection of the side chain protecting groups and cleavage from the resin were performed by incubation with 5 ml of the cleavage mixture TIS:TFA:H₂O (1:97:2) for 8 hours. The peptide solution was separated by filtration and the peptides initially purified by ether precipitation. Cyclization of the remaining cysteine pair was performed as described above, using 2 equivalents of linker.

Determination of inhibitory activity of selected peptides

The inhibitory constants (K_i) of peptides were assessed by measuring the residual enzymatic activities of coagulation factor XIa (FXIa) incubated with serial dilutions of peptides (ranging from 10 μ M to 900 pM final concentration). The activity of FXIa was monitored using the specific substrate Pyr-Pro-Arg-pNA (Bachem). Activity curves were determined at 25°C in an activity assay buffer as mentioned previously (chapter 3). FXIa (Molecular Innovations) was added at 0.5 nM (final conc.) and reactions were started by adding the substrate at 400 μ M (final conc.). The release of p-nitroaniline (pNA) upon substrate cleavage was monitored over 20 min by measuring the increase in absorbance over time at 405 nm using an absorbance microtiter plate reader (Infinite M200 Pro, Tecan). The rate of pNA release is proportional to enzymatic activity. The IC_{50} values were determined using the following equation:

$$y = \frac{100}{1 + 10^{(\log IC_{50} - x)p}}$$

Where y = the residual activity (%) of protease, x = the logarithm of peptide concentration, IC_{50} = the concentration of inhibitor that leads to 50% enzyme inhibition, and p is the Hill coefficient. The inhibitory constants were calculated from the IC_{50} using the following equation:

$$K_i = \frac{IC_{50}}{1 + \frac{[S]_0}{K_m}}$$

Wherein $[S]_0$ = the initial concentration of substrate, K_m = the Michaelis constant for the substrate. The K_m of FXIa for Pyr-Pro-Arg-pNA was determined to be $255 \pm 14 \mu\text{M}$.

Specificity profiling

For specificity profiling, the residual activities of several serine proteases homologous to FXIa in presence of FXIa inhibitors were determined. Two-fold dilutions of the peptides were used, ranging from $40 \mu\text{M}$ to 39 nM . The assays were performed similarly as described above. The final concentrations of the proteases were: 2 nM β -FXIIa, 0.1 nM trypsin, 7.5 nM tPA, 1.5 nM uPA, 2 nM thrombin, 0.25 nM plasma kallikrein, 2.5 nM plasmin. All proteases were obtained from Molecular Innovations, except PK, which was obtained from Innovative research. Fluorogenic substrates (Bachem) were used for activity determination: Z-Phe-Arg-AMC for PK, Z-Gly-Gly-Arg-AMC for thrombin, trypsin, tPA and uPA, H-D-Val-Leu-Lys-AMC for plasmin. The substrate concentration in the assay was $50 \mu\text{M}$. Fluorescence (AMC ex. 368 nm , em. 467 nm) was measured at 25°C over time using a fluorescence microtiter plate reader (Infinite M200Pro, Tecan) as a measure of enzymatic activity.

Determination of binding kinetics

For the determination of binding kinetics, 1 nM FXIa was incubated for 10 minutes with $260 \mu\text{M}$ Pyr-Pro-Arg-pNA. Peptides at final concentrations ranging from 600 nM to 9.4 nM were

then added and the recording of absorbance at 405 nm was started as rapidly as possible and measured every 10 s. The values of the slopes were calculated over 6 time points and were plotted as reaction rate versus time. The k_{obs} values were calculated by fitting the obtained curves using the following equation:

$$[E] = [E_0]e^{-k_{\text{on}} [P]t}$$

where $[E]$ is the concentration of free enzyme, $[P]$ is the concentration of free peptide, and k_{on} is the second order rate constant for the association of E and P. k_{obs} corresponds to $k_{\text{on}}[P]$. The k_{on} value is finally determined by plotting k_{obs} values as a function of peptide concentration, where the slope of the curve corresponds to k_{on} .

For the determination of the on-rate of faster binders, a Kinetasyst (Hi-Tech scientific) stopped-flow system was used. The enzyme was added at a final concentration of 16 nM and the substrate at 520 μM . The solutions of enzyme and substrate were mixed and added to syringe C. The peptide solution was added to syringe D at final concentrations ranging from 600 nM to 37.5 nM. The solutions in syringes C and D were then mixed 1:1 in the flow cell of the instrument and absorbance was recorded at 405 nm at kinetic intervals of 100 ms.

aPTT and PT coagulation activity measurements

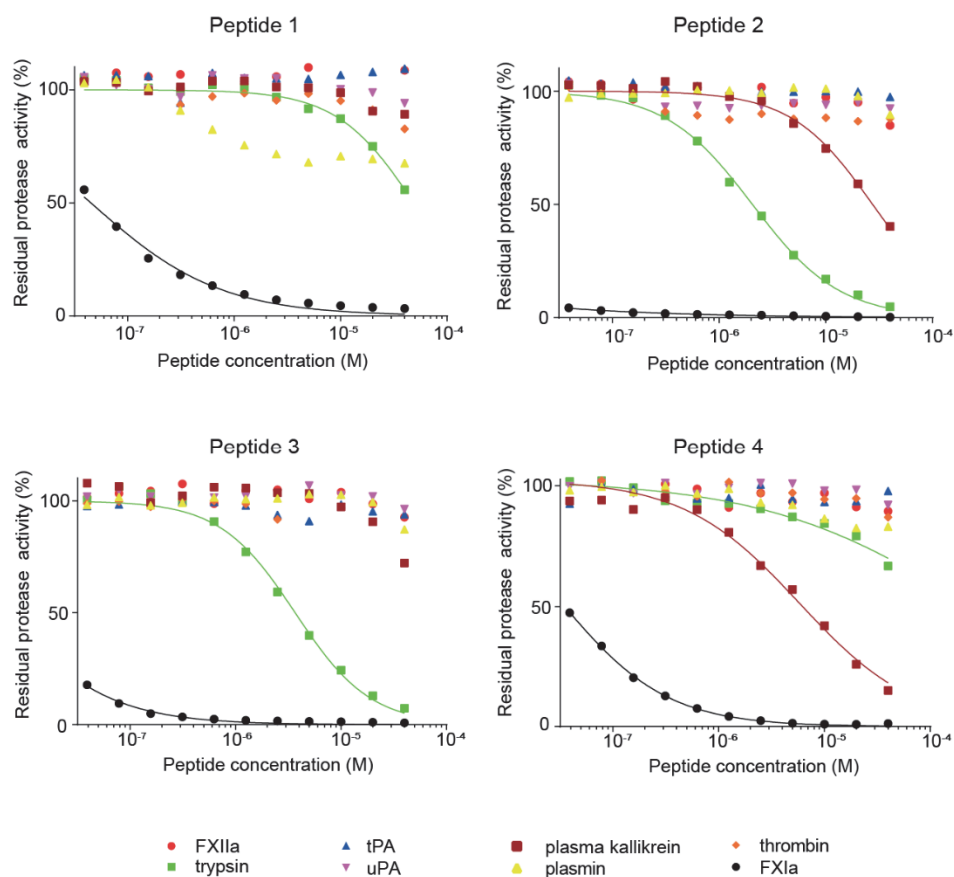
For the characterization of the anticoagulation activity of peptides, aPTT and PT coagulation assays were performed in human plasma using a coagulation analyzer (STAGO Start4, Diagnostica Stago) as described previously (chapter 4). For PT, 50 μL of citrated human single donor plasma with peptides at concentrations ranging from 150 μM to 30 μM were incubated for 2 min at 37 °C in the chamber of the instrument. 100 μL of Innovin (activator of extrinsic pathway of coagulation, Dade Behring/Siemens) were added using the dedicated automatic pipette. The oscillation of a steel ball in the sample, which was induced electromagnetically, was recorded. The PT was defined as the time until the ball movement stopped after addition

of Innovin. For aPTT, 100 μL of citrated human single donor plasma with peptides at concentrations ranging from 30 μM to 0.3 μM were added to 100 μL of Pathromtin SL (activator of the intrinsic pathway of coagulation, Siemens) and incubated at 37 °C for 2 min. 100 μL of CaCl_2 solution (25 mM, Siemens) were then added with the dedicated pipette, thus starting coagulation, and oscillation of the steel ball was monitored as described above.

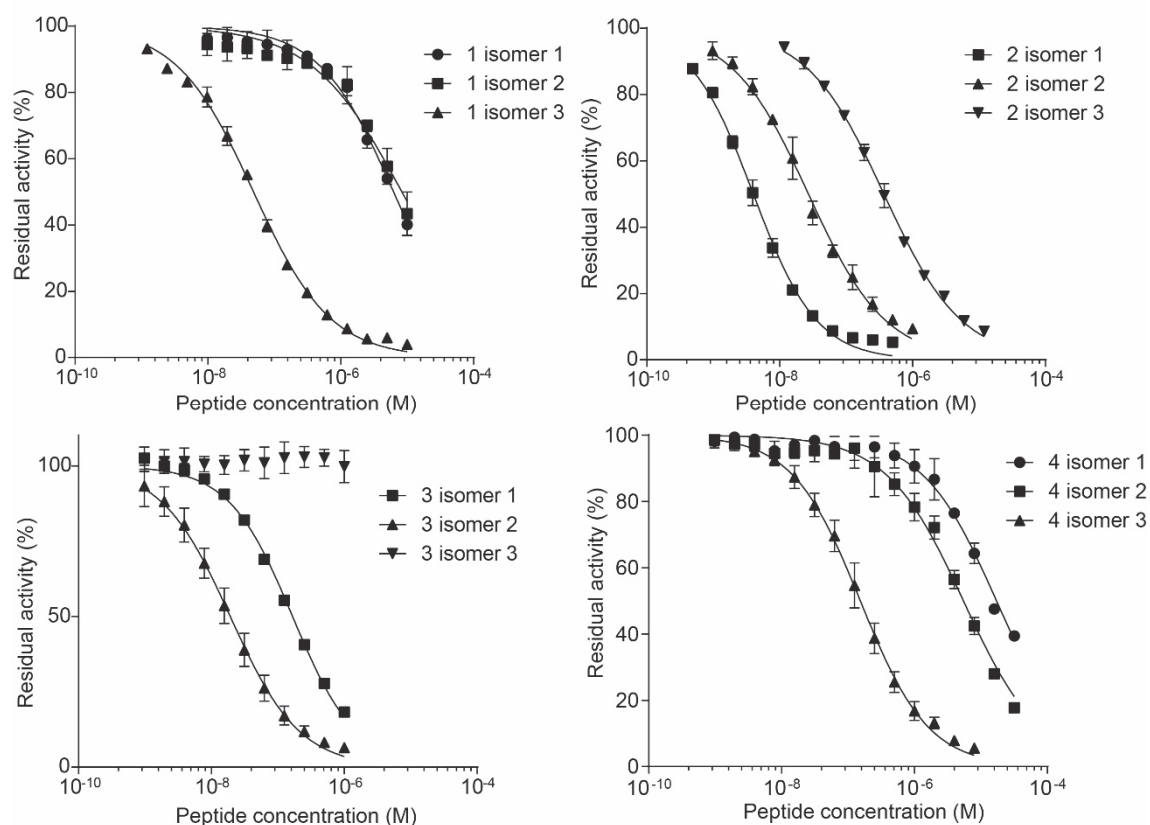
5.6 Supplementary information

Structure-activity relationship of peptide 5

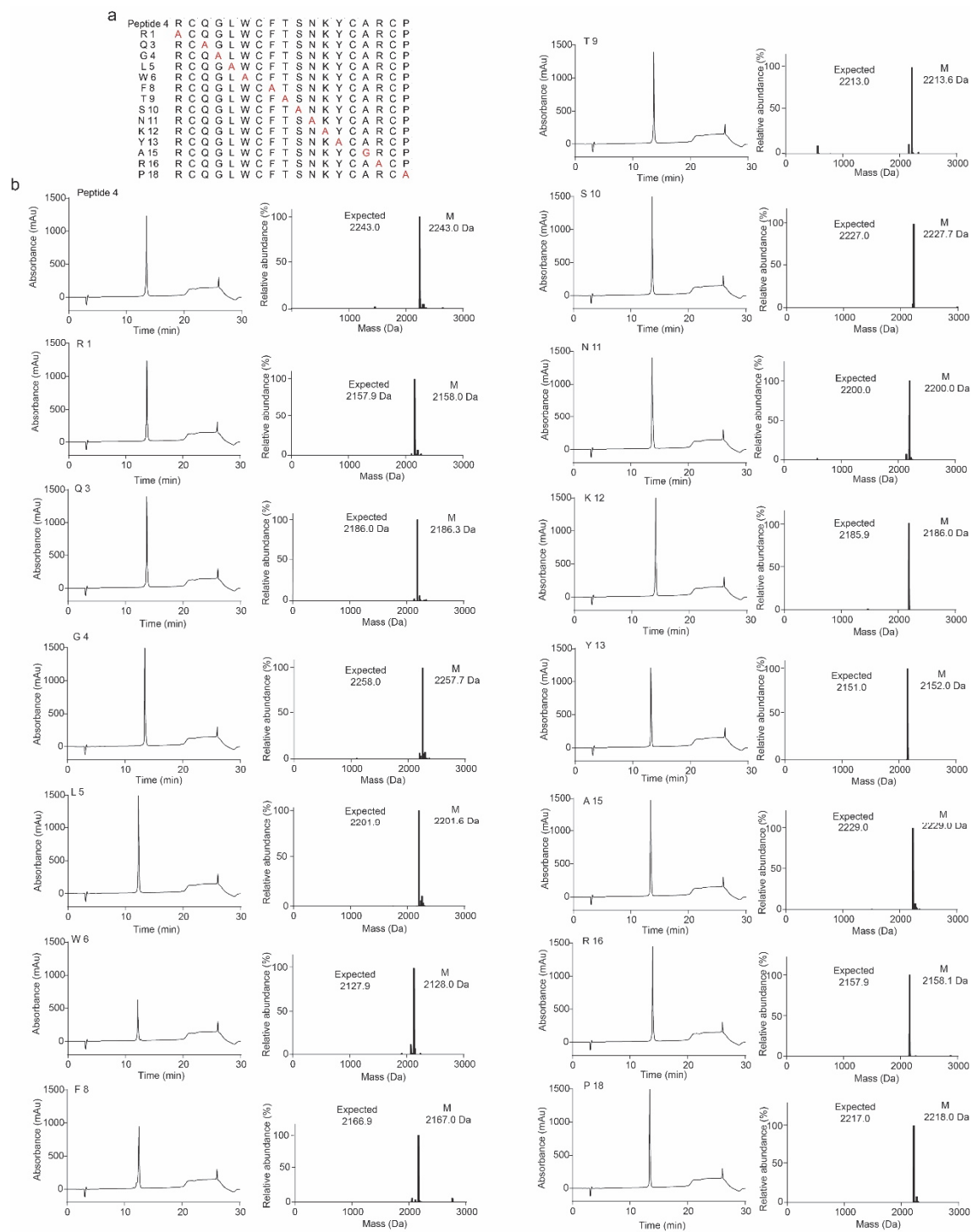
The SAR of peptide 5 ($K_i = 290 \pm 45$ nM) was studied by mutating its residues with analogs (Fig. 27). In particular, three types of substitutions were made: a) natural amino acids with similar side chains; b) residues with inverted stereochemistry; c) unnatural amino acids with side chains similar to the substituted residue. When mutating Asn11, all substitutions led to loss of activity. D/L-glutamine, L-aspartic acid and L-citrulline led to $K_i > 8000$ nM. In the Lys12 position, all mutated residues were chosen to carry a positive charge at physiological pH, in order to avoid loss in k_{on} . None of the mutations led to high loss in activity, supporting the hypothesis of the importance of the positive charge (Fig. 27 and Supplementary Fig. 16 and 17). In the Tyr13 position, all the phenylalanine analogs with different substituents (except 4-nitro L-phenylalanine) preserved the activity, while D-tyrosine and 5-hydroxy L-tryptophan led to great loss of activity ($K_i > 8000$ nM). Substitution with 3 (2-naphthyl) L-alanine led to 3.9-fold improvement in activity ($K_i = 76 \pm 8$ nM) (Fig. 27). Substitution of Cys4 or both Cys4 and Cys7 with L-homocysteine led to complete loss of activity ($K_i > 8000$ nM), suggesting that variations in the cycle size are not tolerated. Similarly, mutation of Ala15 with L- β -homoarginine, which also increases the cycle size by one carbon, was not tolerated. Substitution with D-alanine also led to loss of activity ($K_i > 8000$ nM). L-2-aminobutyric acid and α -methyl alanine, instead, preserved the activity, suggesting that substitutions of alanine with amino acids presenting bulkier side chains might be tolerated. All substitutions with arginine analogs in position 6 led to loss of activity ($K_i > 8000$ nM), suggesting that L-arginine provides optimal binding and even small changes in the side chain perturb the interaction. Finally, substitution of Pro18 with proline analogs yielded the best binder when D-proline was introduced, leading to a 29-fold improvement in inhibitory activity (Fig. 27) and large improvement in the aPTT effect, from 2-fold prolongation at a plasma concentration of 30 μ M to 3.5-fold prolongation (Fig. 27).



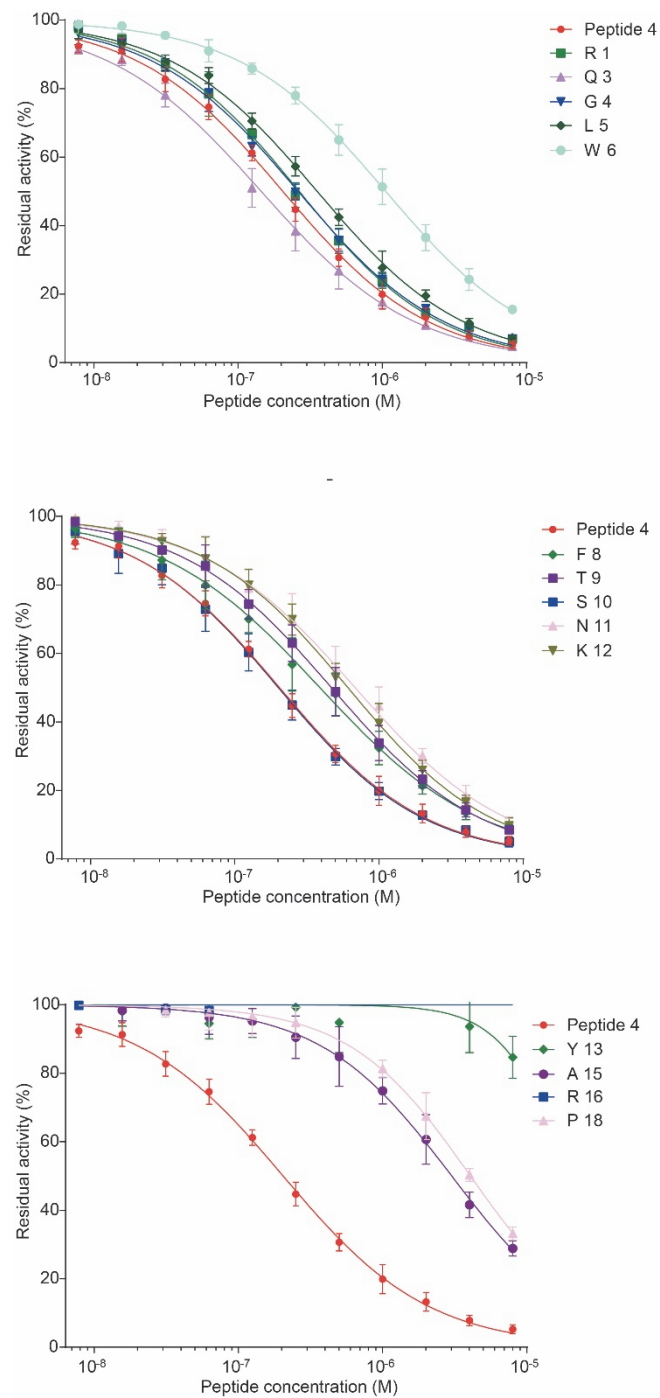
Supplementary Figure 10. Specificity of peptides 1 to 4. Inhibition of human trypsin-like serine proteases by the indicated concentrations of peptides. Residual protease activity was measured with fluorogenic substrates.



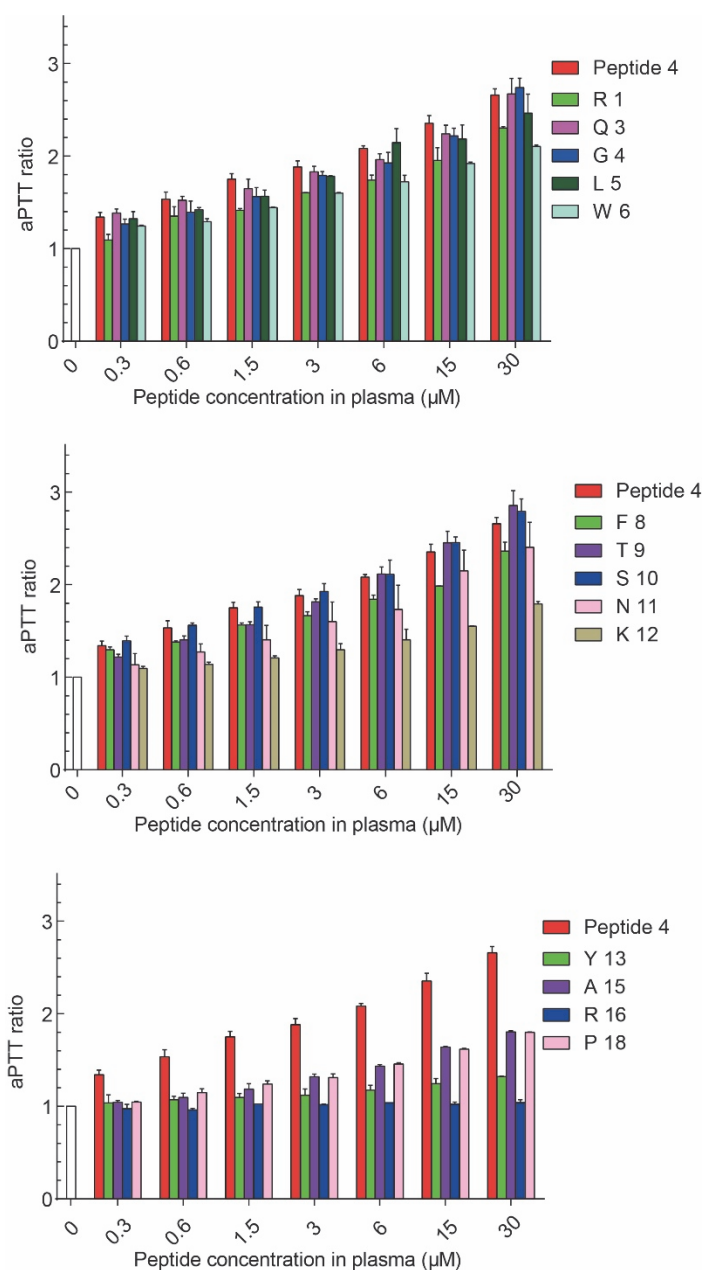
Supplementary Figure 11. Curves of inhibitory activity against FXIa of all the regoisomers of the four inhibitors. The activity of FXIa was determined with a chromogenic substrate. Mean values and SDs are shown for three measurements.






Supplementary Figure 12. Alanine scan of peptide 4. a) Peptides synthesized for the alanine scan. The mutated position in each peptide is highlighted in red. b) Purity assessment by analytical HPLC and mass characterization by LCMS of the peptides from the alanine scan.



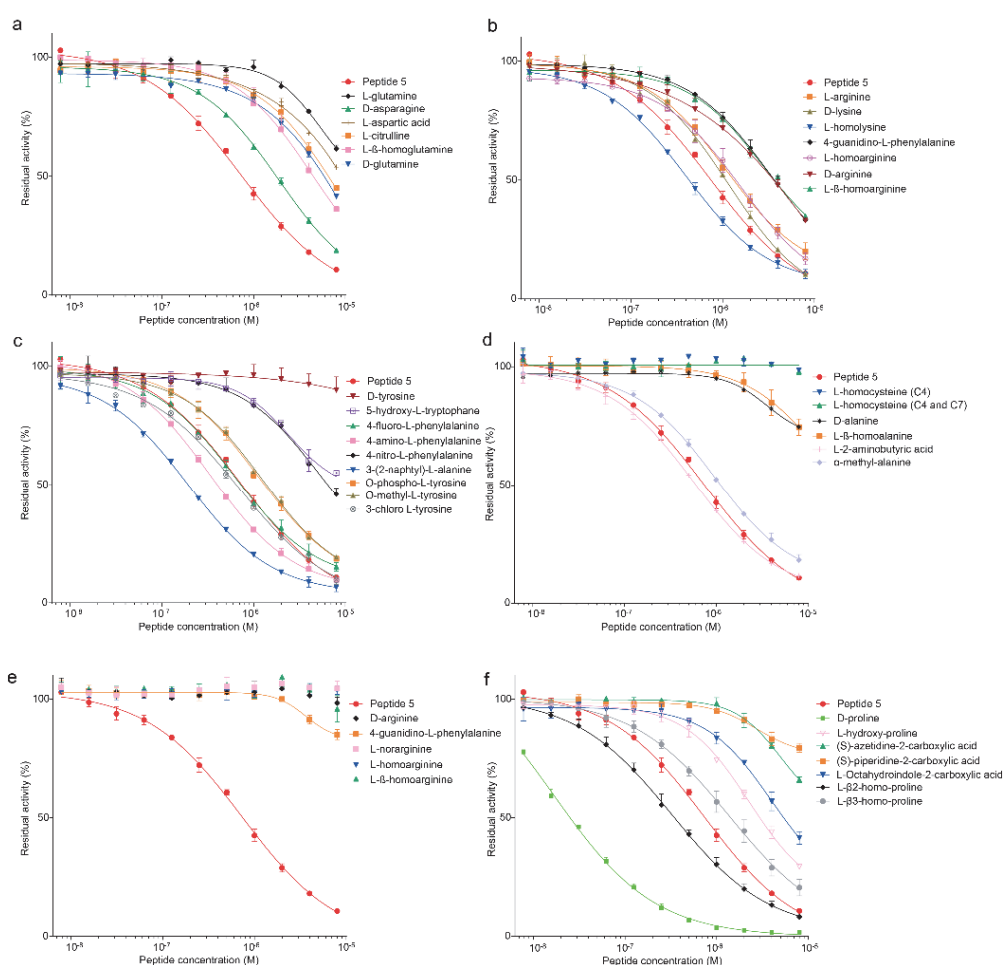
Supplementary Figure 13. Inhibition of FXI by alanine scan mutants. The activity of FXIa was determined with a chromogenic substrate. Mean values and SDs are shown for three measurements.



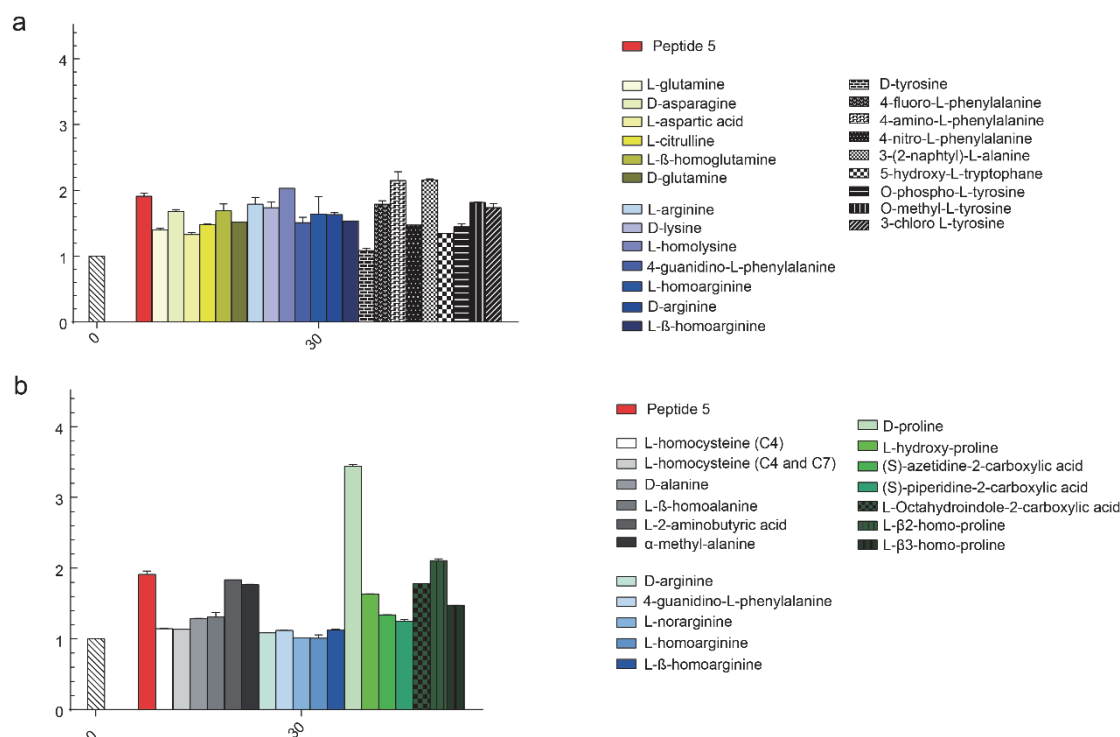
Supplementary Figure 14. Prolongation of aPTT by alanine scan mutants. Peptides concentrations tested ranged from 0.3 to 30 μ M. Mean values and SDs are shown for three measurements.

Isomer	K_i (nM)
	60 → 4 isomer 3
	1190
	1320

Supplementary Figure 15. Synthesis of three regioisomers of peptide 4 and their FXIa inhibitory activity. The first regioisomer, characterized by two monocycles connected via a linear peptide linker, is the most potent and showed inhibition comparable to the peptide 4 previously synthesized by randomly connecting the four cysteines and HPLC separation of the isomers.

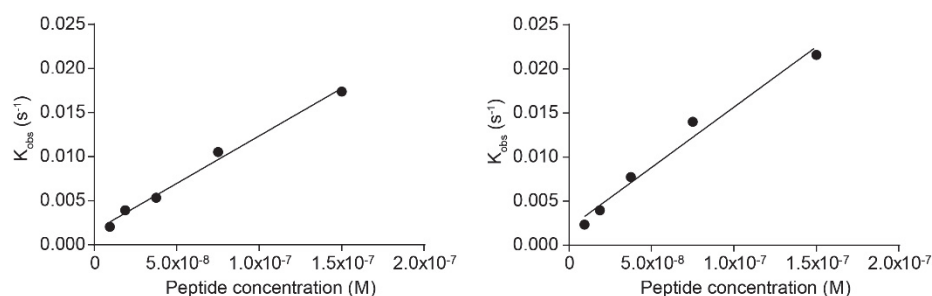


Supplementary Figure 16. Inhibitory activity of peptide 5 variants with unnatural amino acids. Peptide variants with substitutions in positions a) Asn11, b) Lys12, c) Tyr13, d) Cys14 and 17 and Ala15, e) Arg16 and f) Pro18. The activity of FXIa was determined with a chromogenic substrate. Mean values and SDs are shown for three measurements.



Supplementary Figure 17. Anticoagulation activity of peptide 5 variants with unnatural amino acids.

a) Peptide variants with substitutions in positions Asn11 (yellow), Lys12 (blue), Tyr13 (grey). b) Peptide variants with substitutions in positions Cys14 and 17 and Ala15 (grey), Arg16 (blue), Pro18 (green). Mean values and SDs are shown for three measurements.



Supplementary Figure 18. Binding kinetics of peptides 2 and 3. k_{obs} values versus peptide concentration are plotted in order to derive the k_{on} value, corresponding to the slope of the curve.

6 Conclusion & Outlook

Coagulation factor XI has been identified as a promising target for safe anticoagulation, as it is involved in the pathogenesis of thrombosis but is not essential for hemostasis. While several FXI-targeting molecules are currently in development, to my knowledge, no peptide-based inhibitors have been generated. Peptides are an interesting molecular format for drug development as they combine favorable properties of biologics and small molecules. The possibility to encode them genetically by display techniques allows for the rapid and efficient screening of large combinatorial libraries, often yielding high-affinity binders. Peptides have also limitations such as the relatively fast renal clearance, which typically requires optimization in order to develop them into therapeutics.

The general goal of this thesis was to develop potent cyclic peptide inhibitors of coagulation factor XIa, and to improve the pharmacological properties of the peptides to allow for their application as safe anticoagulants.

In this thesis, I have successfully constructed a large and structurally diverse cyclic peptide phage library and have shown that the high diversity is important for the selection of potent binders. I have then successfully developed cyclic peptide FXIa inhibitors characterized by high potency, specificity, stability, and prolonged elimination half-life and shown that such molecules achieve a strong anticoagulation effect both *ex vivo* and after circulation in blood *in vivo*. Finally, I have characterized the molecular basis for strong anticoagulation *ex vivo* and found that the binding on-rate of inhibitors of activated proteases is an important parameter. The specific conclusions for the three individual projects of my PhD thesis are found in the next sections.

Generation and screening of a structurally diverse 100-billion cyclic peptide phage display library

The selection of peptides from large combinatorial libraries using *in vitro* evolution strategies allows for the efficient identification of binders to various therapeutic targets. It is broadly accepted that screening large and structurally diverse libraries is crucial for the selection of binders with desired properties.

In this work, I have developed an unprecedentedly large and structurally diverse cyclic peptide phage library. Its large size has been achieved by applying a cloning strategy that combined whole vector PCR for the creation of the library DNA and the use of a phagemid vector that, being much smaller than phage vectors, simplifies the preparation of library DNA and allows for high transformation efficiency. High backbone diversity has been obtained by designing library peptides having four cysteines positioned in 91 different ways. The diversity is then further increased by the formation of three regioisomers upon cyclization, leading to 273 different formats. In addition, since cyclization reagents can impose different backbone conformations to peptides, the availability of various bifunctional linkers (around 20 molecules tested to date) can further increase the backbone diversity several fold. Finally, upon cyclization one out of the three peptides formed is characterized by two monocycles connected by a linear peptide chain. This allows for the selection of monocyclic peptides, which renders the library even more versatile.

The importance of the large size and high structural diversity achieved with the new library was demonstrated in this work by a) the enrichment of FXI-binding peptides with specific backbones and binding motifs depending on the applied cyclization reaction; b) the large consensus sequences obtained and c) the selection of potent binders (nanomolar affinities). The high value of the library is further supported by the fact that it has yielded potent binders to various targets when applied by other colleagues. Examples of such molecules can be found in Table 4.

Table 4. Examples of cyclic peptide-binders successfully selected with the novel library. The molecular target, affinity and colleague who developed the molecule are listed.

Target	Affinity	Developed by
Tissue kallikrein 5	2 nM	Patrick Gonschorek (unpublished)
Tissue kallikrein 7	10 nM	Patrick Gonschorek (unpublished)
FKBP12	18 nM	Cristiana Berti (unpublished)

Development of selective FXIa inhibitors based on cyclic peptides and their application for safe anticoagulation

The development of potent peptide-based FXIa inhibitors in our laboratory has proven challenging. In particular, the lack of cross-reactivity with FXIa homologs of model animals, which is crucial to perform preclinical efficacy tests *in vivo*, has posed a problem in the past.

In this project I was able to successfully develop a FXIa inhibitor with single-digit nanomolar affinity for the target, high selectivity over homologous serine proteases and strong anticoagulation effect (achieved via specific inhibition of the intrinsic pathway, without affecting the prothrombin time). Importantly, it is the first synthetic peptide in our lab that is cross-reacting with a FXIa homolog, the one of rabbit. This is important as achieving solid preclinical efficacy proof of concept *in vivo* is an essential step to de-risk drug development.

One of the main obstacles for the development of peptides as therapeutics is their short *in vivo* half-life, which hampers their application for several diseases that require prolonged treatment. In this work, I have successfully applied a half-life extension strategy based on PEGylation. The resulting conjugate showed an *in vivo* elimination half-life of around one day in rabbits, which could translate to days in human, and remained functional for over 48 hours when incubated in plasma. One of the main advantages offered by the PEGylation strategy is the possibility to modulate the half-life of the peptide to accommodate the therapeutic needs of different indications, which can be achieved by varying the size of PEG molecules. For example, anticoagulants applied to avoid clotting during hemodialysis (HD)

only need to act throughout the duration of each session (around 3-4 hours) and thus a shorter PEG chain might be applied.

I have then shown that the cyclic peptide inhibitor and the PEG-peptide conjugate achieve a strong anticoagulation effect both in plasma and in whole blood. The *ex vivo* anticoagulation shown by the peptide-based inhibitors compares with the one of the golden standard anticoagulant heparin (UFH). In addition, the therapeutic range of my inhibitor was found to be around 100-fold larger, which further improves its safety profile and can facilitate administration in clinics.

Anticoagulation in HD was identified as a potential indication where application of our molecule would be beneficial. In order to test our conjugate in a model which is the closest possible to the clinical situation, an *ex vivo* model of HD was chosen. In this model, all the blood is in contact with foreign surfaces (blood bag, tubing system and dialyzer), and therefore provides a much more procoagulant environment than in the case of HD applied to patients. Our inhibitor prolonged the HD circulation time similarly to UFH and is expected to have low risk of bleeding side effects. This is particularly important in CKD patients receiving HD, as they are at higher risk of bleeding¹⁸⁴. In addition, patients with HIT would strongly benefit from an effective alternative to UFH.

Finally, I have shown that the PEGylated cyclic peptide administered to New Zealand White rabbits shows an anticoagulation effect for at least 24 hours, thus confirming the suitability of this model animal for further studies.

In conclusion, I have developed an attractive molecule that has the potential to be improved in terms of potency and to be transformed into a therapeutic. The properties of this molecule make it suitable for indications such as HD and post-operative anticoagulation, where there is a clear unmet need for safer anticoagulants. As the plasma concentration of the current inhibitor necessary for adequate anticoagulation is relatively high, I am planning to further

improve the potency of the inhibitor in the future. To this end, I am planning to perform SAR studies to optimize the peptide sequence using natural and unnatural amino acids. My goal is to improve the affinity of the inhibitor to FXIa by at least 10-fold, in order to achieve an optimal anticoagulation effect at low micromolar or even at nanomolar concentrations. This should allow for the administration of a therapeutic dose of the inhibitor in line with approved drugs with similar formats^{69,185,186}, in the range of 1-5 mg/kg (depending on the indication and the administration route), and will reduce the costs per dose. In addition, I am planning to explore alternative PEG conjugate formats. For example, formats with two or more peptide molecules per PEG chain might be interesting, as they would increase the potency per weight and thus allow for the administration of lower doses. Such strategy has already been applied for molecules like APL-2 (currently in clinical development, see section 1.1.2), where two complement C3-peptide inhibitors are conjugated to a PEG 40kDa^{27,187}. Finally, with the improved inhibitor in hand, I am planning to demonstrate efficacy in relevant models, such as the AV shunt thrombosis model in rabbits^{155,156,188}, the FeCl₃-induced thrombosis model in FXI-KO mice supplemented with human FXIa^{131,167}, and in a bigger *ex vivo* HD study. A strong preclinical efficacy proof of concept would offer the basis to develop further a cyclic peptide FXIa inhibitor with the goal of establishing a safe anticoagulation therapeutic.

Fast binding kinetics of a coagulation factor inhibitor are key for strong anticoagulation

In this project, I characterized four FXIa inhibitors that were previously selected from the novel cyclic peptide phage library (chapter 3). A poor correlation between the peptides' inhibitory activities and *ex vivo* anticoagulation effects, tested in the activated partial thromboplastin time (aPTT), was observed. High selectivity over homologous proteases excluded inhibition of other serine proteases as the cause for this observation. One peptide in particular showed a strong effect on the aPTT, while having a less potent inhibitory activity.

Further characterization via an alanine scan suggested that a lysine residue was responsible for this effect, as its mutation to alanine leads to moderate loss in inhibitory activity, but great loss in anticoagulation potency *ex vivo*. As lysine could contribute to binding by forming electrostatic interactions, I speculated that fast binding to the target (often achieved by such long range interactions) could be important for potent anticoagulation¹⁸⁹. Thus, I investigated the binding kinetics of the peptides as a potential parameter influencing the *ex vivo* efficacy profile and I found that the peptide with high anticoagulation potency had a 10-fold faster binding on-rate than the other inhibitors.

It is likely that rapid FXIa inhibition can strongly limit the amount of thrombin that gets activated, and thus hamper thrombus propagation more efficiently than a slow binder. As many endogenous inhibitors of serine proteases of the coagulation cascade were found to be fast binders, with on-rates in the order of $10^7 \text{ M}^{-1} \text{ s}^{-1}$, we could speculate that this is an important factor also for *in vivo* regulation of the coagulation cascade.

Based on the findings of this study, it might be important to take into consideration the binding on-rate of inhibitors of the active form of coagulation proteases (and other proteases that act in similarly fast pathways) in future drug development programs. Since rapid blockage of activated coagulation proteases seems crucial for achieving a strong anticoagulation effect, a promising strategy could involve the development of molecules that can target both the active form and the zymogen of the protease, in order to avoid completely the activation. A mAb currently in clinical development (MAA868) has achieved this dual inhibition and thus might have a competitive advantage. Inspired by these findings, a scientist from our research group is currently developing a cyclic peptide-based dual binder of FXI and FXIa (Kong *et al.*, unpublished).

References

1. Ladner, R. C., Sato, A. K., Gorzelany, J. & De Souza, M. Phage display-derived peptides as therapeutic alternatives to antibodies. *Drug Discov. Today* **9**, 525–529 (2004).
2. Vlieghe, P., Lisowski, V., Martinez, J. & Khrestchatisky, M. Synthetic therapeutic peptides: science and market. *Drug Discov. Today* **15**, 40–56 (2010).
3. Craik, D. J., Fairlie, D. P., Liras, S. & Price, D. The Future of Peptide-based Drugs. *Chem. Biol. Drug Des.* **81**, 136–147 (2013).
4. Fosgerau, K. & Hoffmann, T. Peptide therapeutics: current status and future directions. *Drug Discov. Today* **20**, 122–8 (2015).
5. Cunningham, A. D., Qvit, N. & Mochly-Rosen, D. Peptides and peptidomimetics as regulators of protein-protein interactions. *Curr Opin Struct Biol* **44**, 59–66 (2017).
6. Mathur, D. *et al.* PEPlife: A Repository of the Half-life of Peptides. *Sci. Rep.* **6**, 36617 (2016).
7. Muheem, A. *et al.* A review on the strategies for oral delivery of proteins and peptides and their clinical perspectives. *Saudi Pharm. J.* **24**, 413–428 (2016).
8. Renukuntla, J., Dutt Vadlapudi, A., Patel, A., Boddu, S. H. & Mitra, A. K. Approaches for Enhancing Oral Bioavailability of Peptides and Proteins. *Int J Pharm.* **447**, 75–93 (2013).
9. Naibo, Y., Margaret, A. B., Paul, W. H. & Jingyuan, W. Enhancing the Oral Bioavailability of Peptide Drugs by using Chemical Modification and Other Approaches. *Med. Chem. (Los. Angeles)*. **4**, 763–769 (2014).
10. Davies, M. *et al.* Effect of Oral Semaglutide Compared With Placebo and Subcutaneous Semaglutide on Glycemic Control in Patients With Type 2 Diabetes. *JAMA* **318**, 1460 (2017).
11. Kaspar, A. A. & Reichert, J. M. Future directions for peptide therapeutics development. *Drug Discov. Today* **18**, 807–817 (2013).
12. Lau, J. L. & Dunn, M. K. Therapeutic peptides: Historical perspectives, current development trends,

- and future directions. *Bioorg. Med. Chem.* **26**, 2700–2707 (2018).
13. Zorzi, A., Deyle, K. & Heinis, C. Cyclic peptide therapeutics: past, present and future. *Curr. Opin. Chem. Biol.* **38**, 24–29 (2017).
 14. Pelay-Gimeno, M., Glas, A., Koch, O. & Grossmann, T. N. Structure-Based Design of Inhibitors of Protein-Protein Interactions: Mimicking Peptide Binding Epitopes. *Angew. Chemie Int. Ed.* **54**, 8896–8927 (2015).
 15. White, C. J. & Yudin, A. K. Contemporary strategies for peptide macrocyclization. *Nat. Chem.* **3**, 509–524 (2011).
 16. Góngora-Benítez, M., Tulla-Puche, J. & Albericio, F. Multifaceted Roles of Disulfide Bonds. Peptides as Therapeutics. *Chem. Rev.* **114**, 901–926 (2013).
 17. Sandimmune (Cyclosporine): Side Effects, Interactions, Warning, Dosage & Uses. Available at: <https://www.rxlist.com/sandimmune-drug.htm#description>. (Accessed: 11th May 2019)
 18. Oates, J. A., Wood, A. J. J. & Kahan, B. D. Cyclosporine. *N. Engl. J. Med.* **321**, 1725–1738 (1989).
 19. Räder, A. F. B., Reichart, F., Weinmüller, M. & Kessler, H. Improving oral bioavailability of cyclic peptides by N-methylation. *Bioorg. Med. Chem.* **26**, 2766–2773 (2018).
 20. Lamberts, S. W. J., van der Lely, A.-J., de Herder, W. W. & Hofland, L. J. Octreotide. *N. Engl. J. Med.* **334**, 246–254 (1996).
 21. Wrighton, N. C. *et al.* Small peptides as potent mimetics of the protein hormone erythropoietin. *Science* **273**, 458–64 (1996).
 22. Kaushik, T. & Yaqoob, M. M. Lessons learned from peginesatide in the treatment of anemia associated with chronic kidney disease in patients on dialysis. *Biologics* **7**, 243–6 (2013).
 23. Hermanson, T., Bennett, C. L. & Macdougall, I. C. Peginesatide for the treatment of anemia due to chronic kidney disease – an unfulfilled promise. *Expert Opin. Drug Saf.* **15**, 1421–1426 (2016).
 24. Srinivas, N. *et al.* Peptidomimetic antibiotics target outer-membrane biogenesis in *Pseudomonas aeruginosa*. *Science* **327**, 1010–3 (2010).
 25. Murepavadin (POL7080) | Polyphor. Available at: <https://www.polyphor.com/pol7080/>. (Accessed: 11th May 2019)
 26. Sahu, A., Kay, B. K. & Lambris, J. D. Inhibition of human complement by a C3-binding peptide

- isolated from a phage-displayed random peptide library. *J. Immunol.* **157**, 884–91 (1996).
27. Apellis Pharmaceuticals - Our Focus. Available at: <https://www.apellis.com/focus-pipeline.html>. (Accessed: 11th May 2019)
 28. Chang, Y. S. *et al.* Stapled α -helical peptide drug development: A potent dual inhibitor of MDM2 and MDMX for p53-dependent cancer therapy. *Proc Natl Acad Sci U S A.* **110**, 3445–3454 (2013).
 29. Pipeline — Aileron Therapeutics. Available at: <https://www.aileronrx.com/pipeline>. (Accessed: 11th May 2019)
 30. Dias, D. A., Urban, S. & Roessner, U. A historical overview of natural products in drug discovery. *Metabolites* **2**, 303–36 (2012).
 31. Packer, M. S. & Liu, D. R. Methods for the directed evolution of proteins. *Nat. Rev. Genet.* **16**, 379–394 (2015).
 32. Davis, A. M., Plowright, A. T. & Valeur, E. Directing evolution: the next revolution in drug discovery? *Nat. Rev. Drug Discov.* **16**, 681–698 (2017).
 33. Matsuura, T. & Yomo, T. In vitro evolution of proteins. *J. Biosci. Bioeng.* **101**, 449–456 (2006).
 34. Press release: The Nobel Prize in Chemistry 2018. Available at: <https://www.nobelprize.org/prizes/chemistry/2018/press-release/>. (Accessed: 12th May 2019)
 35. Smith, G. P. Filamentous fusion phage: novel expression vectors that display cloned antigens on the virion surface. *Science* **228**, 1315–1317 (1985).
 36. Smith, G. P. & Petrenko, V. A. Phage Display. *Chem Rev.* **97**, 391–410 (1997).
 37. Qi, H., Lu, H., Qiu, H. J., Petrenko, V. & Liu, A. Phagemid vectors for phage display: Properties, characteristics and construction. *J. Mol. Biol.* **417**, 129–143 (2012).
 38. Bazan, J., Calkosiński, I. & Gamian, A. Phage display--a powerful technique for immunotherapy. *Hum. Vaccin. Immunother.* **8**, 1817–1828 (2012).
 39. Ledsgaard, L., Kilstrup, M., Karatt-Vellatt, A., McCafferty, J. & Laustsen, A. H. Basics of antibody phage display technology. *Toxins (Basel)*. **10**, 236 (2018).
 40. Rondot, S., Koch, J., Breitling, F. & Dübel, S. A helper phage to improve single-chain antibody presentation in phage display. *Nat. Biotechnol.* **19**, 75–78 (2001).
 41. Josephson, K., Ricardo, A. & Szostak, J. W. mRNA display: from basic principles to macrocycle drug

- discovery. *Drug Discov. Today* **19**, 388–399 (2014).
42. Chen, S. & Heinis, C. Phage Selection of Mono-and Bicyclic Peptide Ligands. doi:10.1039/9781849737159-00241
43. Giebel, L. B. *et al.* Screening of Cyclic Peptide Phage Libraries Identifies Ligands That Bind Streptavidin with High Affinities. *Biochemistry* **34**, 15430–15435 (1995).
44. Koivunen, E., Wang, B. & Ruoslahti, E. Isolation of a highly specific ligand for the $\alpha 5\beta 1$ integrin from a phage display library. *J. Cell Biol.* **124**, 373–380 (1994).
45. Koivunen, E., Wang, B. & Ruoslahti, E. Phage libraries displaying cyclic peptides with different ring sizes: Ligand specificities of the rgd-directed integrin. *Bio/Technology* **13**, 265–270 (1995).
46. Bonnycastle, L. L. C., Mehroke, J. S., Rashed, M., Gong, X. & Scott, J. K. Probing the basis of antibody reactivity with a panel of constrained peptide libraries displayed by filamentous phage. *J. Mol. Biol.* **258**, 747–762 (1996).
47. Fairbrother, W. J. *et al.* Novel peptides selected to bind vascular endothelial growth factor target the receptor-binding site. *Biochemistry* **37**, 17754–17764 (1998).
48. Heinis, C. & Winter, G. Encoded libraries of chemically modified peptides. *Curr. Opin. Chem. Biol.* **26**, 89–98 (2015).
49. McConnell, S. J., Uveges, A. J., Fowlkes, D. M. & Spinella, D. G. Construction and screening of M13 phage libraries displaying long random peptides. *Mol. Divers.* **1**, 165–176 (1996).
50. Livnah, O. *et al.* Functional mimicry of a protein hormone by a peptide agonist: the EPO receptor complex at 2.8 Å. *Science* **273**, 464–71 (1996).
51. Heinis, C., Rutherford, T., Freund, S. & Winter, G. Phage-encoded combinatorial chemical libraries based on bicyclic peptides. *Nat. Chem. Biol.* **5**, 502–507 (2009).
52. Timmerman, P., Beld, J., Puijk, W. C. & Meloen, R. H. Rapid and Quantitative Cyclization of Multiple Peptide Loops onto Synthetic Scaffolds for Structural Mimicry of Protein Surfaces. *ChemBioChem* **6**, 821–824 (2005).
53. Angelini, A. *et al.* Bicyclic Peptide Inhibitor Reveals Large Contact Interface with a Protease Target. *ACS Chem. Biol.* **7**, 817–821 (2012).
54. Rebollo, I. R., Angelini, A. & Heinis, C. Phage display libraries of differently sized bicyclic peptides.

- Medchemcomm* **4**, 145–150 (2013).
55. Chen, S., Bertoldo, D., Angelini, A., Pojer, F. & Heinis, C. Peptide Ligands Stabilized by Small Molecules. *Angew. Chemie Int. Ed.* **53**, 1602–1606 (2014).
56. Chen, S., Morales-Sanfrutos, J., Angelini, A., Cutting, B. & Heinis, C. Structurally Diverse Cyclisation Linkers Impose Different Backbone Conformations in Bicyclic Peptides. *ChemBioChem* **13**, 1032–1038 (2012).
57. Baeriswyl, V. *et al.* A Synthetic Factor XIIa Inhibitor Blocks Selectively Intrinsic Coagulation Initiation. *ACS Chem. Biol.* **10**, 1861–1870 (2015).
58. Middendorp, S. J. *et al.* Peptide Macrocycle Inhibitor of Coagulation Factor XII with Subnanomolar Affinity and High Target Selectivity. *J. Med. Chem.* **60**, 1151–1158 (2017).
59. Wilbs, J., Middendorp, S. J. & Heinis, C. Improving the Binding Affinity of in-Vitro-Evolved Cyclic Peptides by Inserting Atoms into the Macrocycle Backbone. *ChemBioChem* **17**, 2299–2303 (2016).
60. Kale, S. S. *et al.* Cyclization of peptides with two chemical bridges affords large scaffold diversities. *Nat. Chem.* **10**, 715–723 (2018).
61. Kim, J. *et al.* Diversity-oriented synthetic strategy for developing a chemical modulator of protein–protein interaction. *Nat. Commun.* **7**, 13196 (2016).
62. Dandapani, S. & Marcaurelle, L. A. Grand Challenge Commentary: Accessing new chemical space for ‘undruggable’ targets. *Nat. Chem. Biol.* **6**, 861–863 (2010).
63. Zorzi, A., Middendorp, S. J., Wilbs, J., Deyle, K. & Heinis, C. Acylated heptapeptide binds albumin with high affinity and application as tag furnishes long-acting peptides. *Nat. Commun.* **8**, 16092 (2017).
64. Kontermann, R. E. Half-life extended biotherapeutics. *Expert Opin. Biol. Ther.* **16**, 903–915 (2016).
65. Strohl, W. R. Fusion Proteins for Half-Life Extension of Biologics as a Strategy to Make Biobetters. *Biodrugs* **29**, 215–239 (2015).
66. Jevsievar, S., Kunstelj, M. & Porekar, V. G. PEGylation of therapeutic proteins. *Biotechnol. J.* **5**, 113–128 (2010).
67. Park, E. J., Choi, J., Lee, K. C. & Na, D. H. Emerging PEGylated non-biologic drugs. *Expert Opin. Emerg. Drugs* **1**, 1–13 (2019).

68. Swierczewska, M., Lee, K. C. & Lee, S. What is the future of PEGylated therapies? *Expert Opin. Emerg. Drugs* **20**, 531–6 (2015).
69. Turecek, P. L., Bossard, M. J., Schoetens, F. & Ivens, I. A. PEGylation of Biopharmaceuticals: A Review of Chemistry and Nonclinical Safety Information of Approved Drugs. *J. Pharm. Sci.* **105**, 460–475 (2016).
70. Caliceti, P. & Veronese, F. M. Pharmacokinetic and biodistribution properties of poly(ethylene glycol)–protein conjugates. *Adv. Drug Deliv. Rev.* **55**, 1261–1277 (2003).
71. Salmaso, S. & Caliceti, P. Peptide and Protein Bioconjugation: A Useful Tool to Improve the Biological Performance of Biotech Drugs. *Pept. Protein Deliv.* 247–290 (2011). doi:10.1016/B978-0-12-384935-9.10011-2
72. CHMP. *Committee for Medicinal Products for Human Use (CHMP) Withdrawal Assessment report for Omontys*. (2013).
73. Zhang, F., Liu, M. & Wan, H. Discussion about several potential drawbacks of PEGylated therapeutic proteins. *Biol. Pharm. Bull.* **37**, 335–9 (2014).
74. Besheer, A., Liebner, R., Meyer, M. & Winter, G. Challenges for PEGylated Proteins and Alternative Half-Life Extension Technologies Based on Biodegradable Polymers. in *ACS symposium series* 215–233 (2013). doi:10.1021/bk-2013-1135.ch013
75. Gaffney, P. J., Edgell, T. A. & Whitton, C. M. The Haemostatic Balance – Astrup Revisited. *Pathophysiol. Haemost. Thromb.* **29**, 58–71 (1999).
76. Davie, E. W., Fujikawa, K. & Kisiel, W. The Coagulation Cascade: Initiation, Maintenance, and Regulation. *Biochemistry* **30**, 10363–10370 (1991).
77. Gale, A. J. P. . Current Understanding of Hemostasis. *Toxicol Pathol.* **39**(1), 273–280 (2011).
78. Hartwig, J. & Italiano, J. The birth of the platelet. *J. Thromb. Haemost.* **1**, 1580–6 (2003).
79. Jackson, S. P. The growing complexity of platelet aggregation. *Blood* **109**, 5087–5095 (2007).
80. Rumbaut, R. E. & Thiagarajan, P. *Platelet-Vessel Wall Interactions in Hemostasis and Thrombosis*. (Morgan & Claypool Life Sciences, 2010).
81. Varga-Szabo, D., Pleines, I. & Nieswandt, B. Cell Adhesion Mechanisms in Platelets. *Arterioscler. Thromb. Vasc. Biol.* **28**, 403–412 (2008).

-
82. De Candia, E. Mechanisms of platelet activation by thrombin: A short history. *Thromb. Res.* **129**, 250–256 (2012).
 83. Halkar, M. & Lincoff, A. M. Dual antiplatelet therapy for acute coronary syndromes: How long to continue? *Cleve. Clin. J. Med.* **83**, 675–688 (2016).
 84. De Caterina, R. *et al.* General mechanisms of coagulation and targets of anticoagulants (Section I): Position paper of the ESC Working Group on Thrombosis - Task Force on anticoagulants in heart disease. *Thromb. Haemost.* **109**, 569–579 (2013).
 85. Gailani, D. & Renné, T. Intrinsic pathway of coagulation and arterial thrombosis. *Arterioscler. Thromb. Vasc. Biol.* **27**, 2507–2513 (2007).
 86. Dahlbäck, B. Blood coagulation. *Lancet* **355**, 1627–1632 (2000).
 87. Mammen, E. F. Physiology and Biochemistry of Blood Coagulation. in *Thrombosis and Bleeding Disorders* 1–56 (Academic Press, 1971). doi:10.1016/B978-0-12-077750-1.50005-2
 88. Hoffman, M. & Monroe, D. M. A cell-based model of hemostasis. *Thromb. Haemost.* **85**, 958–65 (2001).
 89. Anderson, J. A., Hogg, K. E. & Jeffrey I. Weitz. Hypercoagulable States. *Hematology* **31**, 2076–2087 (2018).
 90. Jin, L. *et al.* The anticoagulant activation of antithrombin by heparin. *Medical Sciences Communicated by Max F. Perutz, Medical Research Council* **94**, (1997).
 91. Lwaleed, B. A. & Bass, P. S. Tissue factor pathway inhibitor: structure, biology and involvement in disease. *J. Pathol.* **208**, 327–339 (2006).
 92. Rogers, H. J., Nakashima, M. O. & Kottke-Marchant, K. Hemostasis and Thrombosis. in *Hematopathology: A Volume in the Series: Foundations in Diagnostic Pathology* 57–105 (2017). doi:10.1016/B978-0-323-47913-4.00002-1
 93. Rau, J. C., Beaulieu, L. M., Huntington, J. A. & Church, F. C. Serpins in thrombosis, hemostasis and fibrinolysis. *J. Thromb. Haemost.* **5 Suppl 1**, 102–15 (2007).
 94. Wendelboe, A. M. & Raskob, G. E. Global Burden of Thrombosis: Epidemiologic Aspects. *Circ. Res.* **118**, 1340–1347 (2016).
 95. Mackman, N. Triggers, targets and treatments for thrombosis. *Nature* **451**, 914–918 (2008).

96. Linton, M. F. *et al.* *The Role of Lipids and Lipoproteins in Atherosclerosis*. Endotext (MDText.com, Inc., 2000).
97. Moore, K. J., Sheedy, F. J. & Fisher, E. A. Macrophages in atherosclerosis: a dynamic balance. *Nat. Rev. Immunol.* **13**, 709–21 (2013).
98. Koupenova, M., Kehrel, B. E., Corkrey, H. A. & Freedman, J. E. Thrombosis and platelets: an update. *Eur. Heart J.* **38**, (2016).
99. Byrnes, J. R. & Wolberg, A. S. Red blood cells in thrombosis. (2017). doi:10.1182/blood-2017-03
100. Yang, G., De Staercke, C. & Hooper, W. C. The effects of obesity on venous thromboembolism: A review. *Open J. Prev. Med.* **2**, 499–509 (2012).
101. López, J. A. & Chen, J. Pathophysiology of venous thrombosis. *Thromb. Res.* **123**, 30–34 (2009).
102. Parkin, L. *et al.* Body Mass Index, Surgery, and Risk of Venous Thromboembolism in Middle-Aged Women. *Circulation* **125**, 1897–1904 (2012).
103. Torri, G. & Naggi, A. Heparin centenary – an ever-young life-saving drug. *Int. J. Cardiol.* **212**, S1–S4 (2016).
104. Baglin, T., Barrowcliffe, T. W., Cohen, A. & Greaves, M. Guidelines on the use and monitoring of heparin. *Br. J. Haematol.* **133**, 19–34 (2006).
105. Crowther, M. A. & Warkentin, T. E. Bleeding risk and the management of bleeding complications in patients undergoing anticoagulant therapy: Focus on new anticoagulant agents. *Blood* **111**, 4871–4879 (2008).
106. Ahmed, I., Majeed, A. & Powell, R. Heparin induced thrombocytopenia: diagnosis and management. *Postgr. Med J* **83**, 575–582 (2007).
107. Estes, J. W. Clinical Pharmacokinetics of Heparin. *Clin. Pharmacokinet.* **5**, 204–220 (1980).
108. Mulloy, B., Hogwood, J., Gray, E., Lever, R. & Page, C. P. Pharmacology of Heparin and Related Drugs. *Pharmacol. Rev.* **68**, 76–141 (2016).
109. Hirsh, J. *et al.* Heparin and Low-Molecular- Weight Heparin Mechanisms of Action, Pharmacokinetics, Dosing, Monitoring, Efficacy, and Safety. *Chest* **119**, 64s–94s (2001).
110. Ufer, M. Comparative Pharmacokinetics of Vitamin K Antagonists. *Clin. Pharmacokinet.* **44**, 1227–1246 (2005).

111. Mekaj, Y. H., Mekaj, A. Y., Duci, S. B. & Miftari, E. I. New oral anticoagulants: their advantages and disadvantages compared with vitamin K antagonists in the prevention and treatment of patients with thromboembolic events. *Ther. Clin. Risk Manag.* **11**, 967–77 (2015).
112. Halvorsen, S. *et al.* A nationwide registry study to compare bleeding rates in patients with atrial fibrillation being prescribed oral anticoagulants. *Eur Hear. J Cardiovasc Pharmacother.* **3**, 28–36 (2017).
113. Rubboli, A., Becattini, C. & Verheugt, F. W. Incidence, clinical impact and risk of bleeding during oral anticoagulation therapy. *World J. Cardiol.* **3**, 351–8 (2011).
114. Weitz, J. I. & Linkins, L.-A. Beyond heparin and warfarin: the new generation of anticoagulants. *Expert Opin. Investig. Drugs* **16**, 271–282 (2007).
115. Larsen, T. B., Skjøth, F., Nielsen, P. B., Kjældgaard, J. N. & Lip, G. Y. H. Comparative effectiveness and safety of non-vitamin K antagonist oral anticoagulants and warfarin in patients with atrial fibrillation: propensity weighted nationwide cohort study. *BMJ* **353**, i3189 (2016).
116. Southworth, M. R., Reichman, M. E. & Unger, E. F. Dabigatran and Postmarketing Reports of Bleeding. *N. Engl. J. Med.* **368**, 1272–1274 (2013).
117. Villines, T. C. & Peacock, W. F. Safety of Direct Oral Anticoagulants: Insights from Postmarketing Studies. *Am. J. Med.* **129**, S41–S46 (2016).
118. Erika L Hellenbart, Kathleen D Faulkenberg & Shannon W Finks. Evaluation of bleeding in patients receiving direct oral anticoagulants. **1**, 13–325 (2017).
119. Klok, F. A., Kooiman, J., Huisman, M. V, Konstantinides, S. & Lankeit, M. Predicting anticoagulant-related bleeding in patients with venous thromboembolism: a clinically oriented review. *Eur. Respir. J.* **45**, 201–10 (2015).
120. Crowther, M. & Cuker, A. How can we reverse bleeding in patients on direct oral anticoagulants? *Kardiol Pol.* **77**, 3–11 (2019).
121. Székely, O. *et al.* Expert Opinion on Emerging Drugs Factor XI inhibition fulfilling the optimal expectations for ideal anticoagulation. *Expert Opin. Emerg. Drugs* **24**, 1–7 (2019).
122. Weitz, J. I. Factor XI and factor XII as targets for new anticoagulants. *Thromb. Res.* **141**, S40–S45 (2016).
123. Sen, S. & Dahlberg, K. W. Physician’s fear of anticoagulant therapy in nonvalvular atrial fibrillation.

- Am. J. Med. Sci.* **348**, 513–521 (2014).
124. Gailani, D., Bane, C. E. & Gruber, A. Factor XI and contact activation as targets for antithrombotic therapy. *J. Thromb. Haemost.* **13**, 1383–1395 (2015).
125. He, R., Chen, D. & He, S. Factor XI : Hemostasis , Thrombosis , and Antithrombosis. *Thromb. Res.* **129**, 541–550 (2012).
126. Bane, C. E. & Gailani, D. Factor XI as a target for antithrombotic therapy. *Drug Discov. Today* **19**, 1454–1458 (2014).
127. Weitz, J. I., and Fredenburg, J. Factor XI and factor XII as targets for new anticoagulants. *Front Med* **4:19**, (2017).
128. Gailani, D. & Gruber, A. Factor XI as a Therapeutic Target. *Arter. Thromb Vasc Biol.* **36**, 1316–1322 (2016).
129. Mohammed, B. M. *et al.* An update on factor XI structure and function. *Thromb. Res.* **161**, 94–105 (2018).
130. Sun, M. F., Zhao, M. & Gailani, D. Identification of amino acids in the factor XI apple 3 domain required for activation of factor IX. *J. Biol. Chem.* **274**, 36373–8 (1999).
131. Geng, Y. *et al.* The dimeric structure of factor XI and zymogen activation. *Blood* **121**, 3962–9 (2013).
132. Weitz, J. I. & Fredenburgh, J. C. 2017 Scientific Sessions Sol Sherry Distinguished Lecture in Thrombosis. *Arterioscler. Thromb. Vasc. Biol.* **38**, 304–310 (2018).
133. McMullen, B. A., Fujikawa, K. & Davie, E. W. Location of the Disulfide Bonds in Human Coagulation Factor XI: The Presence of Tandem Apple Domains¹. *Biochemistry* **30**, 2056–2060 (1990).
134. Meijers, J. C., Mulvihill, E. R., Davie, E. W. & Chung, D. W. Apple four in human blood coagulation factor XI mediates dimer formation. *Biochemistry* **31**, 4680–4 (1992).
135. Zucker, M., Zivelin, A., Landau, M., Rosenberg, N. & Seligsohn, U. Three residues at the interface of factor XI (FXI) monomers augment covalent dimerization of FXI. *J. Thromb. Haemost.* **7**, 970–975 (2009).
136. Ponczek, M. B., Gailani, D. & Doolittle, R. F. Evolution of the contact phase of vertebrate blood coagulation. *J. Thromb. Haemost.* **6**, 1876–1883 (2008).

-
137. Sun, Y. & Gailani, D. Identification of a factor IX binding site on the third apple domain of activated factor XI. *J. Biol. Chem.* **271**, 29023–29028 (1996).
138. Meijers, J. C. M., Tekelenburg, W. L. H., Bouma, B. N., Bertina, R. M., Rosendaal, F. R. High levels of coagulation factor XI as a risk factor for venous thrombosis. *N. Engl. J. Med.* **701**, 342:696 (2000).
139. Doggen, C. J. M., Rosendaal, F. R. & Meijers, J. C. M. Levels of intrinsic coagulation factors and the risk of myocardial infarction among men : opposite and synergistic effects of factors XI and XII. **108**, 4045–4052 (2006).
140. Yang, D. T., Flanders, M. M., Ascp, M. T. & Kim, H. Elevated Factor XI Activity Levels Are Associated With an Increased Odds Ratio for Cerebrovascular Events. **126**, 411–415 (2006).
141. Preis, M. *et al.* Factor XI deficiency is associated with lower risk for cardiovascular and venous thromboembolism events. **129**, 1210–1216 (2019).
142. Büller, H. R. *et al.* Factor XI Antisense Oligonucleotide for Prevention of Venous Thrombosis. *N. Engl. J. Med.* **372**, 232–240 (2015).
143. Al-Horani, R. A. & Desai, U. R. Factor XIa inhibitors: A review of patent literature Rami. *Expert Opin Ther Pat.* **26**, 323–345 (2016).
144. Weitz, J. I. & Chan, N. C. Advances in Antithrombotic Therapy. *Arterioscler. Thromb. Vasc. Biol.* **39**, 7–12 (2019).
145. Tucker, E. I. *et al.* Prevention of vascular graft occlusion and thrombus-associated thrombin generation by inhibition of factor XI. **113**, 936–945 (2009).
146. Eder, J. *et al.* US20170022292A1. (2017).
147. Koch, A. W. *et al.* MAA868, a novel FXI antibody with a unique binding mode, shows durable effects on markers of anticoagulation in humans. *Blood* **133**, 1507–1516 (2019).
148. Tucker, E. I. *et al.* Inhibition of factor XI activation attenuates inflammation and coagulopathy while improving the survival of mouse polymicrobial sepsis. *Blood* **119**, 4762–4768 (2012).
149. Cheng, Q. *et al.* A role for factor XIIa-mediated factor XI activation in thrombus formation in vivo. *Blood* **116**, 3981–3990 (2010).
150. Thomas, D. *et al.* BAY 1213790, a fully human IgG1 antibody targeting coagulation factor XIa: First evaluation of safety, pharmacodynamics, and pharmacokinetics. *Res. Pract. Thromb. Haemost.* **3**,

- 242–253 (2019).
151. Buchmueller, A., Wilmen, A., Strassburger, J., Schmidt, M. V. & Laux, V. *The anti-factor XIa antibody BAY 1213790 is a novel anticoagulant that shows strong antithrombotic efficacy without an increased risk of bleeding in rabbit models*. doi:10.3252/pso.eu.ISTH2017.2017
152. Ma, D. *et al.* Desmolaris, a novel factor XIa anticoagulant from the salivary gland of the vampire bat (*Desmodus rotundus*) inhibits inflammation and thrombosis in vivo. *Blood* **122**, 4094–4106 (2013).
153. Wu, W. *et al.* The kunitz protease inhibitor domain of protease nexin-2 inhibits factor XIa and murine carotid artery and middle cerebral artery thrombosis. *Blood* **120**, 671–677 (2012).
154. Younis, H. S. *et al.* Antisense inhibition of coagulation factor XI prolongs APTT without increased bleeding risk in cynomolgus monkeys. *Blood* **119**, 2401–2408 (2012).
155. Wong, P. C., Crain, E. J., Watson, C. A. & Schumacher, W. A. A small-molecule factor XIa inhibitor produces antithrombotic efficacy with minimal bleeding time prolongation in rabbits. *J. Thromb. Thrombolysis* **32**, 129–137 (2011).
156. Pinto, D. J. P. *et al.* Discovery of a Parenteral Small Molecule Coagulation Factor XIa Inhibitor Clinical Candidate (BMS-962212). *J. Med. Chem.* **60**, 9703–9723 (2017).
157. Hayward, N. J., Goldberg, D. I., Morrel, E. M., Friden, P. M. & Bokesch, P. M. Abstract 13747: Phase 1a/1b Study of EP-7041: A Novel, Potent, Selective, Small Molecule FXIa Inhibitor. *Circulation* **136**, 13747 (2017).
158. Sho Kouyama *et al.* Discovery of ONO -5450598 , a highly orally bioavailable small molecule factor XIa inhibitor: the pharmacokinetic and pharmacological profiles. Available at: https://www.postersessiononline.eu/173580348_eu/congresos/ISTH2017/aula/-PB_2139_ISTH2017.pdf. (Accessed: 18th May 2019)
159. Al-Horani, R. A. & Desai, U. R. Designing allosteric inhibitors of factor XIa. Lessons from the interactions of sulfated pentagalloylglucopyranosides. *J. Med. Chem.* **57**, 4805–4818 (2014).
160. Woodruff, R. S. *et al.* Generation and characterization of aptamers targeting factor XIa. *Thromb. Res.* **156**, 134–141 (2017).
161. Yau, J. W. *et al.* Selective depletion of factor XI or factor XII with antisense oligonucleotides attenuates catheter thrombosis in rabbits. **123**, 2102–2108 (2019).

-
162. Ricardo, A. *et al.* Preclinical Evaluation of RA101495, a Potent Cyclic Peptide Inhibitor of C5 for the Treatment of Paroxysmal Nocturnal Hemoglobinuria. *Blood* **126**, 939 (2015).
163. Rentero Rebollo, I. & Heinis, C. Phage selection of bicyclic peptides. *Methods* **60**, 46–54 (2013).
164. Baeriswyl, V. *et al.* Development of a Selective Peptide Macrocyclic Inhibitor of Coagulation Factor XII toward the Generation of a Safe Antithrombotic Therapy. *J. Med. Chem.* **56**, 3742–3746 (2013).
165. Rentero Rebollo, I. *et al.* Development of Potent and Selective *S. aureus* Sortase A Inhibitors Based on Peptide Macrocycles. *ACS Med. Chem. Lett.* **7**, 606–11 (2016).
166. Mackman, N. Triggers, targets and treatments for thrombosis. *Nature* **451**, 914–918 (2008).
167. Wang, X. *et al.* Effects of factor IX or factor XI deficiency on ferric chloride-induced carotid artery occlusion in mice. *J Thromb Haemost.* 695–702 (2005).
168. Crosby, J. R. *et al.* Antithrombotic effect of antisense factor xi oligonucleotide treatment in primates. *Arterioscler. Thromb. Vasc. Biol.* **33**, 1670–1678 (2013).
169. Yau, J. W. *et al.* Selective depletion of factor XI or factor XII with antisense oligonucleotides attenuates catheter thrombosis in rabbits. *Blood* **123**, 2102–2107 (2014).
170. Müller F, Gailani D & Renné T. Factor XI and XII as antithrombotic targets. *Curr. Opin. Hematol.* **18**, 349–355 (2011).
171. Smith, L. M. *et al.* Novel phenylalanine derived diamides as Factor XIa inhibitors. *Bioorganic Med. Chem. Lett.* **26**, 472–478 (2016).
172. David, T. *et al.* Factor XIa-specific IgG and a reversal agent to probe factor XI function in thrombosis and hemostasis. *Sci. Transl. Med.* **8**, 353ra12 (2016).
173. Tucker, E. I. *et al.* Prevention of vascular graft occlusion and thrombus-associated thrombin generation by inhibition of factor XI. *Blood* **113**, 936–944 (2009).
174. Rebollo, I. R., Sabisz, M., Baeriswyl, V. & Heinis, C. Identification of target-binding peptide motifs by high-throughput sequencing of phage-selected peptides. *Nucleic Acids Res.* **42**, e169 (2014).
175. Diao, L. & Meibohm, B. Pharmacokinetics and Pharmacokinetic – Pharmacodynamic Correlations of Therapeutic Peptides. *Clin Pharmacokinet* **52**, 855–868 (2013).
176. Baumann, A., Tuerck, D., Prabhu, S., Dickmann, L. & Sims, J. Pharmacokinetics, metabolism and distribution of PEGs and PEGylated proteins: Quo vadis? *Drug Discov. Today* **19**, 1623–1631

- (2014).
177. Byun, J. H., Jang, I. S., Kim, J. W. & Koh, E. H. Establishing the heparin therapeutic range using aPTT and anti-Xa measurements for monitoring unfractionated heparin therapy. *Blood Res.* **51**, 171–174 (2016).
178. Himmelfarb, J. & Ikizler, T. A. Hemodialysis. *N. Engl. J. Med.* 1833–1845 (2010).
179. Kessler, M., Moureau, F. & Nguyen, P. Anticoagulation in Chronic Hemodialysis: Progress Toward an Optimal Approach. *Semin. Dial.* **28**, 474–489 (2015).
180. Davenport, A. What are the anticoagulation options for intermittent hemodialysis? *Nat. Rev. Nephrol.* **7**, 499–508 (2011).
181. Kyrk, T., Bechara, A., Skagerlind, M. & Stegmayr, B. Heparin and albumin as part of the priming solution limits exposure to anticoagulation during hemodialysis: In vitro studies. *Int. J. Artif. Organs* **37**, 734–740 (2014).
182. Chen, S. *et al.* Improving Binding Affinity and Stability of Peptide Ligands by Substituting Glycines with d -Amino Acids. *ChemBioChem* **14**, 1316–1322 (2013).
183. Villequey, C., Kong, X. D. & Heinis, C. Bypassing bacterial infection in phage display by sequencing DNA released from phage particles. *Protein Eng. Des. Sel.* **30**, 761–768 (2017).
184. Ocak, G. *et al.* Chronic kidney disease and bleeding risk in patients at high cardiovascular risk: a cohort study. *J. Thromb. Haemost.* **16**, 65–73 (2018).
185. Steevens N. S. Alconcel, A. S. B. and H. D. M. FDA-approved poly (ethylene glycol)– protein conjugate drugs. *Polym. Chem.* **2**, 1442–1448 (2011).
186. Reichert, J. M. Antibodies to watch in 2017. *MAbs* **9**, 167–181 (2017).
187. Grossi, F. V *et al.* APL-2, a Complement C3 Inhibitor for the Potential Treatment of Paroxysmal Nocturnal Hemoglobinuria (PNH): Phase I Data from Two Completed Studies in Healthy Volunteers. *Blood* **128**, 1251 (2016).
188. Wong, P. C. *et al.* Nonpeptide Factor Xa Inhibitors: I. Studies with SF303 and SK549, a New Class of Potent Antithrombotics. *J. Pharmacol. Exp. Ther.* **292**, 351–357 (2000).
189. Schreiber, G. & Fersht, A. R. Association of Proteins. *Nat. Struct. Biol.* **3**, 427–431 (1996).

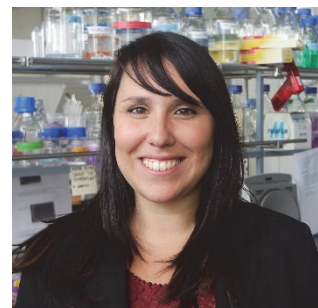
CV Vanessa Carle

vanessa.carle@epfl.ch

+41762907362

Av. de Morges, 63

1004 Lausanne (CH)



Education

2015 – present	PhD in Chemical Biology Doctoral School in Chemistry and Chemical Engineering EPFL, Lausanne, Switzerland (Final exam: 07/2019)
2012 – 2015	International Master of Science in Pharmaceutical Biotechnology Martin-Luther-Universität Halle-Wittenberg, Halle, Germany Degree: Master of Science
2008 – 2012	Bachelor of Science in Biotechnology Università degli studi di Pavia, Pavia, Italy Degree: Bachelor of Science

Experience

2016 – 2019	Supervision of five master thesis research projects and teaching activity in the courses “Biochemistry I” and “Experimental biochemistry and biophysics” EPFL, Lausanne, Switzerland
07/2015 – present	PhD thesis “Development of cyclic peptide inhibitors of coagulation factor XIa for safer anticoagulation” Doctoral School in Chemistry and Chemical Engineering, Laboratory of Therapeutic Proteins and Peptides, Prof. Christian Heinis EPFL, Lausanne, Switzerland
04/2014 – 02/2015	Internship and master’s thesis “Structural-functional characterization of the translocase domain of the enzyme LlaBIII” Faculty of biology, structural biology group, Prof. Saikrishnan Kayarat IISER Pune, Pune, India
10/2013 – 01/2014	Internship “Chemical cross-linking and MS3D analysis of tropoelastin for the characterization of its cross-linking interfaces and specific residues” Faculty of Pharmacy, Elastin group, Dr. Christian Schmelzer Martin-Luther-Universität Halle-Wittenberg, Halle, Germany
03/2011 – 09/2011	Internship and bachelor’s thesis “Preparation of protein-loaded calcium phosphate nanoparticles for oral vaccine delivery” Faculty of Pharmacy, Department of Drug Delivery, Prof. Claus-Michael Lehr Universität des Saarlandes, Saarbrücken, Germany

Conferences, workshops and competitions

06/2018 – 10/2018	Leader of the start-up project “Velox Therapeutics” at Mass Challenge Switzerland, one of the 65 start-ups selected from over 1000 applicants Renens, Switzerland
04/2018	Idea champion at the SwissCompanyMaker workshop Bern, Switzerland
02/2018	Elevator Pitch at the 10th Sachs European Life Sciences CEO forum Presentation of the start-up project “Velox Therapeutics” Zürich, Switzerland
09/2017 – 12/2017	Project leader at CTI (now Innosuisse) Entrepreneurship training “Business Concept” : “A fast track and hands on entrepreneurship training taught by seasoned entrepreneurs” EPFL, Lausanne, Switzerland
12/2016	Oral presentation at the Swiss-Japanese symposium “Frontiers 2017” EPFL, Lausanne, Switzerland
08/2016	Short talk and poster presentation at the Swiss Summer School in Chemical Biology Villars sur Ollon, Switzerland

Awards and grants

09/2019 – 09/2020	SNSF/Innosuisse Bridge Proof of Concept Fellow Laboratory of Therapeutic Proteins and Peptides, EPFL, Lausanne, Switzerland
10/2018	Platinum award at Mass Challenge for the start-up project “Velox Therapeutics” Renens, Switzerland
12/2017	Best project award at the CTI Entrepreneurship training “Business Concept” EPFL, Lausanne, Switzerland
12/2016	Best poster award at the Swiss summer school in Chemical Biology Villars sur Ollon, Switzerland

List of publications

Carle, V. *et al.* Generation and screening of a structurally diverse 100-billion cyclic peptide phage display library. *In preparation.*

Carle, V. *et al.* Development of selective FXIa inhibitors based on cyclic peptides and their application for safe anticoagulation. *In preparation.*

Carle, V. *et al.* Fast binding kinetics of a coagulation factor inhibitor are key for strong anticoagulation. *In preparation.*

Kumar Chand, M., Carle, V., Anuvind, K.G., Kayarat, S. DNA-mediated coupling of the ATPase, translocase and nuclease activities of a Type ISP restriction-modification enzyme. *In revision, Nucleic Acids Res.* (2019).

Kong, X.D., Carle, V., Pojer, F., Abriata, L., Deyle, K., Heinis, C. De novo evolution of target-specific peptides that survive oral administration. *Submitted.*

